



UNIVERSITÀ
DEGLI STUDI
DI PADOVA

UNIVERSITÀ DEGLI STUDI DI PADOVA

Dipartimento di Ingegneria Industriale - DII

Corso di Laurea Magistrale in Ingegneria Energetica

Thermal Energy Storage Tanks as a Source of Flexibility in District Heating Networks

Relatore: Prof. Michele De Carli

Prof. Angelo Zarrella

Mario Silvestri

Matr. 1208994

Anno Accademico 2020/2021

UNIVERSITÀ DEGLI STUDI DI PADOVA
DIP. DI INGEGNERIA INDUSTRIALE

UNIVERSITY OF PADUA
DEPT. OF INDUSTRIAL ENGINEERING

**Tesi Magistrale per il Corso di
Laurea in Ingegneria Energetica**

**In Partial Fulfillment of the
Requirements for the Master's
Degree in Energy Engineering**

**THERMAL ENERGY STORAGE TANKS AS A SOURCE OF
FLEXIBILITY IN DISTRICT HEATING NETWORKS**

**I SERBATOI DI ACCUMULO TERMICO COME STRUMENTO DI
FLESSIBILITÀ NELLE RETI DI TELERISCALDAMENTO**

Prof. Michele DE CARLI
Prof. Angelo ZARRELLA

Candidate: Mario SILVESTRI
Matr. no.: 1208994

April 20, 2021

Abstract

District heating networks are an important part of the strategy to reduce carbon emissions in the heating sector. In order to conserve primary energy and to increase the role of intermittent renewable resources, it is useful to decouple the production of heat from its consumption. Different technologies are used for the storage of heat, over a variety of time spans and in many different sizes. In this thesis, we would like to focus on the role played by tanks of liquid water, and the extent to which they can help a real-life network achieve flexibility.

A simple model of a stratified tank was built, based on a cylindrical control surface divided into a number of sectors of equal volume along the vertical direction. The model, after being deemed satisfactory when compared with a pre-existing numerical representation, was integrated with a model of the complete district heating network of the city of Verona.

The network model is fed with the temperature of the tank top sector and with the value of the circulating mass flow for heat distribution, and gives out the return temperatures to the tank bottom sector. This way, it becomes possible to evaluate the dynamic behaviour of the reservoir when different regulation regimes at the generator level are implemented, and ultimately its energy "costs" and ability to set aside energy for later use.

After considering the energy data previously obtained from the network simulations without purpose-built heat reserves, and by analysing the dynamic evolution of temperature and power parameters, it is possible to say that reservoirs can make a meaningful contribution to flexibility in the district network in Verona.

Riassunto

Le reti di teleriscaldamento sono responsabili per quote molto diverse del calore per usi civili che viene fornito nei diversi Paesi dell'Unione Europea e del mondo, ma vengono generalmente considerate uno strumento importante per la decarbonizzazione dei consumi energetici degli edifici. Grazie alle reti di teleriscaldamento, è infatti possibile utilizzare calore di scarto e integrare fonti rinnovabili, sia termiche che elettriche, anche compensando l'intermittenza delle seconde attraverso la conversione in calore per usi civili.

Nella prima parte della tesi, è data una panoramica delle tecnologie usate nella produzione e nella distribuzione del calore nelle reti di teleriscaldamento. Particolare attenzione viene rivolta alle tecnologie di generazione, e si evidenzia che attualmente si usano sia calore di scarto della produzione di elettricità e dei processi industriali, che fonti rinnovabili (principalmente biomasse) e infine impianti che producono solo calore, generalmente a combustibile fossile. Questi ultimi sono meno convenienti dal punto di vista dell'efficienza, ma spesso necessari per garantire la fornitura di calore, specialmente nei momenti di più forte domanda. Si rende quindi evidente l'utilità dei sistemi che permettono, in una certa misura, di disaccoppiare la produzione di calore dal consumo.

Successivamente, vengono passati in rassegna i principali metodi di accumulo dell'energia per il teleriscaldamento, a partire dalle masse termiche della rete di distribuzione e degli edifici, per arrivare alle strutture dedicate centralizzate. Queste appartengono a diverse famiglie a seconda del mezzo usato per l'accumulo, della durata dello stesso e delle dimensioni. Particolarmente comuni, per la densità di energia e la relativa economicità costruttiva, sono i serbatoi che sfruttano il calore specifico dell'acqua.

Si perviene in seguito al "cuore" della tesi: lo sviluppo della rappresentazione numerica di un serbatoio stratificato a circuito diretto. Il modello monodimensionale discreto è basato su un sistema lineare, costruito a partire dalle equazioni di bilancio di una serie di regioni di uguale volume lungo l'asse verticale. Come si vedrà, l'energia termica viene essenzialmente spostata dalle portate di massa, che percorrono il serbatoio dall'alto verso il basso quando la portata dal lato del generatore di calore di calore supera quella di circolazione nella rete, e verso l'alto nel caso inverso. Benché si manifestino alcune instabilità nel momento in cui le portate sui due lati sono simili, il modello generato è comunque ragionevolmente in linea con quelli consolidati che si trovano in commercio dal punto di vista dei risultati, come il "Type 534" della piattaforma TRNSYS con cui è stato confrontato. Si può considerare soddisfacente anche dato il suo limitato impiego di potenza di calcolo.

Il modello numerico del serbatoio deve poi essere integrato in una rappresentazione di un'intera rete di teleriscaldamento, nello specifico di quella di Verona Centro Città, basata sul metodo NeMo. Questa, date le temperature del fluido in uscita dal serbatoio (predette dal modello) e le portate di massa richieste dai consumatori del calore (fissate secondo dati

storici), fornisce le temperature di ritorno al serbatoio. Nelle simulazioni svolte, si osserva l'effetto su alcuni parametri di diversi regimi di funzionamento del generatore, contraddistinti da diversi andamenti temporali della portata di massa, che quindi entra nel settore più elevato del serbatoio ed esce dal più inferiore.

L'evoluzione delle temperature dei livelli del serbatoio permette di identificare i momenti di accumulo e rilascio dell'energia termica, e nella simulazione con dati reali non si manifestano particolari instabilità malgrado la semplicità della struttura matematica.

I parametri calcolati infine sono diversi, tra cui: la diminuzione del picco di potenza tra domanda e produzione, la variazione dell'energia assorbita dal serbatoio, durante lassi di tempo fissati, rispetto a quella consumata mandando il calore direttamente alla rete; e la quantità di energia "spostata" nel tempo, o meglio accantonata per essere usata successivamente. Si osserva che l'impiego di un serbatoio non causa consumi aggiuntivi rilevanti di energia, e che l'energia accumulata tende ad aumentare man mano che si incrementa il tempo di pre-carica e la capienza del serbatoio.

I principali risultati delle simulazioni permettono, in ultima analisi, di immaginare un utilizzo dei serbatoi di accumulo allo scopo di aumentare la flessibilità delle reti di teleriscaldamento. Occorre tenere presente che l'uso della rete e dei serbatoi hanno costi di diversa natura. La prima, se usata come serbatoio, può causare la mancata soddisfazione delle richieste dell'utenza; i secondi richiedono investimenti e la realizzazione di opere civili. La strategia nella direzione della flessibilità, quindi, dovrà essere scelta dal gestore di rete solo dopo ulteriori studi.

Acknowledgements

Many people and organisations have made this piece of work possible. I shall try to recognise their contributions by starting with the most immediate ones and then taking a broader perspective.

The company AGSM of Verona has provided the research group at the University of Padua with precious data about the heat loads and operation of the district heating network that is the object of our study. The United States National Institute of Standards and Technology maintains the database REFPROP, from which data on the properties of some fluids (like water) can be obtained for free, and Dr. Marco Azzolin has kindly prepared a MATLAB function for us students to easily query the database.

I have been able to access and most importantly use these data, in the context of a much wider research project, thanks to Prof. Michele De Carli and Prof. Angelo Zarrella, who have involved me in a scientific investigation group dealing with a topic as complex and interesting as district heating. I hope I have been up to the responsibility that has been entrusted to me.

All along this project, I have received the help and support of Dr. Jacopo Vivian and Dr. Davide Quaggiotto, who have helped me navigate the intricacies of MATLAB modelling, and have provided the network model which gives context and meaning to the reservoir simulation that we built together.

I would like to also thank my teachers at the University of Padua. It is the concepts received during their courses that have allowed me to produce this work.

Finally, my most heartfelt gratitude cannot go to anyone but my parents Antonio and Nicoletta, who have supported me throughout these more than five years of studying, during joyful moments as well as crises of discouragement.

Acronyms

- ATES** Aquifer Thermal Energy Storage. 33
- BTES** Borehole Thermal Energy Storage. 33
- CHP** Combined Heat and Power. 8
- COP** Coefficient of Performance. 19
- DH** District Heating. 3, 5, 27, 29, 34, 37, 38, 42, 67, 68
- DHN** District Heating Network. 23, 90
- DHW** Domestic Hot Water. 4, 22, 67
- DSM** Demand Side Management. 29
- HOB** Heat-Only Boiler. 13, 67
- HP** Heat Pump. 20
- PCM** Phase Change Material. 30, 32, 38
- PTES** Pit Thermal Energy Storage. 34
- TTES** Tank Thermal Energy Storage. 35, 89, 90

Contents

1	Introduction	1
2	An Overview of District Heating Networks	3
2.1	Historical Notes	5
2.2	Sources of Heat	7
2.2.1	Combined Heat and Power	8
2.2.2	Waste heat recovery	12
2.2.3	District heating boilers	13
2.2.4	Renewable and non-fossil sources	14
2.2.5	Heat pumps for district heating	18
2.3	Heat Distribution	21
2.3.1	Transmission pipelines	21
2.3.2	Substations	22
2.4	Flexibility: Needs and Possible Sources	23
3	Thermal Storage in District Networks	27
3.1	Main Sources of Flexibility	27
3.1.1	The network	27
3.1.2	Customers	29
3.2	Dedicated Systems: Classification	31
3.2.1	Sensible heat	31
3.2.2	Latent heat	32
3.2.3	Environment media: ground and groundwater	33
3.3	Hot Water Storage	34
3.3.1	TTES: classification	35
3.4	Tank Thermal Storage: Structure and Organisation	37
3.4.1	Hydraulic connections	38
3.4.2	Geometric design	39

4	Modelling the Storage Tank	41
4.1	One-dimensional Models	41
4.2	Fundamental Equations	43
4.2.1	Tank sector energy balance	44
4.3	Explicit Model	47
4.4	Implicit Tank Model	48
4.5	Preliminary Results	50
5	Model Validation	55
5.1	The Reference Model: TRNSYS Type 534	55
5.2	Validation Procedure	57
5.3	Results and Observations	60
6	The Verona Case Study	67
6.1	Network Description	67
6.2	The Network Model	68
6.2.1	The hydraulic problem	69
6.2.2	The thermal problem	70
6.2.3	Network analysis and results	70
6.3	Model Integration and Application	74
6.3.1	Computer model structure	75
6.3.2	Performance indicators	77
7	Conclusions	89
A	MATLAB Code	91
A.1	Tank Model	91
A.1.1	Tank Linear System Function	91
A.2	Code for TRNSYS Validation	92
A.2.1	Main Script	92
A.2.2	Support Functions	95
A.3	Full Simulation	96
B	Tables and Charts	101
B.1	General Notes	101
B.2	Validation Results	104
B.3	Selected Simulations	108
	Bibliography	112

1. Introduction

District Heating is considered an important technology for the reduction of carbon dioxide emissions in the heating sector. Renewable energy sources, which are quickly growing in importance, so far have mostly contributed to changes in the production of electricity. This is due to physical reasons, since hydraulic, wind, and solar photovoltaic energy come in electrical form, as well as to technological and system integration issues, because the size and interconnected nature of the electric grid allows to integrate large amounts of intermittent resources, which can be out of phase with consumer needs. The main source of renewable heat is biomass, that is dispatchable to a certain extent, but whose environmental impact is discussed from both a land consumption and an air pollution standpoint. District heat networks allow to pool the needs of a large number of customers, in order to make more efficient use of fossil fuels and exploit alternative resources as well, by mitigating their disadvantages. In order to make the existing district networks more efficient, it can be useful to decouple in time the production of heat from its consumption.

In the present thesis, we shall firstly give an overview of the current state of district heating technology and of its likely developments in the near future, with particular attention to generating technologies. As will be shown, energy production in both district and individual heating is still dominated by fossil fuels. Therefore it is important, at least for the foreseeable future, to also evaluate flexibility solutions in the context of higher efficiency and more rational utilisation of conventional energy sources.

Afterwards, flexibility solutions will be briefly reported on, in order to arrive to stratified tanks of warm water. These are the core subject of this work; more specifically, we wish to carry out a comparative evaluation of the contribution that stratified tank can give towards flexibility of district heating networks. To this purpose, a finite difference numerical model of a stratified tank will be prepared. The model relies on the use of linear systems that, once solved, will give the temperature of water at some points along the vertical axis of a large reservoir.

The model shall then be compared to an existing computational routine for the prediction of tank temperatures, provided by an established simulation software library. After validation, the tank model is to be integrated into a wider model of the whole district heating network of the city of Verona. The latter model, prepared by researchers at the University of Padua, has already been used to measure the extent to which the mass of circulating water in the network can help smooth peaks of energy consumption and make heat generation more flexible.

Ultimately, the purpose of our model is complex. Firstly, it is expected to provide elements that can help compare the amount of flexibility provided by an optimised circulation of water, against the operational liberty given by the use of large dedicated reservoirs. Moreover,

we would like to obtain some understanding of the evolution of operational parameters in a dynamic network that includes a heat storage facility.

2. An Overview of District Heating Networks

A district heating network is any system that aims to connect a large number of heat users in order to centralise the production of the heat. The heat consumers are generally households, but industrial heat (which tends to be of higher thermodynamic quality) can also be delivered by means of a district network.

The English expression *district heating* underscores the large-scale nature of the consumer base of this sort of energy service. It is assumed in the name itself that the network must serve a city or at least a neighbourhood, with a minimum of hundreds or even thousands of users. The plant that produces the heat shall therefore be much larger than any household boiler, or than any of the heating systems used in pre-industrial times and countries. Between the plant and the households, a network of pipes transports the heat. The network is easier to build and operate if the users are concentrated in a small area. The development of such systems would not be feasible without urbanisation and industrialisation, as we are reminded by the French expression for the technology, *chauffage urbain* or "urban heating". In Italian, district heating (DH) is called *teleriscaldamento*: the emphasis is on the *distance* between producer and user, as is the case in the German-speaking world, where the word is *Fernwärme*.

If we wanted to summarise, at the cost of some inaccuracy, we would say that the typical district heating system is made of large machines, producing heat for many customers far away from them, with a heat carrier fluid to transport the "product" and a large network of pipes to move the fluid and bring it to the consumers. The fundamental goals of DH engineering will then be to maximise the advantages of large sizes, large distances and large pools of interconnected users, while mitigating the drawbacks.

Which are these advantages and drawbacks? Which conditions are more conducive to the deployment of DH, and which are the situations in which we should prefer decentralised heating?

We will start by listing succinctly the pros and cons, and then giving a short overview of the ways in which the need for DH has been met historically.

The main **advantages** of district heating are:

- *economies of scale*. Larger generators can be built and operated at a smaller cost per unit of energy delivered. This is due, among other reasons, to lower staffing per unit of installed power, smaller use of land and space (in an urban setting, space savings on the consumer side can be particularly important), fewer components such as gauges, valves, pumps et cetera. These savings result in manifold advantages, that can be described from other points of view: for example, in a large machine it can be cheap enough to install a more efficient pollution control system, or a different boiler can be used, that can withstand "difficult" fuels such as wood or municipal waste;

- *economies of scope*: in a centralised system, multiple services can be produced at once. Typically, low-grade civil heat production is associated with the delivery of electric power, or with an industrial process that requires high-grade heat. But not only energy services are tied together: the incineration of waste with heat recovery for the city is an example of hybrid¹ public service.
- *Flexible energy sourcing*: multiple sources of energy can be integrated in a DH system, especially the ones that would be too expensive, or dangerous, or polluting, for individual generation. The operating company can increase or decrease the relative importance of each energy source in response to market conditions or environmental concerns. The heat supply source of an entire city can be changed by modifying a central plant, which is not necessarily simple but, on the other hand, can be quicker than involving the entire citizenry.
- *smaller local environmental impact*. The environmental impact from residential heat generation is moved away from the customer households. It should be noted that this often encourages the use of "dirtier" fuels like coal, biomass and municipal waste, but larger plants, as mentioned above, can allow more significant pollution control systems to be installed.
- *Benefits on the user side*: generally speaking, the consumers of district heat obtain the final product by using a water-to-water heat exchanger. A water heat exchanger takes up less space than a furnace, is cheaper to install and maintain, and does not use a chemical reaction to heat the cold side fluid - so there are no combustible materials to store and transport, which is a public safety benefit. Moreover, heat delivery can be more reliable and contracts can be signed where only the heat is purchased, and not, for example, a boiler (boilers can be under-used and are generally sized for DHW production, which requires a much larger capacity than space heating).

On the other hand, the very traits of citywide heat service produce some **disadvantages**:

- *inequality* between the individual customer and the monopolistic heat provider.
- *Inflexible planning and implementation*: the infrastructure has a long lifetime, which can make it complex to correct mistakes made, for example, in the prediction of consumption patterns. Such a system might involve stakeholders that could develop different interests and no longer want or be able to participate after a while (for example the owners of an industrial activity that provides waste heat).²
- *Complexity and high investment costs* on the side of the operator, that has to build a network of pipes to connect all the users without dissipating too much heat and keep them in good condition. This can result in DH being viable only in areas where there is strong heat demand during the year and per unit of area: i. e., for practical purposes, a densely populated city where the weather is consistently cold during a large portion

¹"hybrid" here means energy and non-energy

²Such unforeseen consequences can be averted with strong binding contracts, but these could deter companies or communities from taking part in the DH project.

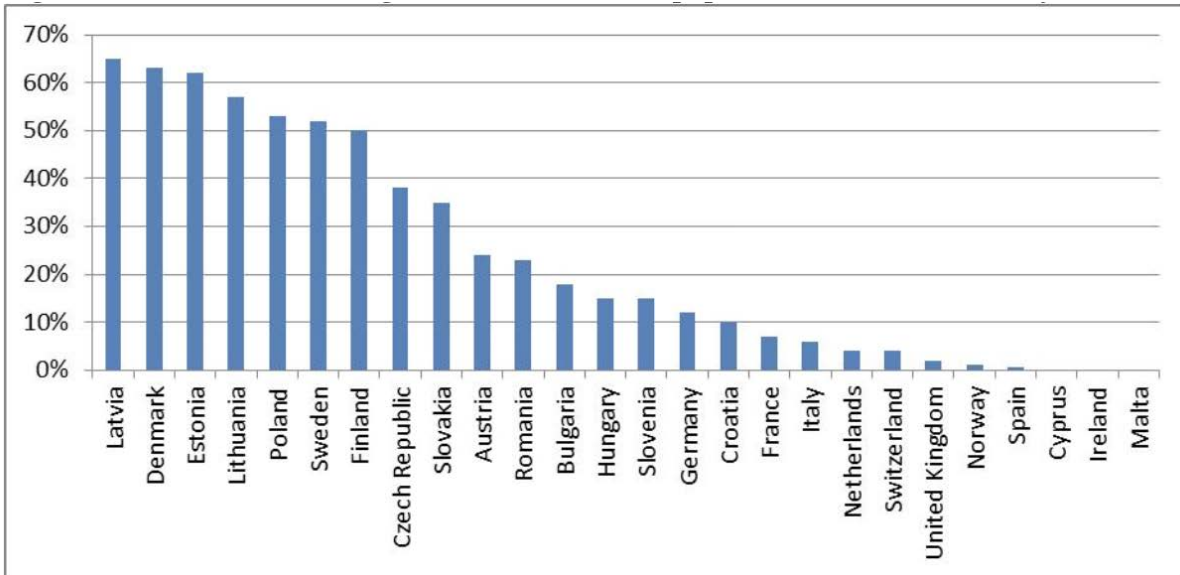


Figure 2.1: The share of the population served by DH in EU countries in 2013 (Euroheat and Power)

of the year. The parameter of linear heat density (LHD) is sometimes used to evaluate the economic feasibility of DH: it is the ratio of the energy delivered yearly to the length of the supply pipes. It has been estimated that the minimum LHD that allows DH is around $3 \text{ MWh}/(\text{yr} \cdot \text{m})$ [10].

2.1 Historical Notes

An overview of the history of district heating can be found in several works, such as [38], that generally identify four or five successive eras, called *generations*. Every generation is characterised by different thermodynamical parameters, materials, and to a certain extent heat sources, and the systems built in each era were and are often retrofitted, where economically feasible, with the devices of the successor generations.

The *first generation* of DH dates back to the Second industrial revolution. In late 1800s cities, heat was supplied by boilers that served one building each, heating or boiling water at high pressures by burning solid fuel, typically coal. The furnaces had to be stoked manually around the clock, were complicated to build and maintain, suffered from important heat losses at the chimney³ and through the walls, and were at risk of malfunction or even explosion because of the high operating pressure. It was thought simpler to build large boilers and connect them with the buildings by way of pipes that carried high-pressure, high-temperature steam. The water evaporated in the boilers and condensed in heat exchangers located in the served buildings.

³hot gas was not the only thing to escape the chimney: the air pollution from decentralised coal boilers was very significant, however this was not a major concern at the time.

Steam posed significant challenges in terms of mechanical losses caused by speed and friction, heat losses due to the high temperatures and safety risks related to the high pressures. Today, of the many steam DH systems developed in northern Europe and North America only a few are still operational in the original form, but among these are notable the networks of Paris and New York City.

The *second generation* of DH was developed starting around the year 1930. Before then, hot water had been identified as a better alternative to steam, but it required the use of electric pumps to be moved around, which at the time were becoming widely available. Water systems required smaller supply pipes but larger returns, and were installed in concrete ducts. The supply temperatures were still high (over 100° C), but 2nd-generation DH allowed easier operation nonetheless. The interest was not only to centralise production, but also to integrate the production of electric power and heat in order to conserve primary energy according to the mechanisms described in section 2.2.1.

This type of networks, with combined generation and water pipes, became widely adopted in central Europe and the standard for urban space heating in the Soviet Union. Still today, over one third of all global district heat is delivered in Russia alone [73].

The *third generation* started being introduced in northern European countries around 1970, and is marked by the use of hot water with reduced operating thermodynamic parameters - it attempts to go near atmospheric pressure and below the 100 degree Celsius mark. This allows the operator to use lighter and cheaper materials such as polymers, to simplify the installation of components (it is important to mention *pre-insulated* pipes) and to integrate different sources of heat, even large heat pumps.

A decrease in the thermal level of the heat delivered results, for easily understandable physical reasons, in the generation of more electric power if a combined plant is used and in smaller thermal losses.

The *fourth generation* of DH systems is being implemented in response to the need to integrate greater shares of renewable energy into heating and to further reduce the losses. It is an evolution of the third generation in the general direction of lighter components, cheaper materials and most importantly lower pressures and temperatures (around 1 bar and 70° C). Decreasing the operating temperatures is not free: it requires the use of household heating systems that accept lower temperatures (like radiant floor heating or lower-temperature radiators) and also demands smaller heating requirements, because with lower temperatures the same district network delivers less heat.

Some concepts have been developed and used in *fifth generation* district networks, particularly since around 2010. The network temperatures, in this case, could be lowered even further, essentially to ambient levels, in the 0-45° C interval. These levels of temperature, sometimes called "ultra-low temperature DH", require the use of heat pumps by the customers and are intended to allow both extraction of heat from the network and release of heat to the network from those customers that need cooling. This new generation of DH should thus enable a higher level of decentralisation of heat and cold production, and new

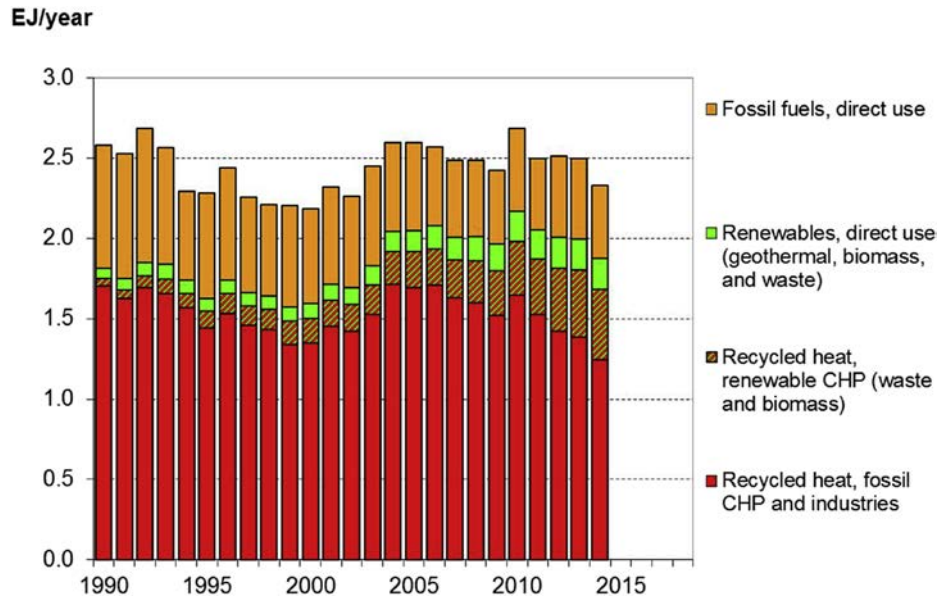


Figure 2.2: The technologies used in the EU to produce district heat [73]

business models in which the consumers also act as producers [7].

2.2 Sources of Heat

The large size, distance and centralisation allow to choose sources of energy that are free from the constraints imposed under modern standards upon the generation of heat in proximity to the consumer. Any heat source can be used, including challenging ones like biomass, waste and even nuclear power.

We have already talked about the interest in the reduction of primary energy consumption, which generally means a reduction in the amount of fuel that we need to burn. However, district heating is about the production and delivery of *heat*, and we know that when a fuel is burnt, nearly all of its chemical potential energy is turned into heat, relatively independently of the context of combustion. A large boiler only marginally increases the amount of thermal energy extracted from the fuel if compared to a smaller one, and this increase is largely outweighed by the losses caused by separating generation and use and by requiring the heat to be transported. After all, in a household furnace even the wall losses end up inside the building and, if the goal is space heating, contribute to the useful effect. So we understand that - unlike what happens in electricity generation - the size of the machines does not save fuel, and obviously neither does the distance between generator and user. What conserves primary energy is the fact that large-scale connections allow to tap into heat that needs to be generated anyway, and would otherwise be lost (dissipated into the environment).

A detailed overview of heat generation for district heating is given in [15].

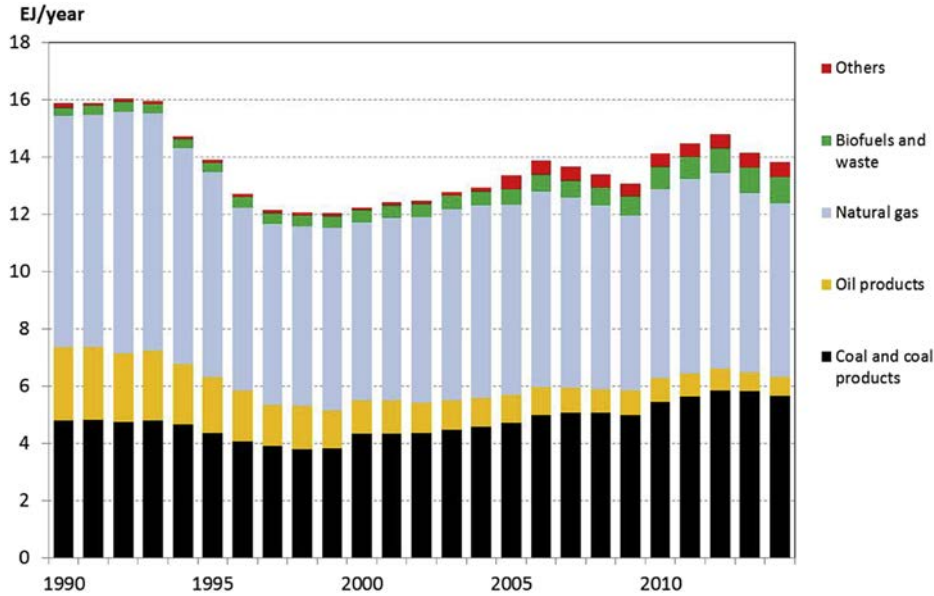


Figure 2.3: The primary fuels used in the DH sector in the world [73]

2.2.1 Combined Heat and Power

Most electric power today is generated in thermal stations which operate by transforming into mechanical work a part of the heat that flows from a hot source to a cold sink. Combined Heat and Power (CHP, also known in North America and Italy as "cogeneration") aims to use the heat that is discharged at the cold sink of a thermal power station. From thermodynamics, we know that for the power station to be efficient with respect to electricity generation the heat must be released at the lowest possible temperature. DH requires relatively low-grade heat to meet the needs of its customers and therefore is very much compatible with CHP, but we need to remember that the higher the heat quality, the larger the sacrifice in terms of electricity generation. As will be shown, the smaller the amount of electricity that is produced, the more similar a CHP plant will be to a heat boiler, which is a machine that does not gain much thermodynamically from being large and far away from the users, indeed quite the opposite.

As we know, the *electrical efficiency* of a power plant is ratio between the electrical power generated and the rate at which thermal power is consumed:

$$\eta_e = \frac{P_e}{Q} = \frac{P_e}{\dot{m}_{fuel} \cdot LHV} \quad (2.1)$$

a CHP plant also produces (we should say "makes available") thermal energy, and there will be a parallel, and subordinated, thermal efficiency:

$$\eta_t = \frac{P_t}{Q} = \frac{P_t}{\dot{m}_{fuel} \cdot LHV} \quad (2.2)$$

more typical of CHP is a third parameter, that defines the share of input energy that is transformed into the final products, known as *total plant efficiency* or *global energy utilisation*

ratio:

$$\varepsilon = \frac{P_e + P_t}{Q} \quad (2.3)$$

some authors question the use of a parameter where mechanical and thermal power are added together. If we want to treat the problem from the perspective of exergy, we could consider the absolute temperature T_i at which a stream of heat is provided:⁴

$$\varepsilon_X = \frac{P_e + \sum_i^N P_{t,i} \cdot (1 - \frac{T_0}{T_i})}{Q} \quad (2.4)$$

Exergy as a measure is often considered too abstract, distant from the need to evaluate the attainment of practical goals. With the goal of primary energy conservation in mind, we can try to compare CHP with a default solution where heat and electricity are produced separately, that will have a global energy utilisation ratio easily defined as:⁵

$$\begin{aligned} \tilde{\varepsilon} &= \frac{P_t + P_e}{Q_t + Q_e} \\ &= \frac{P_e(1 + \alpha)}{\frac{P_e}{\tilde{\eta}_e} + \frac{P_t}{\tilde{\eta}_t}} \\ &= \frac{P_e(1 + \alpha)}{\frac{P_e}{\tilde{\eta}_e} + \frac{P_e \alpha}{\tilde{\eta}_t}} \\ &= \frac{1 + \alpha}{\frac{1}{\tilde{\eta}_e} + \frac{\alpha}{\tilde{\eta}_t}} \end{aligned} \quad (2.5)$$

where α is the ratio of the heating to the electrical power. Similarly, we can define the total efficiency of the combined solution as:

$$\varepsilon = (1 + \alpha) \cdot \eta_e \quad (2.6)$$

the amount of energy that is conserved, relativised to the amount that would be used in a separate solution, is

$$i_R = \frac{Q_e + Q_t - Q}{Q_e + Q_t} = 1 - \frac{Q}{Q_e + Q_t} = 1 - \frac{\tilde{\varepsilon}}{\varepsilon} \quad (2.7)$$

which equals

$$i_R = 1 - \frac{\frac{1}{\tilde{\eta}_e} + \frac{\alpha}{\tilde{\eta}_t}}{\eta_e} \quad (2.8)$$

It appears that the energy conservation of a CHP plant also depends on the efficiencies of the competing conventional solutions, from a thermal and electrical standpoint, as could be predicted from the moment we started making a comparison. What is important to notice is the role of the parameters α and η_e : an "efficient" CHP plant tends to generate a significant amount of electric power compared to how much heat it provides, and turns a large portion

⁴ T_0 is instead the reference absolute temperature

⁵N. B.: we are defining with P the outputs, thermal and electric, and with Q the thermal inputs to produce each output or both

of the fuel energy into electricity. This is also predictable, since we know that electricity is significantly more primary energy-intensive than heat to produce.

There is, for each type of CHP plants, a threshold electrical efficiency only above which primary energy is conserved. With the increase in efficiency of condensation boilers and small heat pumps, new challenges are posed to DH operators who want to conserve energy and reduce emissions of pollutants [32].

Steam plants

The cold sink of a steam plant is the condenser. So in this case the condensing steam needs to heat the carrier fluid of the DH network. In an electric power station, on the cold side of the condenser there is a fluid, like sea or river water, even air in some rare cases, that is warmed as little as possible before being released into the environment or cooled via contact with the atmosphere in a cooling tower. In a station that provides heat to a district heating network, the steam has to condense at a slightly higher temperature than the network supply.

The pressure at the turbine outlet, therefore, could be significant (typically higher than atmospheric with 3rd-gen DH) and we shall have what is called a *backpressure steam cycle*, as opposed to the "vacuum-condensed" cycle of electric-only plants. This results in a very significant reduction of electrical efficiency. Some electrical efficiency can be recovered due to the return DH water "seeing" a large temperature difference between itself and the condensing steam. By splitting the steam in many streams, which expand until different condensation pressures, it is possible to reduce the temperature difference between the two sides of the heat exchanger: the incoming DH water (the "return" water) will receive heat from the lowest pressure steam first, and then move on to higher values of the outlet pressure. A balance needs to be stricken between the complexity of the system and the production of electric power.

In a backpressure steam plant, the total plant efficiency is quite high: the only losses are, theoretically, the ones caused by the enthalpy of flue gas at the chimney. On the other hand, there is a fixed proportion between the heat and the work produced at any given time and the electrical efficiency is strongly reduced.

A different configuration is the one in which the vacuum condenser is maintained, and with it the turbine low-pressure stages, but in parallel a higher-pressure DH water heater is installed (such a condenser, also in the case of a backpressure plant, is called a *calorifier*) where it is possible to deviate a part of the steam instead of sending it to the following expansion stages.

This structure is called an *extraction and condensation steam cycle*, and is somewhat akin to what is done in order to pre-heat feedwater to a power station boiler, only generally at lower pressures and with the possibility to control the flow of steam exiting the turbine.

Some of the steam must always reach the vacuum condenser in order to keep the low-pressure expansion stages lubricated and cooled. This produces a certain decrease in the total plant efficiency compared to the backpressure system, but on the other hand allows

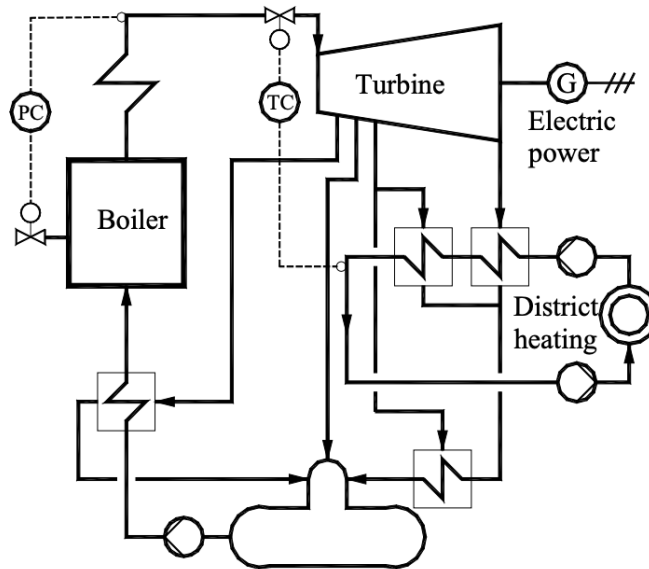


Figure 2.4: The structure of a simple CHP steam plant: the district heating water creates a "back-pressure" in the first heat exchanger of the loop, then steam is extracted from the turbine to supply additional energy. From [39].

a large degree of flexibility in the choice of how much electric power to produce and how much energy is to be left for water heating.

Generally speaking, it could be said that what characterises extraction and condensation plants is a larger degree of flexibility at the cost of some energy losses caused by condensation.

In some plants, for the sake of flexibility, there is even a line that takes steam from the high-pressure turbine stages or the boiler outlet and sends it to the calorifiers, which is inefficient thermodynamically but can help meet the demand for heat in the peak moments, during the coldest hours of the year.

Gas plants

In gas cycle power stations, a gas (atmospheric air, in essentially all industrial applications) is compressed, heated and expanded to produce work, and finally discharged into the environment.

This happens with continuous flow and steady-state parameters in a gas turbine, where an axial turbo-compressor compresses atmospheric air, which is then heated by internal combustion of the fuel, up to over 1500° C in more recent models, and then expanded in an axial multi-stage turbine until discharge at atmospheric pressure, and at a temperature which is typically between 350 and 500° C. With no steady-state, the same happens in an "internal combustion engine", or - more precisely - an intermittent combustion gas cycle, where a piston compresses the gas (where the fuel can already be present) which is then

ignited and expanded. The maximum temperature reached can be much higher⁶ than in a gas turbine with continuous combustion, which gives higher efficiency for a machine of the same power rating, at the cost of added complexity, with a higher discharge temperature as well.

Gas cycles work with smaller pressure ratios when compared to steam cycles, but the heat source temperature is significantly higher; the thermal efficiency is, in the case of gas turbines, somewhat lower than in steam cycles of the same capacity, but the internal combustion of the fuel and the open path of the gas, by allowing direct discharge into the atmosphere, eliminate the need for heat exchangers and make the power plant more compact, cheaper to install and simpler to operate [37].

As far as district heating is concerned, the most important characteristic of gas cycles is the high discharge temperature, which is very far away from the temperature of the environment. This means that with a gas-to-water heat exchanger virtually all the waste heat can be recovered, without reducing the electricity production. There are some limits to the recovery of heat: in this case, the total energy losses depend exclusively on the temperature of the flue gas at discharge, after heat recovery.

$$\varepsilon = 1 - \frac{P_L}{Q} \quad (2.9)$$

$$P_L = \dot{m}_{gas} \cdot c_{p,gas} \cdot (T_{flue,gas} - T_{amb}) \quad (2.10)$$

the temperature of gas at the final outlet needs to be higher than the temperature of DH return water, and needs to be high enough to guarantee dispersal at the chimney and prevent condensation of water, a phenomenon that could corrode the structures, especially if the fuel contains sulphur.

Heat recovery reduces the production of electric power only marginally, insofar as it increases the pressure at the turbine or piston engine outlet. It is important to design a heat exchanger with low pressure drop on the gas side, in order not to reduce the pressure ratio at the turbine. The largest gas turbines have electrical efficiencies around 40%, and the largest piston engines⁷ reach 50%: the large majority of the rest of the fuel heat content can be used for DH or other uses, at temperatures well above 100° C, which causes a larger saving of primary energy that can be obtained with a steam CHP plant.

The main disadvantage of gas cycles is the need to consume gaseous or liquid fuels to avoid clogging of the turbine. This condition decreases the range of fuels that it is possible to use and increases the unitary cost of primary energy.

2.2.2 Waste heat recovery

All industries and activities that need to cool a product, a byproduct or an intermediate substance and do not have an immediate on-site use for the heat are potential providers of

⁶nearly 4000° C in the Otto cycle, close to 3000° C in the Diesel cycle

⁷the power rating of the largest piston engines is one order of magnitude smaller than the rating of the largest gas turbines: this makes the former quite widespread in small CHP systems

district heat.

The experience of Nordic countries and especially Sweden shows that there are four main industries that can provide heat to DH: oil refining, paper and pulp, chemicals production and steel and metal making [15].

The city of Gothenburg⁸ uses waste heat from two nearby oil refineries as its second most important energy source, essentially as important as the combustion of municipal solid waste (27% and 28% of the heat provided respectively). It should be noted that, according to data provided by the city utility and the St1 refining company and quoted in [15], refining waste heat is the second source in the order of merit, after waste combustion and ahead of CHP, heat pumps and finally biomass (which although has a significant share of the supply, 16%, is used as a "last resort").

Other cities, notably Dunkerque in the Nord-Pas de Calais region of France, rely on the waste heat of steel-making facilities. In blast furnaces, coke coal is burned to extract oxygen from iron minerals, a process creating hot gas that is generally used in a steam power station to provide the plant with electricity. These steam power stations can be used as district heating CHP plants, like in Dunkerque; otherwise, the hot gas can be cooled to produce electricity and subsequently to produce district heat, until temperatures not much higher than the ambient levels.⁹

Smaller steel producers use electric arc furnaces, that also give off hot exhaust gas, which is often cooled in heat exchangers where water is evaporated. The steam that is obtained can be used for the internal needs of the facility, such as moving pumps or fans, but also to produce electric energy or heat for sale to a third party [42]. In the city of Brescia, an electric arc furnace facility for the production of steel uses exhaust gas to boil water, which in turn is used to provide heat to an organic Rankine cycle with a net installed power of about 1.8 MW; the input steam, that carries a power of 10.4 MW, can be used to heat district heating water when electricity demand is low or when, like during the winter, the DH network demands heat. It is interesting to notice that, while relatively constant "macroscopically" over the course of the year, heat production is strongly variable during the working day and a steam storage tank with a volume of 150 m³ and a capacity of 6 MWh is needed [57].

In the metallurgical sector, there are waste heat streams within a broad range of temperatures, for example from 30 to about 100 °C in copper smelting, that are complex to integrate in district heating: it is particularly useful to reduce the network return temperature [13].

2.2.3 District heating boilers

Some of the heat is produced in facilities that do not provide electricity or other products, commonly called Heat-Only Boilers (HOB). They can consume some sort of biomass, natural gas, coal or Diesel fuel, or electricity in those rare cases in which it is particularly abundant and inexpensive. In the European Union the direct use of fossil and renewable fuels is of lesser importance, but definitely not negligible since, as late as 2014, it accounted for about one fifth of the total DH production, with fossil fuels representing more than three

⁸sometimes known by the Swedish name Göteborg

⁹This is true from a theoretical standpoint, that does not consider the possible effects of condensation or the need for chimney effect, that often discourage complete heat extraction from exhaust gas

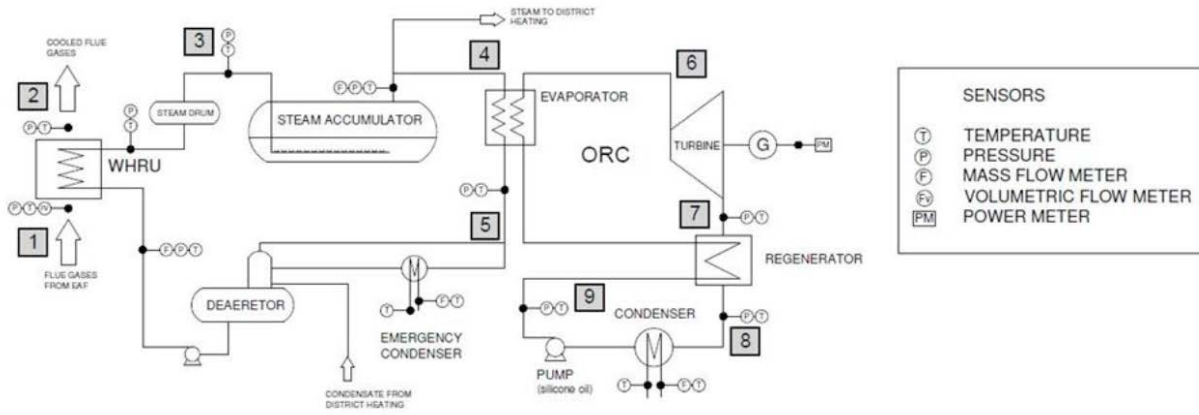


Figure 2.5: The complex system installed to recover heat and electricity from a steel production facility in Brescia, from [57]

quarters of the total energy supplied by direct combustion. In other contexts, direct fuel combustion is much more significant: it provides around 50% of the urban heat consumed in Russia and China, which raises its share of the world total to well over 40% [73].

Electric boilers are sometimes used to accommodate "excess" production of electricity. Nowadays, there is sometimes the need to make use of wind power on particularly windy days, and in Nordic countries DH has been investigated as a possible "production peak shaving" instrument. Historically, the same Nordic countries, in particular Norway and Sweden, developed electric boilers to make use of hydroelectricity in particularly rainy periods or to consume the excess power produced when a large station was inaugurated and it exceeded local electrical consumption. This has been true with hydroelectricity since the first half of the 20th century, and with nuclear power in Sweden in the 1970s. The desire to integrate electricity into the Swedish heating sector led to both the deployment of resistive DH boilers and to the first experiences with DH heat pumps [3].

As we have discussed in the CHP sections, heat-only systems do not entail a saving in primary energy, and are often used to match demand for heat when other sources with lower marginal costs are already exploited to their limit, or are unavailable because of an extraordinary occurrence like a malfunction. There is a large variation in heat demand over the course of the day and the year, and expensive (per unit of power) systems such as CHP plants and heat pumps cannot be sized for the highest level of demand.

2.2.4 Renewable and non-fossil sources

The most important source of renewable heat for DH is, by far, the combustion of biomass and waste [73].¹⁰ Another significant source of heat that can be considered renewable is geothermal power, especially in certain countries (Iceland, Turkey). Some small systems even use solar energy. Sometimes in legislation heat pumps are considered a renewable

¹⁰waste is often, but not always, considered a renewable source; the use of biomass itself is sometimes criticised for habitat destruction and depletion of forestry resources if not managed correctly

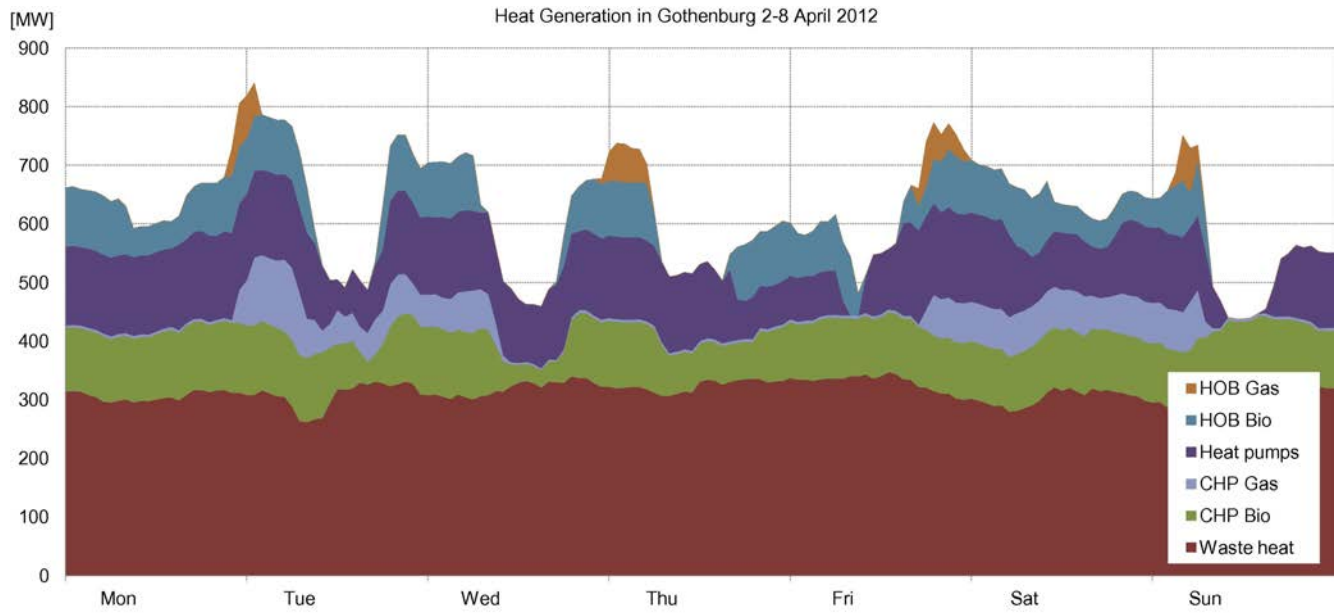


Figure 2.6: The sources of heat used for DH in Gothenburg during a mid-season week (courtesy of [30]). Waste heat is used as much as possible and HOBs meet demand peaks, with priority given to those fuelled by biomass

energy source¹¹ since they bring important benefits like the reduction in primary energy use and the absence of chemical reactions that can produce dangerous effluents.

Legal considerations aside, district heating can be considered, with reasonable certainty, renewable or non-fossil whenever it relies on electricity or heat that are produced by these kinds of sources.

Biomass and waste

Biomass and municipal waste are generally consumed in Rankine cycle power stations, that require special boilers to handle these fuels in pure form; as an alternative, they can be mixed with conventional fuels (typically coal) in more conventional steam plants.

To preserve the components of the boiler from corrosion, it can be necessary to lower the operating temperature. Particularly challenging are those fuels whose ashes melt at relatively low temperatures: "liquefied" ashes stain the boiler walls and heat exchange surfaces, causing severe corrosion and resistance to heat transfer.

In most boilers, heat transfer happens through the walls of tubes lining the walls of an insulated chamber where the fuel is burnt; often, especially in waste incinerators and biomass power plants, fuel is burnt in one chamber and then the fumes are cooled in a separate heat exchanger, to protect the water tubes from direct contact with thermal radiation from the flame. This also gives the opportunity to control the temperature with an auxiliary burner to prevent the formation of certain pollutants.¹²

¹¹although they are not even a source of energy

¹²municipal waste incinerators nearly always use a natural gas or oil "afterburner" to prevent the formation of dioxins, which happens below a certain temperature threshold

If the boiler is used to produce DH, the temperatures of the water circulating in the heat exchangers can be set to much lower values than those found in electric power production units, and electricity can be produced in an Organic Rankine Cycle, that is more suitable to lower pressure ratios and smaller power ratings.

The most common biomass burners are of the *fixed-bed* type, where there is a grate on which combustion takes place, that often moves horizontally to remove the ashes and receives air from beneath. In larger machines, the air flow from the bottom to the top is strong enough that the fuel burns while suspended, while mixed with a series of minerals like dolomite or limestone, called a *fluidised bed*. The bed acts as a thermal reservoir which "protects" the boiler operation from dis-homogeneous fuels and controls certain pollutants, especially by reacting with sulphur oxides. If the air flow is even faster, and the size of the fuel bits is reduced further, the bed leaves the combustion chamber together with the fumes, and is retrieved with a cyclone separator located downstream, before being sent back: a *circulating fluidised bed* or CFB combustor is obtained [15].

Other biomass burners use gaseous fuels, whether directly obtained by bio-chemical reaction (called "biogas", which is produced in significant amounts but is very difficult to transport to central plants) or by gasification of solid biomass, which is still a nascent technology.

The use of waste incineration as a heat source, and particularly its environmental impact, is the subject of intense research interest, since it can reduce carbon emissions but can produce non insignificant amounts of pollutants [6]; with biomass, the reduction in carbon emissions is more pronounced but so can be the production of particulate matter and NOx.

A significant barrier to the use of biomass for DH is the 'diluted' character of the energy source, which makes it complicated to collect in sufficient amounts for plants that serve entire cities: in fact, Italian biomass DH facilities have an average power rating of about 6 MW and are generally located in small municipalities [8]. It can be understood that in urban settings the combustion of municipal waste is often preferred as the resource is more abundant and its disposal is a service for which the heat producer can be paid (the fuel price, so to speak, is negative).

In northern Italy, a famous example of waste CHP plant is the one in Brescia, which has a thermal power of 160 MW and an electrical capacity of 84 MW [28].

Geothermal district heating

District networks can provide an opportunity to exploit geothermal resources, which are often concentrated and far away from cities. We shall discuss the cases in which the geothermal resource is available at a significantly higher temperature with respect to the environment; otherwise, its exploitation falls into the *heat pump* category.

High-enthalpy geothermal heat is often used to produce electricity and heat in combined plants. A description of the technologies used to provide electric power from geothermal sources would go beyond the scope of the present work, but a few remarks should be given to understand the integration of heat production.

The geothermal fluid is extracted from the borehole; if it is steam of a sufficiently high enthalpy, it can be directly expanded in a turbine; more often, it is first "flashed", *i. e.*,

separated in liquid and vapour phase, of which the latter is expanded (sometimes with a second flashing afterwards) and the former re-injected. If the fluid is hot water not much beyond atmospheric pressure, it can be used to heat a low-boiling fluid that performs a Rankine cycle to generate electricity.

If a secondary fluid is heated (which has the added advantage of preventing the "dirty" geothermal fluid from hitting the turbine blades), it receives most of the energy during the phase change. This means that the geothermal water is cooled down until a temperature above the boiling point of the working fluid, after which only a limited amount of heat can be extracted for use in the pre-heating line. The re-injected water can be therefore at a relatively high temperature, which causes a significant loss of energy. This phenomenon is often limited by using a working fluid with a larger ratio of specific heat capacity to latent heat¹³; otherwise, some energy could be recovered by transferring heat to district heating water, which has a return temperature not much above ambient levels [15].

A famous example of geothermal district heating is the Hellisheiði power station in Iceland. A mixture of water and steam is extracted from about 30 production wells, then flashed at a pressure of 10 bar; the steam is directly expanded in a turbine until the pressure of 2 bar, where it exists in two-phase form, which is flashed again to extract new power, until a pressure of approximately 0.22 bar. The fluid is finally condensed, which provides heat to the district network at temperatures up to about 57° C. More heat at higher temperature levels is taken from the separated water; the total electrical power, from seven production units, is 303 MW, while the thermal power is about 400 MW [24].

The city of Reykjavik also relies on heating supplied by heat-only geothermal plants drawing power from several different hydro-thermal fields at different temperature levels. Water is heated in boilers, mixed with cold water and finally brought to a common level of about 80° C on a standard day, before being directly sent to the users. After passing through heating and DHW heat exchangers it is at a temperature of about 35° C, and can be used to melt snow on the roads. It is interesting to remark that the geothermal production is very constant, and therefore tanks with a capacity of tens of thousands of cubic metres have been installed to meet the needs of the coldest days [22].

Solar district heating

Solar thermal energy is integrated into certain (relatively small) DH networks, generally up to 10 to 50% of the total heat demand. It is provided by large installations of solar thermal collectors, with ratings of up to 50 MW; the most commonly used technology is the flat-plate collector, which suits the relatively low temperatures of third and fourth generation DH [49].

Historically, one of the world's largest solar DH systems has been the one serving the town of Marstal¹⁴ in Denmark, with an installed power of 13 MW complementing an oil boiler and providing about 30% of the total demand, with the help of several hot water tanks, the largest of which has a volume of 10,000 cubic metres [15].

The experience of Danish district heating networks has shown that, without thermal storage, the contribution of solar energy cannot go beyond 5 to 8% of the total annual energy

¹³typically, organic fluids are used, in plant configurations known as ORC, Organic Rankine Cycle

¹⁴population: about 6,000

demand. With diurnal storage, this can be raised to about 20%, a threshold that requires seasonal storage in order to be exceeded. In order to obtain a solar penetration of 40%, it has been estimated that about 1.2 cubic metres of storage are needed for every square metre of solar collectors [64].

Nuclear district heating

The most common type of nuclear power plants, based on LWRs or "Light Water Reactors", are steam power stations with roughly 30 to 35% electrical efficiency. This provides the opportunity to exploit a large amount of low-temperature waste heat, as would be done in any backpressure or extraction-and-condensation steam cycle. To exclude the possibility of radioactive materials entering the DH network, it is recommended to include an intermediate cooling loop between the one that cools the reactor and the water circuit that carries heat away from the power station; it is included by default in pressurised water reactors (PWRs).

The large size of nuclear plants, made of several reactors with a combined thermal output that easily exceeds 10,000 MW, hampers the development of nuclear cogeneration, since it is not easy to find consumers for this much energy within a reasonable distance - a problem made worse by the tendency to locate nuclear power stations relatively far away from large cities. To move these amounts of heat, large investments are required, that are often not considered "safe" due to the political uncertainties surrounding nuclear power [35].

Nevertheless, several nuclear district heating projects exist, mainly in the countries of the former Soviet Union and Warsaw Pact; some others are found in China, Slovenia and Switzerland. We shall remember the largest such systems, that serve the cities of Zaporizhzhya (Ukraine, installed capacity of 1400 MW), Temelin in the Czech Republic and Sosnovy Bor in Russia (near Saint Petersburg, capacity of 290 MW) [36].

2.2.5 Heat pumps for district heating

As it is known, a heat pump is an inverse cycle, in which a fluid is evaporated, then compressed and condensed at a higher saturation, before being finally expanded, generally isenthalpically. In some ways, it is the mirror image of a power station, which means that in the design of heat pump heating (and cooling) there are unique complexities, for example related to the need to increase efficiency - *i.e.* reducing the consumption of mechanical work. However, heat pumps are the most efficient known way to obtain heat from electric power, and their use is seen as a key instrument to reduce carbon emissions in the heating sector.

With a certain degree of trivialisation, we can easily identify three main advantages given by the integration of heat pumps into a DH network.

The first is that larger machines can be cheaper to build and operate.

The second is the possibility to use warmer heat sources (and colder heat sinks in district cooling, sometimes even colder than the refrigerated buildings) like the sea, rivers or sewers, that are better exploited with centralised plants; it also makes possible to use low-temperature geothermal heat outside the boundaries of a city, in case there is not enough ground to use in the populated areas.

The third important advantage is that in a large plant it becomes possible to use a more challenging, but thermodynamically optimised, refrigerant. An example is ammonia: it is environmentally benign and has excellent thermodynamical and heat transfer properties, but it is flammable and toxic, which generally makes it unsuitable for individual household applications [18].

The first district heating heat pumps were commissioned in Switzerland in 1942, in response to the shortage of fossil fuels during World War II, in a system powered by three units with a combined heating rating of 5.9 MW [75]. An important stimulus to the development of the technology came from Nordic countries in the 1970s, the period also marked by the development of the third generation of DH - whose lower service temperatures are useful to make the most of inverse cycles. In Norway and Sweden, the authorities chose heat pumps as a more efficient way to use hydroelectricity for heating and reduce the consumption of chemical fuels during the oil shocks of the 1970s [3].

Hydraulic schemes

Due to the particular characteristics of heat pumps, that become less efficient as the temperature of the heat made available increases, different configurations are often put in place, modifying the traditional structure of district heating networks based on one centralised source of heat.

One possibility is to use large centralised heat pumps to heat water until a certain temperature, and then a combustion or resistive boiler to attain the temperatures required by the customers.

Alternatively, heat pumps partially heat the network water, which is then heated again by the users with combustion or electric boilers. Conversely, any source of low-grade heat can be used by the network to provide heat to the evaporator of individual heat pumps, in a "booster" configuration [70]. In this scheme, the network temperature can be lowered and brought close to the "fifth generation" levels, which greatly reduces energy losses and allows to install little to no insulation.

Sometimes, HPs move heat inside the network, by cooling return water at the evaporator and heating supply water before the customers. Generally speaking, the heating of supply water negatively affects the COP, but allows to avoid modifications of the heat generator; besides, if it also reduces the return temperature, it can favour integration of lower-grade waste or renewable heat [17].

Heat sources

The use of water as a source for heat pumps is favoured over air or ground because of the higher thermal capacity and conductivity of water and the evaporation temperatures that are higher than those allowed by ambient air. The ground is thermodynamically not inferior to water, since at a depth of just 10 metres we find a constant temperature year-round, equivalent to the average atmospheric temperature. However, the ground has lower thermal conductivity and as a result tends to exhibit non-steady state behaviour, which limits the amount of energy that can be extracted per unit of surface [29].

If we take into account the urban location of DH systems, a natural source of heat for inverse cycles can be *sewage* water, which is abundant in settlements and already warmed by human use. In Sweden, over 700 of the 1200 installed MW of large-scale heat pumps rely on sewage, producing roughly 2.5 of the total 4 TWh of heat. It is interesting to notice that "only" 47% of the about 1500 MW of historically installed district heat pumps relied on waste water: in recent times, many heat pumps have been decommissioned due to the higher electricity prices, but this has happened particularly with ambient water HPs (27% of installed power) and especially waste heat HPs (13%) [3].

As an alternative source or sink of heat, *seawater* can be used. The DH network of Helsinki draws about 4% of its heating energy and rejects about 33% of its cooling load in the Gulf of Finland through five heat pump units with a combined power of 84 MW, installed in 2006 [14]. In the Värtan neighbourhood of Stockholm, the installed power is 180 MW, and it is interesting to notice that the plant has been installed in 1985, with the original use of R22 as a refrigerant, which has since been replaced with R134a, in compliance with the stricter regulations on chlorinated and then fluoridated refrigerant enacted after the Montréal Protocol [52].

Seawater is, of course, one of the many forms of *surface water* that can be used, which include river or lake water.

It is not uncommon to extract heat from *groundwater*. In Milan, for example, there is a pair of large heat pumps serving the neighbourhoods of Canavese and Famagosta, with a combined heating power of 15.5 MW. The water is drawn from the ground at the temperature of 15°C and reinjected at 7.6 °C; it is necessary to send 1150 cubic metres of groundwater per second through the system. On the other side, district heating water is heated from 65 to 90 °C. The network supply temperature is more typical of the third generation of DH, fairly high for modern heat pump standards, which gives a COP of 2.68 and an electrical power consumption of about 5.8 MW. A much larger system has recently been conceived for installation in the municipality of Boulogne-Billancourt near Paris, with a heating power of 73 MW (provided at 80 °C) and a cooling power of 23 MW. The HPs used are two-stage machines with the possibility to extract power from both ground water and the cooling network; when the cooling effect is considered, COP leaps from about 2.7 to over 4.3. Other HPs in the systems can alternatively work to extract groundwater energy for use by the customers or to reject heat into the groundwater (in which case COP is over 5.1).

In certain contexts, *waste heat* can be used as a warm source, often not alone. This is the case in Aosta, where heat from a steel plant is used to pre-heat the groundwater until 18 °C. The gas used is R134a, and heat is supplied at 90 °C like in Milan, but (predictably) the COP is somewhat higher: around 2.9 [51].

2.3 Heat Distribution

The history of the infrastructure that bring heat to the consumers is as complex as the history of district heat itself. We will try to give a brief overview of historical advancements of the major network components, and finally of the current situation and state of the art.

2.3.1 Transmission pipelines

First generation DH used steam, which was transported inside steel pipes in turn contained inside tunnels called *ducts*, originally made of masonry and then of concrete slabs. Still today, steam is sometimes delivered at pressures that, while obviously not superior to the saturation point, are as high as 20 bar, with a temperature that can reach 300° C; this makes the heat quite expensive to produce but allows the survival of complex steam systems to this day, since high-pressure steam is useful for many applications beyond space heating. A typical energetic application of hot steam is the operation of absorption heat pumps for cooling. The pipes always have a mildly sloping configuration, and compensate the fall with a short vertical tract every 30 to 50 metres called a *condensate trap*, that collects the liquid water formed in the pipelines whenever there is a heat loss. The condensate is removed by a system of pipes parallel to the main one; in some systems, that have no return of the liquid water to the boiler, all the condensate ends in the sewers.

The hot water pipelines of the second generation were housed in concrete ducts as well, that also sloped in order to make possible the extraction of leaked water; from the sloped pipes, gases were extracted with valves. Around the water pipes there often was a layer of mineral wool which considerably reduced heat losses. In the ducts there were (and still are) thermal expansion compensators, structural supports and guiding elements to prevent excessive stresses and contacts between components. Large ducts with chambers and vaults to contain the valves and joints are prone to flooding, which can produce heat losses and corrode the pipes, especially if there are contaminants such as salt. Towards the end of the second generation, experiments were made to fill the ducts with protective materials such as cellular concrete or bituminous substances, that tended to be not watertight enough and did not offer particularly relevant cost savings.

The third generation of heating networks is marked by the *direct burial* of pipes; at first, the fluid carrier pipe was housed inside a double concentric surface, generally made of asbestos fibre cement and filled with an insulating material on the inside: a narrow gap was left between the inner cement surface and the pipe, to allow for expansion of the former. The established technology, however, is the *all-bonded* directly buried pipe. It generally consists of a carbon steel carrier pipe surrounded by cellular polyurethane, which is in turn encased in a "jacket pipe" made of high-density polyethylene. Expansion is dealt with by supporting the pipes with elastic materials like polymeric foams or lighter beds like gravel, or with shapes like Z- and U- curves. The flow of water is directed with *ball* and *plug valves* in small-to-medium diameter pipes and with *butterfly valves* in large-diameter pipes.

The tendency of the fourth and fifth generation of DH is towards the reduction of the need for insulation, with essentially uninsulated polymer pipes in the newest systems. It should be remarked that, particularly in the fifth generation, the small temperature difference be-

tween supply and return can cause large amounts of water to be moved, resulting in large pipe sizes [7].

Different configurations can be employed to connect the network, of which we can remember the most common:

- *single-pipe* networks only have a supply line, that provides water to the hot side of heating and DHW heat exchangers, or sometimes directly DHW; this way, a part of the energy is lost but it makes the installation of long-distance pipes significantly cheaper.
- *Double-pipe* networks have supply and return lines that go through customer heat exchangers; sometimes, there is an entirely separate network for DHW, that diverges from the larger (but used only in winter) heating network. In some systems, the return lines are used to supply energy to customers that require low-temperature heat (like greenhouses, swimming pools, roads to be kept from freezing).
- *Triple-pipe* networks are made of two distinct supply pipes for heating and hot water, and a single return.
- *4-pipe* systems have two independent networks with supply and return for both heating and DHW.

2.3.2 Substations

We call "substations" the facilities which group together all the devices needed to achieve the interconnection of the network and the customer plants.

The main machines contained within a substation will be, in the vast majority of cases:

- *heat exchangers*, to transfer the heat;
- *valves*, to regulate the flow of water on both sides of the heat exchangers and to reduce the network pressure so that it is compatible with the consumer heat exchangers;
- *meters*, to measure the amount of energy delivered.

There are different hydraulic connections at the substation level, that are related to the transmission configuration.

1. Network water can be directly delivered for use as DHW and space heating, with no hydraulic separation at all. This is an inexpensive solution since neither heat exchangers nor return lines (at least for DHW, often also for space heating) are required. On the other hand, much water and energy is wasted, especially when radiator water is rejected to the environment after a small temperature decrease. Moreover, the oxygen typically dissolved in water for domestic uses can corrode the network and user infrastructure.
2. It is possible to directly use DH water for DHW, and a heat exchanger to extract energy for space heating. This option eliminates the waste of water but is vulnerable to corrosion.

3. Alternatively, DH water circulates in radiators and heats DHW through a heat exchanger. This is a very common configuration as it represents a good compromise of low cost and infrastructural protections, as long as heating units must be compatible with the DH water, chemically and pressure- and temperature-wise.
4. Heat is often passed through heat exchangers to both the space heating and DHW circuits. This *indirect connection* configuration allows the maximum protection of consumer devices from corrosion and pressure transients; furthermore, it protects customers from noise and more importantly limits losses that are caused when peripheral pipes break. This configuration is favoured in networks that value reliability. It is generally found in the Nordic countries, as well as in the Verona network introduced in chapter 6.
5. Sometimes, the DHN warms an intermediate circuit, that releases heat to the indoor air and, by means of a new heat exchanger, to the DHW circuit. Scale formation is thus reduced, but the network is forced to provide water at a relatively high temperature, and the hydronic heating circuit temperature is also constrained.
6. Finally, it is possible to have an indirect connection in which an intermediate circuit is dedicated to DHW exclusively. This configuration is expensive but allows a great degree of protection of the drinking water from leaks of the DH heat carrier fluid.

Heat exchangers used in DH are of the *brazed plate* type, generally made of stainless steel, which have gradually replaced shell-and-tube models. In a brazed plate heat exchanger, the structure cannot be disassembled for cleaning; therefore, cities where the mains water is particularly 'hard' often prefer *gasketed plate* heat exchangers, which are bolted together and allow easier inspections and removal of scale.

The valves of DH substations can be either *self-operated* or *motorised*. The most common type of valve in the former category is the thermostatic one, moved by a gas which expands or contracts according to higher or lower temperatures of the fluid downstream; thus, it allows more or less fluid to bypass the heat exchanger on either side, decreasing or increasing heat transfer respectively. It could be said that there are two components to power regulation: the bypass valve and the bypass line, which is equipped with a one-way valve to prevent water backflow. Motorised valves have the same function but are operated by an electric motor. This solution requires an external power supply but gives the possibility to introduce a more complex control logic: typically, a PID controller can be used instead of a purely proportional one.

All substations have *meters* which evaluate the amount of heat transferred: they typically consist of temperature sensors upstream and downstream of the heat exchanger and of a mass flow rate sensor.

2.4 Flexibility: Needs and Possible Sources

It has been shown how many different sources of heat it is possible to use, and choices are made according to the peculiar location, structure and operation of each DH network. We

have also sketched a concise portrait of the diversity and complexity of heat sources. For a variety of reasons, such as the ones listed in [16] and generally for mechanisms that are easily understandable from the characteristics of heat sources discussed above, it becomes clear that it can be interesting to store heat produced in one moment for later usage.

We shall now provide some examples of the many situations in which it can be useful to *decouple* the production of heat from its consumption.

A common heat supply structure is the one where CHP plants provide the base heat load by working at or near full capacity, and heat only boilers are used to match demand peaks. HOBs consume more primary energy per unit of useful heat, and therefore it can be beneficial to limit their use by responding to peaks in consumption with stored CHP heat. In Turin, it has been proposed as a strategy to reduce primary energy consumption by up to 12% and costs by about 5% [68].

The use of CHP itself presents complexities related to the relationship between heat and electric power.

In a backpressure steam plant, for example, there is always a nearly fixed proportion between the amount of heating power and electrical power provided: this could be acceptable to a certain extent, since both the demand for heat and for electricity are higher during the day. However, it has been observed that electricity demand has two peaks during the day, the higher of which tends to happen in the late afternoon and evening (around 6 to 7 PM, depending on the region), while heat is demanded at the highest rate in the morning, around 6 to 7 AM. It could be therefore useful to store some heat during the day and the night to meet the heating peaks, as an alternative to only following the heat demand and "importing" and "exporting" electricity from the served area, which could be economically counterproductive since the imports would happen when the costs are higher.

In an extraction and condensation steam power station, the proportion of heat used to produce electricity can be changed with time, but all the same it can be difficult to follow the demand for heat at its peak, and it is preferable not to direct valuable boiler-outlet steam to the calorifier.

Heat pumps, on their part, are expensive devices that should ideally operate with high capacity factors and not follow too much the instantaneous variations of demand [18]. Besides, we know that a heat pump consumes electric power (or more seldom heat from a fuel or high-temperature steam) to extract heat from the environment. Thermal storage can allow the heat pump to operate in moments in which electricity is less expensive or the environmental conditions are more conducive to heat extraction or rejection: it has been found that thermal storage in hot weather can reduce the energy input of refrigeration [58].

If waste heat is used, it might come from an industrial activity that needs to work at all times, on triple shifts, and provides the same amount of heat during the whole year, quite similarly to geothermal wells. What often happens is that cooling towers are employed to discard most of energy when the network demand is far from the design rating [13].

At the opposite of this situation is the use of intermittent renewable sources like solar power, which is concentrated in the time of the year in which there is no demand for heating, and requires seasonal storage.

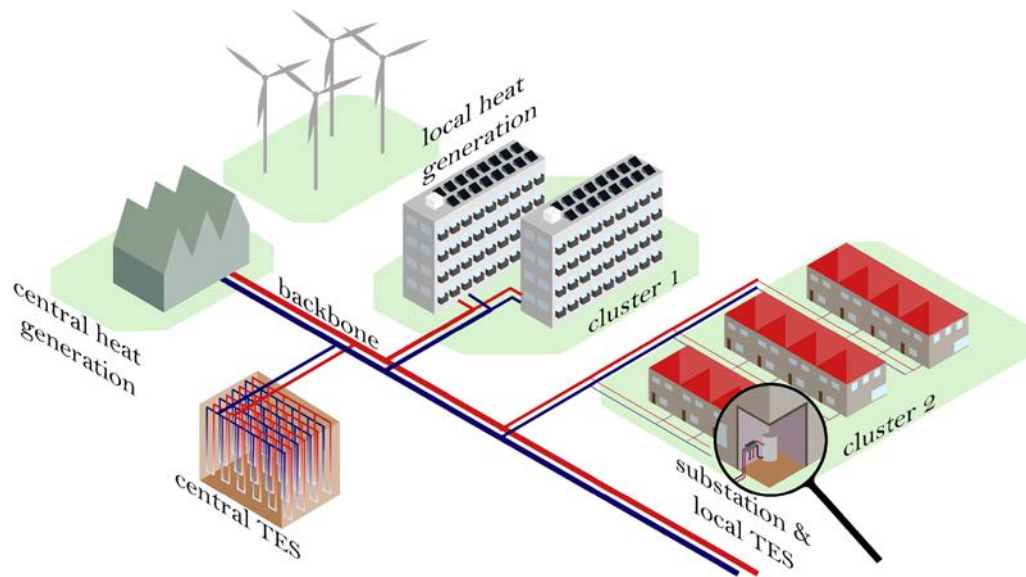


Figure 2.7: In newer and future DH networks, the need to include decentralised and renewable energy production arises, which in turn can rely on both centralised and decentralised energy reservoirs. Picture from [66].

For all these reasons, it appears that it is quite useful to have a certain reserve of heat to decouple in time the production of heat from its consumption. This can be obtained by using the water stored in the network itself, which is a reservoir of thermal energy, or by installing facilities built with this goal.

3. Thermal Storage in District Networks

As we have mentioned, it can be useful to decouple the instants in which heat is produced from the ones in which it is consumed. We shall see how this is accomplished, with particular attention to facilities that can hold heat reserves.

In fact, the instruments of flexibility in a DH network can be as manifold as the origins of the need for the flexibility itself. CHP plants can change the ratio of heat to electric power produced; flexible heat pumps have also been studied, as well as other power-to-heat technologies. The focus on thermal energy storage is due to the object of the present thesis and to the fact that it is a particularly inexpensive and technologically attainable form of energy storage [26].

3.1 Main Sources of Flexibility

A body that is at a different temperature from a standard point can be considered a heat reservoir. Therefore, we can identify several tools to achieve non-steady state operation, related to all the different masses that compose a district network, such as the transport and distribution networks, the substation heat exchangers, the building heating circuits and heating devices, the building masses, and dedicated storage devices installed at the network or customer level [19].

3.1.1 The network

The first thermal mass to exploit for flexibility is the network itself, which at any given time contains a large amount of water. The evolution of DH networks in non-steady state conditions has been studied quite extensively, often with the help of models similar to the one described in section 6.2. The network is modelled as a heat reservoir, whose charge and discharge are respectively analogous to absorption of heat from the generators and heat release to the consumers.

In Predictive Model Controllers (PMC), all the information available about the current thermal and hydraulic situation of the network, along with forecasts about heat demand and more generally operating conditions in a certain period of time in the future, is fed to an optimisation problem. The optimisation problem is solved with the help of a certain *objective function* to be minimised (or maximised) in the interval of time ahead. The solution of the objective function tells the operator what is the optimal way of running the system in the following period of time.

As an example: if we had the objective of minimising carbon emissions, the objective function could give as output the carbon emissions of the network by taking as input variables various forcing terms such as the heat demand of the consumer base, the weather, and the operating conditions of the non-controllable heat generators in every given instant. The optimisation problem consists then in setting the parameters of the objective function so that, at any moment, its value is the minimum. The parameters could be the operating conditions of the dispatchable heat generators and of the storage devices, and therefore the optimum set of parameters, in any given instant, would be the combination of generators that saves the most carbon emissions. The development in time of the set of controllable parameters is equivalent to the *optimal scheduling* (from the point of view of carbon emissions) of the generators.

A typical objective function is the operating cost, and the generators of heat are used and combined in order to reduce its value as much as possible at any moment.

After finding the optimal scheduling of generators (under the hypothesis that we are interested in this peculiar problem), the mass flow rates and temperatures, and more generally the hydro-thermal parameters that reflect the optimal generator operation, are fed into a physical model of the system. The physical model of the system, that includes its ability to store thermal energy, allows us to predict the evolution of the network parameters of interest in the immediate future interval of time. The parameters, such as for example the return temperatures, are used as new inputs for the function to minimise in the following time interval.

The network is therefore an energy resource that can be used to meet the consumer needs if it is necessary, provided that the energy has been supplied beforehand.

One possibility is increasing, to a certain extent, the amount of water circulating during the hours that precede the peak, generally with the help of expansion-managing devices. Thus, for the same amount of heat withdrawn by the customers, there is a smaller temperature drop on the hot side of the substation heat exchangers. This results in an increase of the network return temperature and consequently of the network average temperature. When heat needs to be discharged, it is sufficient to reduce the circulation of water in the network, which by the same mechanism described above causes the difference between supply and return to increase again and the network average specific enthalpy to fall [71].

It must be remarked that a return temperature rise can increase thermal losses to the environment and decrease the efficiency of the heat generators.

Another possible strategy is the increase in water temperature before the demand peak. This can be done by having the heat generators work at a higher power rating and provide warmer carrier fluid. A more widely discussed method is based on decreasing the amount of heat withdrawn by the substation heat exchangers before and during the demand peak, in order to increase the return and network average temperature.

Control of heat exchangers is at the heart of the use of networks for energy storage: evolutionary control strategies provide multi-faceted benefits. For example, they enable the heat provider to distribute heat equally when it is in short supply (like after a malfunction or during a challenging peak in demand), by reducing the withdrawals by customers that are

closer to the generating stations, which normally would "starve" of heat the users located further away [66].

There can be two important limits to the use of the network as a reservoir: the first in time, since the water in a DH network generally undergoes a complete turnover every one or two hours and therefore it is not possible to conserve the heat reserve for longer. The second limit is in the temperature increase that the network components can tolerate; ideally it should be limited to prevent the formation of significant thermal stresses and to limit the effects of fatigue [16][26][72].

3.1.2 Customers

The most important daily peak in heat demand corresponds to the moments in which domestic hot water is consumed, especially in the morning: it has been observed in the Turin DH system that the demand around 6 AM can be as high as twice the average during daytime and as four, sometimes six times the night-time average, which generally coincides with the demand immediately before the peak itself [20] [67].

It seems therefore reasonable that a major source of flexibility could be found on the premises of the customer, by acting on the dynamics of heat withdrawal from the network.

The flexibility solutions that involve the customer are collectively known as *demand side management* (DSM). It is apparent that DSM often requires to find a balance between the needs of the heat provider and those of the consumers.

The end users can help smooth peaks in demand by using energy more constantly, which results in an energy demand shift towards periods in which the producer finds it less expensive to provide. Sometimes the nature of the heat demand helps the generators: industrial consumption, for example, is much more constant and therefore with a user base with a large proportion of industries will demand heat in a way that improves the capacity factor of the DH plants.

If the customers are mostly residential, the network operator could encourage them to store energy by charging tariffs that are at any instant proportional to the production cost of energy, or that include a component based on the installed power. However, it has been noticed that pricing heat at different rates could create other demand peaks in the hours with the lowest rates. It is therefore important to maintain real-time communication between users in different areas and the network controllers, and to send different price signals to the different users at the same moment.

Buildings themselves can act as a storage medium, without dedicated facilities. Many researchers have studied *demand response* (DR) control methods, that essentially aim to disconnect the space heating load of a building from the network during peak demand hours. The main instruments to achieve DR are building properties such as insulation and thermal capacity, that give a certain degree of "thermal autonomy" [11].

A building automatically acts as a thermal reservoir when it is sufficiently insulated. As a benefit of insulation, the building can be heated and then it can use that same heat for

a relatively long time, which makes it tolerant to interruptions in heat supply. It has been found that a residential building with wall U-value in the order of $0.1 \text{ W m}^{-1} \text{ K}^{-1}$, in spite of somewhat lower thermal capacity when compared to more traditional buildings, exhibits a time constant of about 105 hours, which results in the ability to remain unheated for about 24 hours in $0 \text{ }^\circ\text{C}$ weather without a considerable loss of inhabitant satisfaction [33]. It becomes clear that this enables the customers to be disconnected for a short while, helping the network meet its demands.

Sometimes, the structural and plant design of the building, and not just the envelope conception, can be a resource to achieve a greater degree of independence and decouple thermal needs from the energy supply. This strategy is adopted in a family of technologies which collectively go under the name of *Thermal Mass Activation* (TMA). TMA can involve the use for energy storage of the building structure ("Building Core Activation"), the facades, the ceilings, or the ventilation systems.

A relatively widespread load management strategy is known as Thermo-Activated Building System (TABS). In TABS, the concrete structure (especially the horizontal floor slabs) is cooled during the summer nights with cold water pipes and then absorbs the thermal load of the daytime, slowing down the rate at which the rooms heat up; in the winter the heating load is less irregular but the mass of a building can still be heated at night to a certain extent, and rely mostly on the solar and activity gains during the day.

Otherwise, buildings can rely on Forced Air Activation,¹ where energy is charged and discharged from concrete masses by the movement of air flows. Certain forms of this technology are called Ventilated Concrete Slab (VCS) [43].

All buildings, regardless of whether they employ peculiar design solutions, and especially if they have a large mass per unit of floor area (as it is common in stone or masonry structures) accumulate heat, and knowledge of this property can help in the operation of a district heating network. The use of building masses is the object of significant research interest due to the fact that the cost of storage is essentially zero, and no space needs to be reserved for this special kind of heat reserve. It has been observed, however, that adding thermal mass to a building with the goal of shifting its heat demand can be counterproductive from an environmental and energy consumption standpoint because of the high energy and carbon footprint of concrete per unit of mass. It is advisable to only use the mass of the building that has already been provided for structural reasons [46].

Phase-change materials have also been studied for integration inside thermally activated structural components, or more generically inside concrete slabs; in the heating and cooling regime, energy needs to be stored at different temperatures, and therefore two different materials are used. It has been observed that there is the risk of worsening the energy efficiency of the system due to the resistance to heat transfer produced by a significant amount of PCMs, but it is thought that further research into these solutions is needed to evaluate their potential [54].

¹as opposed to hydronic activation, which relies mixtures of water and additives and is called "Hydronic TABS"

3.2 Dedicated Systems: Classification

There are several criteria on the basis of which thermal storage systems can be classified.

- By *medium*, or by the substance acquiring and releasing heat with a thermal, physical or chemical transformation. Different media result in very different values of energy density (from the high levels of some phase change materials to the relatively low ones of rock and concrete), and a wide variety of sizes.
- By *duration*. The time passing between the loading and unloading of energy can be months in seasonal storage, days in weekly storage, hours in daily storage and an even shorter span in hourly energy management peak shaving
- By *organisation*: thermal reservoirs can be centralised at the network level or scattered between many locations, like the different substations [21].

We shall give a brief overview of the main DH storage technologies within the general framework of a classification by medium, in order to gradually narrow the interest to the hot water tanks used in DH networks [2, chapter 50].

Storage media can be grouped in broad families according to their working principle: there are *sensible* heat storage media, whose temperature increases and decreases when being charged or discharged with energy, *latent* heat storage media, which undergo a phase change, and *thermo-chemical* media in which a chemical reaction occurs.

3.2.1 Sensible heat

The most common sensible systems are based on *liquid water*, accumulated in tanks that range in size from hundreds (or even dozens) of litres in households, to hundreds of cubic metres in tanks for daily and hourly balancing in DH networks, and up to hundreds of thousands of cubic metres in large reservoirs sometimes used for seasonal energy storage [21].

Let us remember that water has relatively high thermal conductivity and density, and the highest sensible heat capacity per unit of mass of all naturally occurring substances. It is liquid and therefore easy to move and to use as a heat transfer fluid as well, has low viscosity, is chemically inert, non-toxic, inexpensive and widely available. The main constraint on the use of water is the need to increase its pressure beyond the equilibrium with the atmosphere in order to heat it past 100 °C. More detail will be given about the use of hot water, that is the focus of the present work.

Other important sensible media are thermal oils and molten salts, that present the important advantage of remaining liquid at high temperatures with little to no need for pressurisation. Molten salts are used to conserve heat at temperatures above 400 °C [1]. On the other hand, these substances can present fire and corrosion hazards, and are significantly more expensive than water. Water is accepted as an optimal medium for energy stocks at temperatures

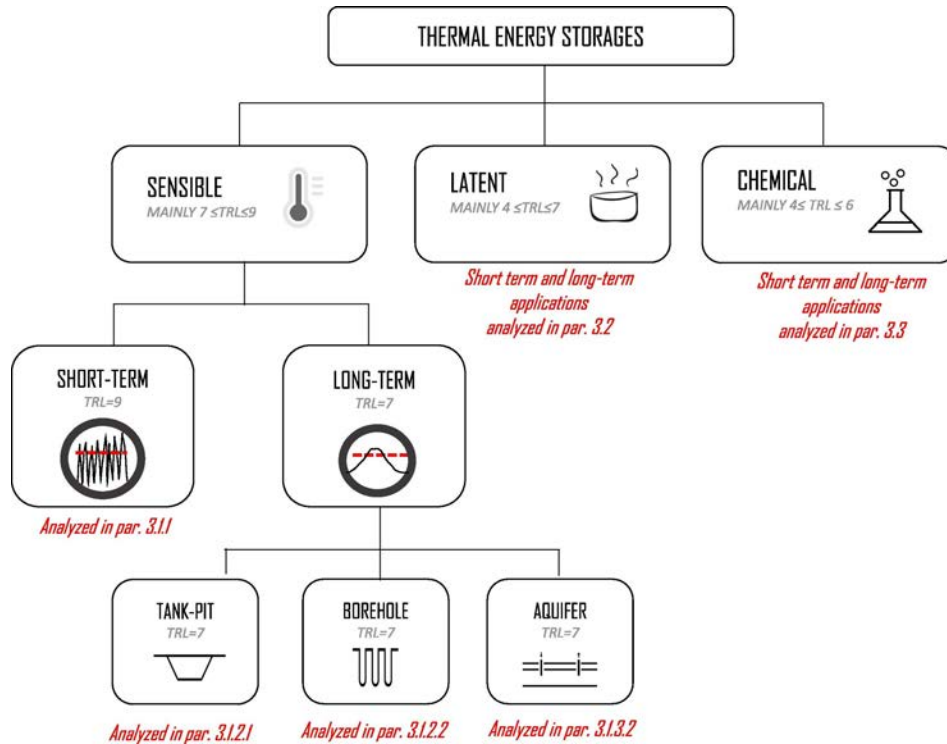


Figure 3.1: A classification of DH thermal storage facilities, as proposed in [21]

around or lower than 100 °C (more so when energy density and cost are important), which has been the thermodynamic grade of district heat since at least the "third generation" developed in the 1970s. Other common sensible storage materials are solid, like sand, gravel, rocks, minerals or concrete. They are generally used in packed-bed structures, with a liquid or gaseous heat transfer fluid adding or removing the heat. Solid materials also have temperature limits beyond which chemical degradation and erosion can occur [1]. More will be said on the facilities that exploit sensible storage in minerals of the ground in section 3.2.3.

3.2.2 Latent heat

Systems have been studied that rely on *phase change materials* to perform what is called *latent heat storage*. Phase-change materials are special substances that melt or evaporate when heat is provided to them and then solidify or condense while releasing energy. They can be divided into inorganic substances, organic substances and salt hydrates. The first group comprises salts like aluminium chloride or potassium carbonate and hydrates like lithium hydrate, that melts at 699 °C releasing 2.68 MJ per kilogram of mass. The temperatures of district heating are closer to the phase change points of inorganic compounds like paraffins and fatty acids - let us remember arachidic acid, that melts at 74 °C releasing "only" 227 kJ per kilogram of mass: much less than inorganic materials but equivalent to water when it is cooled down by more than 50 K [50].

The main advantages of PCMs are considered to be the significant energy density (indi-

cated at $100\text{-}300 \text{ MJ}/\text{m}^3$, or $30\text{-}80 \text{ kWh}/\text{m}^3$ for household materials, in [44]) and the fact that, while they are liquid and "loaded" with energy, they do not risk to lose exergy because of the mixing of colder and warmer fluid. PCMs, therefore, do not require specially shaped tanks, that in sensible storage need to be at least twice or three times as tall as their diameter, and as a consequence can be more suitable for household or substation installation. The advantage in installation has been reported in [63], a work in which a particular substance, namely Sodium Acetate Trihydrate, has been identified as acceptable for heat storage, with the main obstacle of its high cost.

Of course the original "phase-change material" used in cold storage, very widely and inexpensively, is ice, or ice slurry [2], whereas steam is also a substance that changes its phase and conserves heat in industrial and higher-temperature applications [1]. A different option could be the integration of PCM or *solid storage media* in systems that also use liquid substances to move, store and transfer energy [55].

3.2.3 Environment media: ground and groundwater

Other media are the ones from the environment, such as the ground or water in natural subterranean reservoirs.

- Borehole Thermal Energy Storage (BTES) is a technology that requires the drilling of deep boreholes, in which polymer water pipes are placed, along with a filling material. When the reservoir is filled with thermal energy, warm water from a solar plant or a heat pump condenser circulates in the boreholes heating the ground, and energy is discharged by heating cold water, typically during the winter.

An important advantage of BTES is the minimal amount of civil engineering works, the small occupation of space above ground and the relative simplicity when it comes to expansion of the reservoir.

On the other hand, ground energy storage suffers from low energy densities, in the order of 15 to 30 kWh per cubic metre, and is difficult to insulate, with the possible exception of the upper boundary surface. In order to reduce costs, heat exchangers can be designed with a horizontal rather than vertical geometry, which keeps them closer to the ground. This results in even greater space occupation and increased energy losses due to the larger surface-to-volume ratio. What is more, maintenance can be difficult or impossible once the system is built, since the buried pipes are almost beyond human intervention [9].

- The water table can be used for thermal energy storage as well. Warm water can be injected in the summer, and then replaced during the winter with cold water, in the systems that rely on Aquifer Thermal Energy Storage (ATES). Extraction wells are typically located at a distance in the order of magnitude of 100 m from the injection. The temperature difference between cold and warm water is relatively small: the former is at 5 to 12 °C, while the latter is at around 15 to 30 °C [61]. As a result, these systems often work together with reversible heat pumps that extract heat in the winter

to increase its thermodynamic grade and "produce" the warm water in the summer. To design such systems, it is necessary to know the speed and direction of the movement of the water table.

Despite the low temperature differences, the presence of water results in a significant energy density gain compared to BTES systems: it is possible to attain values of 60 to 80 kWh per cubic metre [9]. The second main advantage of this technology is the low construction cost, since no engineering work is needed besides the drilling of the wells.

The temperature differences need to be small because ATEs facilities are uninsulated: it is very difficult to stop the water table from moving, and therefore warm (or cold) water will tend to mix with ambient water over long periods of time and temperature gradients tend to become less and less steep. A particularly significant instrument for the control of thermal losses is the large size of reservoirs, with the goal of reducing the surface-to-volume ratio.

Heat losses are often considered the main obstacle to the use of ATEs; other drawbacks are the limitations on the choice of possible locations and the risk of contamination of the groundwater. It is necessary to find an underground volume of permeable material containing a water table and limited above and beneath by layers of impermeable rock. In most countries, permits are needed to extract or alter the temperature of ground water, and there are often limits to the temperature difference between extraction and reinjection [23].

The most important systems to store thermal energy in DH networks, at least from a quantitative standpoint, however, are known as Pit or Tank Thermal Energy Storage (PTES, TTES). These storage facilities are based on accumulating water in purpose-built structures at temperatures that are as close as possible as those used for heat supply in the system, while ATEs and BTES systems conserve heat at lower temperatures, that are closer to the environment, so that they often work together with heat pumps [9].

3.3 Hot Water Storage

The tanks used for hourly and diurnal storage constitute the main object of the present work.

They belong to a wider family of *stratified* storage reservoirs, in which the temperature is relatively high and there is a strong temperature difference between the top and bottom region, that must be maintained. The two main types of storage systems in this family go under the name of "Pit" and "Tank" Thermal Energy Storage.

- Pit Thermal Energy Storage (PTES) systems represent the main strategy for DH seasonal storage, for example in the networks with a large proportion of solar energy. A PTES facility is built by excavating the ground to form a large empty space in the shape of a truncated inverted cone, or inverted pyramid, which is then lined with a watertight material like polymers, cement, or bentonite, and covered with an insulated vaulted surface, that either floats or is supported by pillars or a filler solid

material like gravel [45]. The sheer *volume* of these chambers is one of the main characteristics of PTES: it is in the order of hundreds of thousands of cubic metres, or one order of magnitude larger than the largest reservoirs of the 'tank' type.

The storage medium is typically not pure water, but rather a mixture of water and sand or gravel, introduced for structural reasons. The higher the share of solid materials, the smaller the energy density, which at around 30-50 kWh per cubic metre is intermediate in the hierarchy of hot water storage.

The perimeter walls of a PTES tank are sloped², which means that the surface occupied by the top can be significant and the design and civil engineering works are sometimes quite challenging, especially with respect to the cover. What is more, maintenance is nigh impossible.

- Tank Thermal Energy Storage (TTES) relies on steel or pre-stressed concrete structures built in large part above ground³, with volumes ranging from hundreds to tens of thousands of cubic metres.

This type of basins is thought to have the highest energy density, typically around 60-80 kWh per cubic metre. Another advantage of TTES is their civil engineering characteristics, more akin to a 'tall building' than it is the case with PTES, which gives more freedom in the design phase and allows to take up a smaller surface area. The important height of such structures allows the greatest degree of thermal stratification, and they can be built in such a way as to extract or inject large amounts of energy per unit of time. Furthermore, inspection and maintenance is greatly simplified.

The main drawback of the technology is the relatively high installation cost [9].

- A third family of higher-temperature reservoirs is called Cavern Thermal Storage Systems (CTES): in this case, the storage tanks are entirely built underground to withstand fluids at high temperature (up to the order 200 °C) and pressure (dozens of atmospheres). CTES is not widely adopted yet, and is believed to be useful for electric power storage rather than the needs of district heating [45].

3.3.1 TTES: classification

Generally speaking, a first discrimination of DH tanks can be based on the pressure levels of the fluid they contain.

- An important family is composed of *pressurised tanks*, which are, as it is easily imaginable, tanks where water is stored at higher-than-atmospheric pressure, typically in equilibrium with the network supply pressure.

The tank is linked via a simple line to the network supply, and via two lines with throttling valves to the network return, at the suction and discharge of the circulator pump. The network supply connection is used for both charging and discharging the hot water, while the return pipes are used to inject and withdraw colder water, from

²the slope is only 26° in the reservoirs of the town of Marstal in Denmark [9]

³in which case are sometimes referred to as *freestanding TTES*, perhaps the favoured configuration in the DH sector, where ease of access for maintenance is often valued.

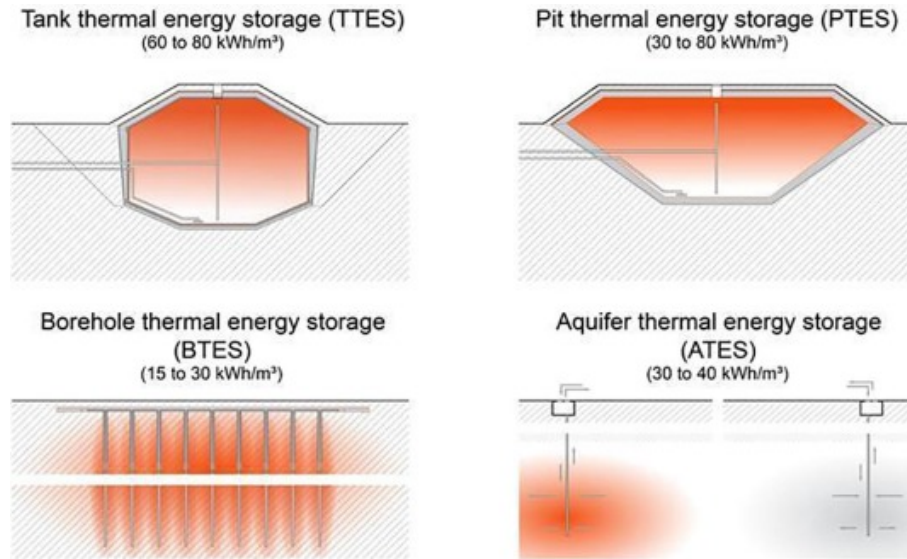


Figure 3.2: The main types of underground heat storage facilities, from [59]. Tanks are often built overground or "freestanding"

the pump outlet and inlet respectively, and during discharge and charge respectively [15].

The main advantages of pressurised tanks, that can be as large as 50'000 cubic metres, are the relative hydraulic simplicity, the possibility of accumulating more energy per unit of volume (since they can hold water at temperatures above 100° C), and their effectiveness at balancing flow rates in the network with no need for pumps or regulated valves. On the other hand, pressurised tanks entail disadvantages such as higher costs due to the more complex structures needed for the high values of pressure and temperature, and the reported difficulty at being used as a network pressure control [15], [4].

- The other main group of reservoirs is *atmospheric tanks*, that store water at atmospheric pressure, even if their depth is such that the pressure can be significantly higher than one atmosphere at their bottom.

To accumulate water at relatively low pressure, the connection lines with the network supply (which is used in discharge) and with the network return (used for charging) are equipped with a pump in parallel with a throttle valve and in series with a no-return valve.

Atmospheric pressure structures are easier to build⁴ and can be used as regulators of the network water volume. Conversely, these reservoirs accumulate less energy per unit of volume and are sensitive to geodetic variations inside the network: if they are at a similar altitude to the rest of the system, they can be used to balance flow rates, but if the DH system spans many different altitudes the pressure needs to be carefully managed with valves, pumps and expansion vessels. Moreover, the pressure

⁴sometimes they can be built for other purposes and then converted [15, p. 254]; however, it has been noticed that the cost savings are not significant because of the need to clean up the previous fluid, and the thermal performance can turn out to be not fully satisfactory [9].

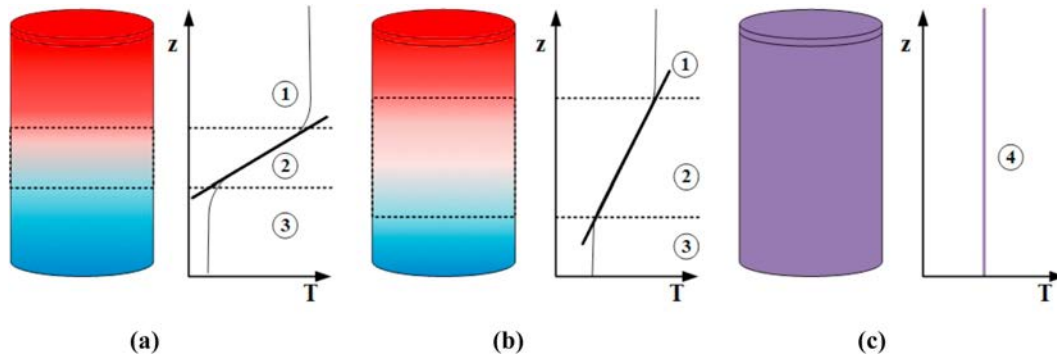


Figure 3.3: The three reservoirs shown contain the same energy but different levels of exergy, so that the third one is essentially useless. From [9]

difference needs to be bridged with a strong electric energy consumption [47].

Pressurised tanks can be divided in two categories according to whether they perform pressurisation of the rest of the system [47]:

- tanks *with a gas buffer* can be used to control the system pressure and compensate brisk volume variations, with the help of a "bubble" of air or nitrogen;
- Tanks *without a gas buffer* are entirely filled with water, and the network requires a separate, dedicated vessel to manage its pressure.

3.4 Tank Thermal Storage: Structure and Organisation

A typical DH storage tank is a steel cylinder that contains hundreds or even thousands of cubic metres of water. To ensure stratification, it must have a relatively high ratio of height to diameter. These tanks are generally nearly or completely full, with both water for network supply and water that comes from the network return. It is of vital importance to prevent the warmer water for supply to the customers from mixing with the rest of the liquid, which would conserve the amount of energy but destroy exergy and reduce the thermodynamic quality of the heat provided. This is the goal of stratification: let all the cold water move to the bottom of the tank, and all the warmer water to the top.

The design of TTES systems is essentially based on averting two main kinds of losses (while minimising cost): *energy losses* caused by heat transfer through the external surface, and *exergy losses* caused by energy transfer inside the tank.

It has been observed that in unmixed water tanks it is possible to identify two regions of relatively homogeneous temperature that correspond to the two main temperature levels of the tank content, separated by a region called a *thermocline*. The thermocline is comprised between two horizontal surfaces separated by a distance that is reported to be measured in the tens of centimetres ([2], [74]). It is lowered by the injection of hot water, while it rises when hot water is withdrawn. Nearly all the vertical variation of temperature in the tank

happens in the thermocline, and this makes it a volume that is not usable for the purpose of storing heat.

In summary, there are two important criteria in the hydraulic design of a cylindrical hot water vessel: the water must not mix and therefore cannot be stirred, and the thermocline must be as narrow as possible to increase efficiency [2, ch. 50].

3.4.1 Hydraulic connections

There are many different ways to connect the storage facility with the rest of a district network.

- *Direct connection systems*, also known as *open systems*, are tanks in which the DH distribution water is directly stored; charging and discharging are performed with a mass stream that is respectively injected and extracted via one or two pairs of ports. If there is only one pair of inlet/outlet ports, the two operational phases must be performed at separate instants in time, while with two pairs of ports (a configuration sometimes said to have "dual loops") charging and discharging are independent of each other. Open systems, where the heat transfer fluid also acts as a storage medium,⁵ are often preferred in Italian DH networks[4] [47].
- In *indirect connection* or *closed* systems, the heat transfer fluid and the storage medium remain separate, and energy is transferred through the walls of a heat exchanger, typically an immersed coil. Charging and discharging can be performed with a single coil by reversing the mass flow direction, or independently with two immersed coils. With closed systems it is easier to separate the pressure levels of storage and network, and to use different storage media. What is more, separating the heat carrier fluid with a heat exchanger wall helps maintain the water still and reduces the risk of stirring and mixing different temperature levels [25]. On the other hand, the heat exchangers are more expensive to install and maintain and heat transfer degrades the thermodynamic quality of energy.
- *Hybrid systems* use both direct injection and immersed heat exchangers. There are configurations in which charging happens via heat exchangers and discharging is operated through the inlet/outlet ports (sometimes called CO systems⁶) and configurations in which the reverse happens (OC systems) [56].

Multiple tanks can be connected together:

- in *series*, when the bottom of each tank is connected with the top of the following one: this way, the warm fluid expands into a new tank once it has completely filled the previous one.

⁵sometimes, not as the only storage medium, since they can contain a solid or PCM filler to reduce costs or increase power density

⁶"closed-open"

- in *parallel* when the tops of a number of tanks are connected together, and so are their bottoms; the one advantage of this configuration is that it allows more flexibility when it comes to finding space for these structures [9].

3.4.2 Geometric design

The behaviour of water inside stratified containers is the subject of detailed analytical and numerical simulations, and is also studied experimentally; let us report on some of the most commonly found results in the literature.

To prevent the water inlet from mixing the tank, we must design the geometry so that gravitational effects prevail over kinetic phenomena; remembering the Froude number,

$$Fr = \frac{w}{\sqrt{g \cdot L}} \quad (3.1)$$

it is generally considered that it must be kept to low values, ideally below 1 (according to [41], quoted in [2]).

Besides, the Richardson number, evaluated as

$$Ri = \frac{g}{\rho} \frac{\frac{\partial \rho}{\partial z}}{\left(\frac{\partial u}{\partial z}\right)^2} \quad (3.2)$$

should be prevented from going below 0.2 everywhere in the control volume, and ideally, if kept to values around 10, stratification could be produced quite independently of the shape taken by the inlet water stream [25].

In simplified representations, water flows through ports on the lateral walls of the tanks. In reality, water is injected and extracted with specialised components called *diffusers* (whether they perform one or the other function). These are of critical importance to reduce the speed of the fluid, with the goal of avoid impingement of the water flow on the boundary surfaces, which can generate turbulent movement of the liquid and vortices that mix together the different temperature layers [65]. The most common shape they take is the one of pipes that "run around" a horizontal section of the tank, close to the top and the bottom, and are open on one side, typically the inferior one, so that water passes through a longitudinal slot or series of holes, typically taking up a 90 to 120 degree section of the pipe circumference [2].

Other important design choices to consider in order to conserve the stratification are:

- the location of "ports" (diffusers) inside the tank. They should be located as close as possible to the tank ends, to avoid injecting warm water into a cold layer (or the other way around); this is particularly true with respect to inlets [25],[9].
- The insertion of horizontal *baffle plates* to separate the fluid layers.
- The conduction through tank walls: it has been observed that a particularly thick layer of structural material can transport heat from one region of the water to another [25].

The structure of a DH tank essentially consists of a series of prefabricated components, assembled on the construction site to form a large cylinder. The two most common materials are steel and pre-stressed concrete. It is also quite common for the main structure to be lined with a layer of stainless steel, generally facing the water. The natural purpose of this layer is preventing the corrosion of the main structure, and, especially in the case of concrete tanks, preventing leakage and vapour transport. When leaks happen, the main effect is the degradation of the insulation layer that can cause a long-term energy loss, which is more important than the fluid loss itself [45].

The shape of the cylinder is generally advised to be such that the height is larger than its diameter. The values of the aspect ratio (height to diameter) encountered in the literature are typically between 2 and 3.5 [74]. This range of values is found in many large structures, but there are more than a few tanks, generally of the buried type, which are not as tall as they are wide - see table B.1 in the Appendix.

Around the cylinder, a layer of insulating material is wrapped. Common insulants include polyurethane, glass wool, expanded polystyrene, foam glass, and extruded polystyrene. Especially in buried TES facilities, the insulating layer is often thicker towards the top and thinner near the bottom - it roughly follows the temperature difference profile in the vertical direction. In freestanding TES, the insulation is in part provided by atmospheric air and the insulating layer can be significantly less cumbersome [9].

Outside of the insulating layer there is often a structure that protects the reservoir from precipitations, guarantees access for inspection and maintenance and "hides" it from the view of the public [4].

4. Modelling the Storage Tank

4.1 One-dimensional Models

There are many different types of storage tank models, with different degrees of complexity. For the purpose of studying the dynamics of water injection and extraction, and more generally the functioning of a tank and the details of its hydraulic design, three-dimensional models with CFD software have been developed [41] [74]. However, these models are too complex for examining the use of hot water tanks in the much larger context of a DH network.

Often, in large plants, the individual components and machines are represented by a single value of each parameter, whether it is extensive or intensive; in the case of a storage tank, the balance of energy and mass flows exiting and entering the control volume would yield, for every instant in time, a single value of the mass and enthalpy contained inside, and of course a single value of temperature, which would be an average for the whole tank. This would be called a *zero-dimensional* model. As common as zero-dimensional models are in the analysis of large energy systems, they do not take into account the gradients of properties inside components, which in the case of hot water reservoirs are a fundamental characteristic.

An average value of temperature, for example, tells us how much energy is contained inside a volume, but nothing about the thermodynamic quality of the heat that can be extracted; nor will it tell us about the mass flow rates needed to exchange a certain heating power. This is due to the fact that mass flow rates are inversely proportional to the temperature difference between the warmest and coldest regions, from which water is extracted and in which water is re-injected respectively.

For this reason, *one-dimensional* models are needed, which study the evolution of parameters along the vertical axis and provide a sufficient level of detail on the water situation. In one-dimensional models, there is no variation of properties in the horizontal plane of the Cartesian representation or, equivalently, along the radial direction if we represent the tank in cylindrical coordinates. Nevertheless, it should be noted that a properly one-dimensional model evaluates temperature at every height in the tank, in some sort of continuous function of z , that could also be too cumbersome to obtain and work with, even with the help of a calculator.

Quasi-one dimensional models have sometimes been retained as a compromise: they divide

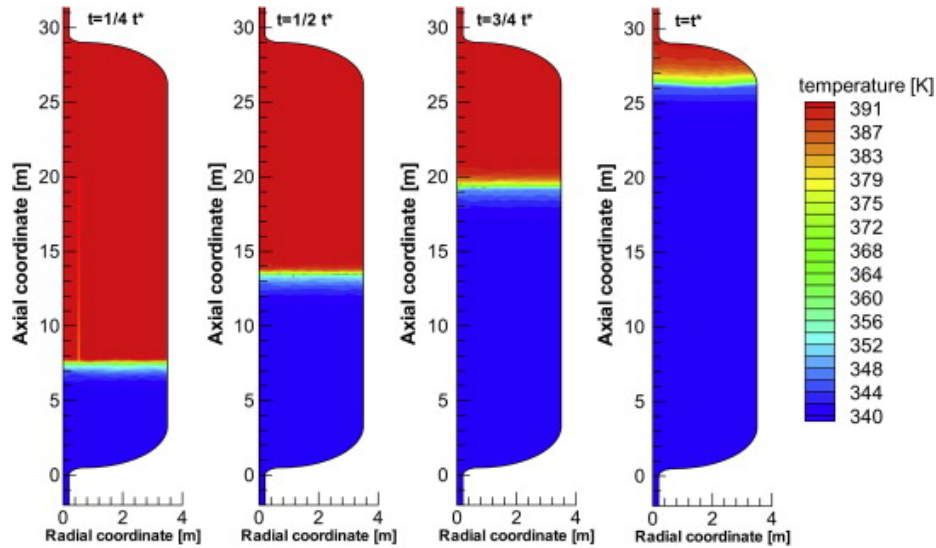


Figure 4.1: The distribution of temperatures inside a stratified DH storage reservoir being discharged, as found with a CFD model by Verda and Colella [68]

vertically the control volume in two homogeneous regions, separated by a *moving boundary* [56]. These models aim to represent, with approximation, the tank in its fundamental characteristic of being divided into two regions by a thermocline: the fundamental output variable shall be the height (or depth) z of the separation between hot and cold water. When the thermocline, simplified in the shape of a surface without volume, is lowered, the tank is being charged; when it rises, the tank is being discharged of its heat.

The fundamental concept at the basis of the tank model here described is the division into a certain number of homogeneous sectors, along the vertical direction. In other words, the tank will be divided by imaginary horizontal surfaces into volumes that each have a specific temperature and are therefore represented as lumped-parameters, zero-dimensional entities. We could name this the *hypothesis of discrete one-dimensionality*.

The tank communicates with the heat generator by means of direct injection of hot water in the top sector and extraction of colder water from the bottom sector. The connection with the heat distribution network, on the other hand, is obtained by extracting water to be sent to the users from the top sector and by injecting return water in the bottom sector.

There is also communication between the different sectors of the tank by way of mass flow and heat conduction through the water. It is important to remark that it has been demonstrated that, in a properly stratified tank, natural convection is negligible and mass transfer happens only by forced movement of the water, that also acts as the main medium of heat transport. Even conduction, which as we shall show is much less important than mass transfer, is more relevant than natural convection according to [27, chapter 9.1].

Lastly, we need to include in our model the flow of heat through the tank boundaries, to the environment. We evaluate it as the product of the surface separating each sector from the environment, the heat transfer coefficient and the difference between the temperature of the sector and a fixed environment temperature.

4.2 Fundamental Equations

Under the hypotheses discussed above, therefore, the main input variables shall be the temperatures of the two incoming flows: the generator-side supply and the distribution network-side return, which enter the top and bottom sectors respectively. Other necessary input variables shall be the mass flow rates associated with these temperatures, that are exactly equal to the mass flow rates being simultaneously extracted from the tank for return to the generator or supply to the network.

This is another important hypothesis: *mass conservation* in the tank control volume and in the generator and network circuits.

As a first approximation, we choose to assume a certain temperature difference between the injection and extraction of hot water on one side, and then calculate the mass flow from the thermal power Q that we want to transfer, with the well known formula:

$$\dot{m} = \frac{Q}{c_p \cdot \Delta t} \quad (4.1)$$

the temperature difference is maintained even when the actual temperature inside the tank changes, and as a result the mass flow rate is always proportional to the power that the reservoir is expected to deliver to the consumers or withdraw from the generator. In the codes that we want to develop, as will be shown, the actual power delivered or withdrawn is defined afterwards by using the calculated temperatures in the tank regions.

As we know, our model will be based on thermal energy balance equations. These are directly derived from differential equations such as:

$$\frac{\partial}{\partial t} \int_V \rho c_p T dV = - \int_S \rho c_p T \mathbf{w} \cdot \mathbf{n} dS - \int_S \lambda \nabla T \cdot \mathbf{n} dS \quad (4.2)$$

it is known that, generally speaking, partial derivative differential equations cannot be exactly solved, and even an approximate numeric solution is challenging for most computer programmes, since they exhibit strong non-linearity and cannot be easily computed into scripts. To allow solution with simpler mathematical tools, especially with linear algebra, the *finite difference method* is used.

In a finite difference model, all the derivatives are transformed into ratios called "finite differences". As an example, the derivative in time becomes the ratio of temperature increase over a small enough but finite amount of time. The gradient, meanwhile, becomes a series of ratios of temperature differences (in space) over distances and, in case of heat transfer, every ratio is multiplied by a finite surface and the products are finally summed together to obtain total conduction heat flow.

It is evident that we need to *dicretise* time and space, which explains the division of the tank into a certain number of vertical sectors, and the fact that the temperature is calculated in a series of successive time instants, separated by a certain duration of time. For the sake of precision, we are tempted to set short amounts of time and small distances in

space: however, doing so increases the work load requested from the machine. Conversely and perhaps more importantly, very "rough" discretisations can put the model at risk of hypothesis falsification. If the time interval between re-calculations were too long, for example, in the physical reality enough water would be injected into the tank to change the temperatures significantly, but all the while the model would have been calculating heat flows with the initial temperatures, which are the only ones it knows.

The degree of accuracy of a finite difference model is measured with a dimensionless parameter known as the Courant number. If we consider a phenomenon that propagates itself in space, for one reason or another, with speed u , and a model that evaluates properties at a distance of Δx at intervals in time separated by the time duration Δt , the Courant number (Co) will be calculated as:

$$Co = \frac{u\Delta t}{\Delta x} \quad (4.3)$$

the lower the Courant number, the more accurately the model will depict phenomena that move in space (like, in our situation, the expansion or removal of hot water inside a tank), with a lower risk of mistakes. It is generally thought that, in explicit models of physical systems, stability cannot be achieved if $Co > 1$ [69].

4.2.1 Tank sector energy balance

Let us finally write out the energy balance equations, in which we see the effect on temperature of the mass flows from the generator and the network, and of the heat transfer to other sectors and through the walls. In the first tank sector, the balance is of the type:

$$C_1 \frac{dT_1}{dt} = \dot{Q}_{mass} + \dot{Q}_{cond,bottom} + \dot{Q}_{cond,wall} \quad (4.4)$$

regarding the intermediate sectors of thermal capacity C_j , the equation is not much different:

$$C_j \frac{dT_j}{dt} = \dot{Q}_{mass} + \dot{Q}_{cond,top} + \dot{Q}_{cond,bottom} + \dot{Q}_{cond,wall} \quad (4.5)$$

and in the tank bottom:

$$C_n \frac{dT_n}{dt} = \dot{Q}_{mass} + \dot{Q}_{cond,top} + \dot{Q}_{cond,wall} \quad (4.6)$$

These balances can be developed as the generic:

$$\rho V_j c_p \frac{dT_j}{dt} = \sum_i \dot{m}_{j,i} h_{j,i} + \sum_k \frac{\lambda S_{j,k}}{\Delta x_{j,k}} \Delta T_{j,k} \quad (4.7)$$

Relatively to the first sector, it is reasonable to linearise the enthalpy function by introducing specific heat capacity c_p , and obtain an equation which can be inserted as a software command.

Let us define some variables, parameters and conventions:

- t is time and T is the temperature;
- ρ is the fluid density;
- V is the total tank volume;
- $\dot{m}_{d,in}$ is the mass flow rate entering the tank (*in*) from the distribution network (*d*);
- $\dot{m}_{g,in}$ is the mass flow rate entering the tank (*in*) from the generator (*g*);
- the *subscripts* $1 \dots j \dots n$ refer to the model nodes, while the *superscripts* 0 and 1 represent the beginning and the end of the timestep.

It is now possible to write, for the first sector starting from the top:

$$\rho \cdot V \cdot c_p \cdot \frac{T_1 - T_1^0}{\Delta t} = \dot{m} \cdot c_p \cdot T_{g,in} - \dot{m} \cdot c_p \cdot T_{d,in} - \lambda_w \cdot \frac{S}{\Delta z} (T_1 - T_2) - U \cdot A (T_1 - T_{amb}) \quad (4.8)$$

then for the intermediate sectors where, in first approximation, we only have heat transfer:

$$\rho \cdot V \cdot c_p \cdot \frac{T_j - T_j^0}{\Delta t} = \lambda_w \cdot \frac{S}{\Delta z} (T_{j-1} - T_j + T_{j+1} - T_j) - U \cdot A (T_j - T_{amb}) \quad (4.9)$$

There is another important phenomenon to be taken into consideration: the movement of fluid from one sector to another, that as will be shown acts as the most important means of energy transfer inside the tank. The internal mass flow rate will necessarily be equal to the difference between the incoming water flow in the top sector and the outgoing flow rate in the same sector, under the convention of having positive values for the flow direction from the top sector downwards.

$$\dot{m}_{net} = \dot{m}_{g,in} - \dot{m}_{d,out} \quad (4.10)$$

Under the effect of this phenomenon, the equations shall become:

$$\rho V c_p \frac{T_1 - T_1^0}{\Delta t} = \dot{m} c_p T_{g,in} - \dot{m} c_p T_{d,in} - \dot{m}_{net} c_p T_1 - \lambda_w \frac{S}{\Delta z} (T_1 - T_2) - U A (T_1 - T_{amb}) \quad (4.11)$$

$$\rho c_p \frac{T_j - T_j^0}{\Delta t} = \dot{m}_{net} c_p (T_{j-1} - T_j) - \lambda_w \frac{S}{\Delta z} (T_{j-1} + T_{j+1} - 2T_j) - U A (T_j - T_{amb}) \quad (4.12)$$

The geometric parameters V , S , A and Δz are fairly straightforward once the tank volume and height, and the number of model sectors, are set. The fluid properties c_p , ρ and λ_w are quite constant in the temperatures considered but can be provided at every timestep by calling a database such as REFPROP (the option chosen, thanks to [34]) or with a polynomial. The global heat transfer coefficient U could instead require some justification. It can be estimated, relatively to the inner tank surface, with the well known formula :

$$U_i = \frac{1}{\frac{1}{\alpha_i} + \frac{r_i}{\lambda_m} \ln \frac{r_1}{r_i} + \frac{r_i}{\lambda_{is}} \ln \frac{r_{ext}}{r_1} + \frac{r_{int}}{r_{ext} \alpha_{ext}}} \quad (4.13)$$

where λ_m is the thermal conductivity of the structural material and λ_{is} is the conductivity of the insulation. r_1 is the radius of the cylindrical surface separating structure from insulation

[5].

The most challenging coefficient to define is α_i , or h_{in} , that regulates heat transmission to the inner tank wall by natural convection. It needs to be calculated for every tank sector by starting from the widely known formula for the Rayleigh number:

$$Ra_D = \frac{g\beta|T - T_s|D_i^3}{\nu\alpha} \quad (4.14)$$

which allows us to find the Nusselt number:

$$Nu_D = CRa_D^m \quad (4.15)$$

and finally the inner natural convection coefficient:

$$h_{in} = \lambda_{water} \frac{Nu_D}{D_i} \quad (4.16)$$

the coefficients C and m are found in [40]. A major issue with the use of these formulae is that they take as input the temperature of the tank wall (T_s), which needs the water heat transfer coefficient to be calculated. In our model, to avoid the complexities introduced by recursive calculations, the wall temperature is calculated at every timestep with the heat exchange parameters found in the previous one, starting from an ideal situation in which the tank wall is isothermal and slightly colder, on average, than the water inside the reservoir. If the thermal resistances of the tank structure and the environment are grouped together and determine a heat transfer coefficient called U^1 , we can define the new global coefficient as:

$$U_{tot} = \frac{1}{\frac{1}{h_{in}} + \frac{1}{U}} \quad (4.18)$$

and, after evaluating the new values of the node temperatures, with these coefficients the inner wall temperature is immediately re-calculated:

$$T_s = T_{amb} + \frac{U_{tot}}{U}(T - T_{amb}) \quad (4.19)$$

The temperature in each sector is calculated at regular time intervals: the energy flows discussed all happen, in our model, in steady state for a fixed amount of time, during which all the values of temperature and mass flow rate are the same of the initial instant. The energy balance in each time interval give new values of temperature, that along with the mass flow inputs of the following time interval will constitute the state of the system at the beginning of the new time interval.

There is therefore a third important hypothesis, that we could call of *instantaneous mixing*: the water newly injected or extracted is not able to change the temperature of the tank sector, and therefore its losses and energy outflow, until the end of the time interval.

1

$$U = \left(\frac{r_i}{\lambda_m} \ln \frac{r_1}{r_i} + \frac{r_i}{\lambda_{is}} \ln \frac{r_{ext}}{r_1} + \frac{r_{int}}{r_{ext}\alpha_{ext}} \right)^{-1} \quad (4.17)$$

4.3 Explicit Model

Our work started with a simplified model of a tank divided into a small, fixed number n of sectors (originally $n = 5$). Its initial temperature is represented by a vector called T_0 , and is one of five inputs:

- the temperature $T_0 = [T_0^1, T_0^2, T_0^3, T_0^4, \dots, T_0^n]$;
- the inlet temperatures $T_{g,in}$ and $T_{d,in}$;
- the mass flow rates $\dot{m}_{g,in}$ and $\dot{m}_{d,in}$;

first the mass flow rate from a sector to another is found;

$$\dot{m}_{net,0} = \dot{m}_{g,in,0} - \dot{m}_{d,in,0} \quad (4.20)$$

then the values of temperature at the end of a time interval, from the top sector to the bottom:

$$T^1 = T_0^1 + \frac{\Delta t}{\rho V c_p} \cdot \left[\dot{m}_{g,in,0} c_p T_{g,in} - \dot{m}_{d,in,0} c_p T_0^1 - \dot{m}_{net} c_p T_0^1 - \frac{\lambda S}{\Delta z} (T_0^1 - T_0^2) - U \cdot (A + S) (T_0^1 - T_{amb}) \right]$$

(4.21)

$$T^2 = T_0^2 + \frac{\Delta t}{\rho V c_p} \cdot \left[\dot{m}_{net} c_p (T_0^1 - T_0^2) + \frac{\lambda S}{\Delta z} (T_0^1 - T_0^2) + \frac{\lambda S}{\Delta z} (T_0^3 - T_0^2) - U A (T_0^2 - T_{amb}) \right]$$

(4.22)

$$T^3 = T_0^3 + \frac{\Delta t}{\rho V c_p} \cdot \left[\dot{m}_{net} c_p (T_0^2 - T_0^3) + \frac{\lambda S}{\Delta z} (T_0^2 - T_0^3) + \frac{\lambda S}{\Delta z} (T_0^3 - T_0^2) - U A (T_0^2 - T_{amb}) \right]$$

(4.23)

and so on, until the final section of the tank:

$$T^n = T_0^n + \frac{\Delta t}{\rho V c_p} \cdot \left[\dot{m}_{d,in,0} c_p T_{d,in} - \dot{m}_{g,in,0} c_p T_0^n - \dot{m}_{net} c_p T_0^{n-1} - \frac{\lambda S}{\Delta z} (T_0^n - T_0^{n-1}) - U \cdot (A + S) (T_0^n - T_{amb}) \right]$$

(4.24)

this series of values is recalculated for the end of the time interval of length Δt , and then used as a starting point for the following interval.

There is an important use of the temperature values: the evaluation of the thermal power injected or extracted from the tank, which depends on the (relatively fixed) mass flow rate multiplied by the specific heat capacity and the difference between the generator supply, or network return, temperature and the temperature of the bottom, or top, tank region. In other words, the outflow minus inflow temperature on the distribution side and the inflow minus outflow temperature on the generator side.

$$Q_{g,eff} = \dot{m}_g c_p (T_{g,in} - T^n) \quad (4.25)$$

$$Q_{d,eff} = \dot{m}_d c_p (T^1 - T_{d,in}) \quad (4.26)$$

In a numerical rendering of these equations using the computer programme MATLAB, the n equations are solved in sequence and, with the help of a `for` loop, for every successive interval of time, until the end of the simulation duration. To obtain this, at the end of each iteration of the `for` loop the new value of T^0 is set at T .

4.4 Implicit Tank Model

For the sake of compatibility with other software used to model the rest of the DH system (described in section 6.2) and in order to make the script convergence faster, the algorithm was then restructured to become *implicit*.

The n temperatures of the tank layers are each multiplied for the parameters that give the energy flows out of the related sector in the given time instant; the temperature vector T becomes the unknown quantity. The terms containing the ambient temperature, the inlet temperatures from generator and distribution network, and the temperatures of the layers at the beginning of the time interval, meanwhile, become the known part of the equation. All the terms that in each equation multiply the sector temperatures will become elements of a square matrix called \mathbf{A} , that is multiplied for the unknown vector to give the vector \mathbf{b} of the known terms, in a typical linear system:

$$\mathbf{A} \cdot \mathbf{T} = \mathbf{b} \quad (4.27)$$

Let us give an example for the first sector; for the sake of brevity, we shall first define:

$$C = \frac{\Delta t}{\rho \cdot V \cdot c_p} \quad (4.28)$$

$$G = \frac{\lambda \cdot S}{\Delta z} \quad (4.29)$$

the rewritten first energy balance equation

$$\frac{T^1}{C} = \frac{T_0^1}{C} + \dot{m}_g c_p T_{g,in} - \dot{m}_d c_p T^1 - \dot{m}_{net} c_p T^1 - G(T^1 - T^2) - U(A + S) \quad (4.30)$$

becomes

$$\left[\frac{1}{C} + \dot{m}_d c_p + \dot{m}_{net} c_p + G + U(A + S) \right] T^1 - GT^2 = \frac{T_0^1}{C} + U(A + S)T_{amb} + \dot{m}_g c_p T_{g,in} \quad (4.31)$$

and the j -th sector inside the tank is represented by an analogous equation of the type:

$$\frac{T^j - T_0^j}{C} = \dot{m}_{net} c_p (T^{j-1} - T^j) + G(T^{j-1} - T^j) + G(T^{j+1} - T^j) - UA(T^j - T_{amb}) \quad (4.32)$$

which can be rearranged into

$$(-\dot{m}_{net} c_p - G)T^{j-1} + \left(\frac{1}{C} + \dot{m}_{net} c_p + 2G \right) T^j - GT^{j+1} = \frac{T_0^j}{C} + UA T_{amb} \quad (4.33)$$

and for the final sector,

$$(-\dot{m}_{net}c_p - G)T^{n-1} + \left[\frac{1}{C} + \dot{m}_g c_p + G + U(A + S) \right] T^n = \frac{T_5^0}{C} + U(A + S)T_{amb} + \dot{m}_d c_p T_{d,in} \quad (4.34)$$

We finally arrive at the assembly of the matrix \mathbf{A} , where first we define:

$$k_{11} = \frac{1}{C} + \dot{m}_d c_p + \dot{m}_{net} c_p + G + U_{tot}(A + S)$$

$$k_D = \frac{1}{C} + \dot{m}_{net} c_p + 2G + U_{tot}A$$

$$k_{nn} = \frac{1}{C} + \dot{m}_g c_p + G + U_{tot}(A + S)$$

making it possible to write:

$$A = \begin{bmatrix} k_{11} & -G & 0 & 0 & 0 & \dots & 0 \\ -\dot{m}_{net}c_p - G & k_D & -G & 0 & 0 & \dots & 0 \\ 0 & -\dot{m}_{net}c_p - G & k_D & -G & 0 & \dots & 0 \\ & & & \vdots & & & \\ 0 & \dots & \dots & 0 & -\dot{m}_{net}c_p - G & k_D & -G \\ 0 & \dots & \dots & 0 & 0 & -\dot{m}_{net}c_p - G & k_{nn} \end{bmatrix}$$

while the known vector equals:

$$b = \begin{bmatrix} \frac{T_0^1}{C} + U(A + S)T_{amb} + \dot{m}_g c_p T_{g,in} \\ \vdots \\ \frac{T_0^j}{C} + UAT_{amb} \\ \vdots \\ \frac{T_0^0}{C} + U(A + S)T_{amb} + \dot{m}_d c_p T_{d,in} \end{bmatrix}$$

It needs to be remarked that the convention used for the sign and the position of \dot{m}_{net} refers to water flowing from a sector to the immediately *inferior* one. When, because of the evolution of heat demand, the flow through the ports on distribution side is larger than through the ports on the generation side, water flows upwards and therefore the mass balance equations are falsified.

The logic of MATLAB helps us with this eventuality; the solution is to introduce an `if` loop, where if the value of \dot{m}_{net} is negative, a different matrix \mathbf{A} is used where:

1. the sign of the terms containing \dot{m}_{net} in the diagonal are reversed;
2. the terms containing \dot{m}_{net} outside of the diagonal are moved along the line until they are in the position symmetrically opposite, across the diagonal.

It has been mentioned that our first-attempt equation systems have been assembled with a small and fixed number of equations; it was then decided to generalise for a tank with any number n of vertical sections.

To achieve functionality for any² number of tank sections, the matrices are initialised in the code by, at first, only writing lines 1 and 2, that are completed by a vector of zeroes of variable length in order to have n line elements in total. The first two lines are followed by a `for` loop that writes out the following $n - 3$ lines of code, with "filler" vectors of zeroes in the areas far away from the diagonal, and finally, outside the loop, by the n -th line of the matrix.

The matrices are inserted inside an `if` loop which is followed by a `for` loop that writes the vector **b**. In the final part of the forward path of the loop we find:

1. the line of code that solves the system, by finding the vector of temperature values satisfying the linear system composed above:
 $T=b \setminus A;$
2. the setting of the new values of T_0 for the next iteration, equivalent to the most recent result T ;
3. the lines charged with memorising into new vectors the newly found values of temperature, mass flows on the two sides, net mass flow and power effectively delivered to the customers and consumed from the generator.

These subsequent code sections are inserted into a `function` that is called in each iteration of a `for` loop in the main script, in order to calculate and memorise the data during the whole duration of the simulation.

4.5 Preliminary Results

As an initial example of use of the model, the mass flow from the generator to the tank top declines from a maximum value in six successive steps of the same duration, until in the last step no fluid enters the reservoir. The network, on the other side, always withdraws the same mass flow from the tank top layer.

We shall show the results of simulations with a different number of tank sectors, and different values of the duration in time of the whole experiment.

Concerning the intermediate simulation results, it is interesting to note that the power transported by mass flows is in the order of megawatts or at least hundreds of kilowatts. The parameter G , that as shown in equation 4.29 is proportional to the conduction energy flow between sectors, is in the order of 10 WK^{-1} or lower, which results in a power of only *dozens of Watts* between two adjacent tank sectors. It is apparent that the conduction effects are negligible next to the mass flows, and could be ignored if the need to simplify the model arises.

²at least theoretically

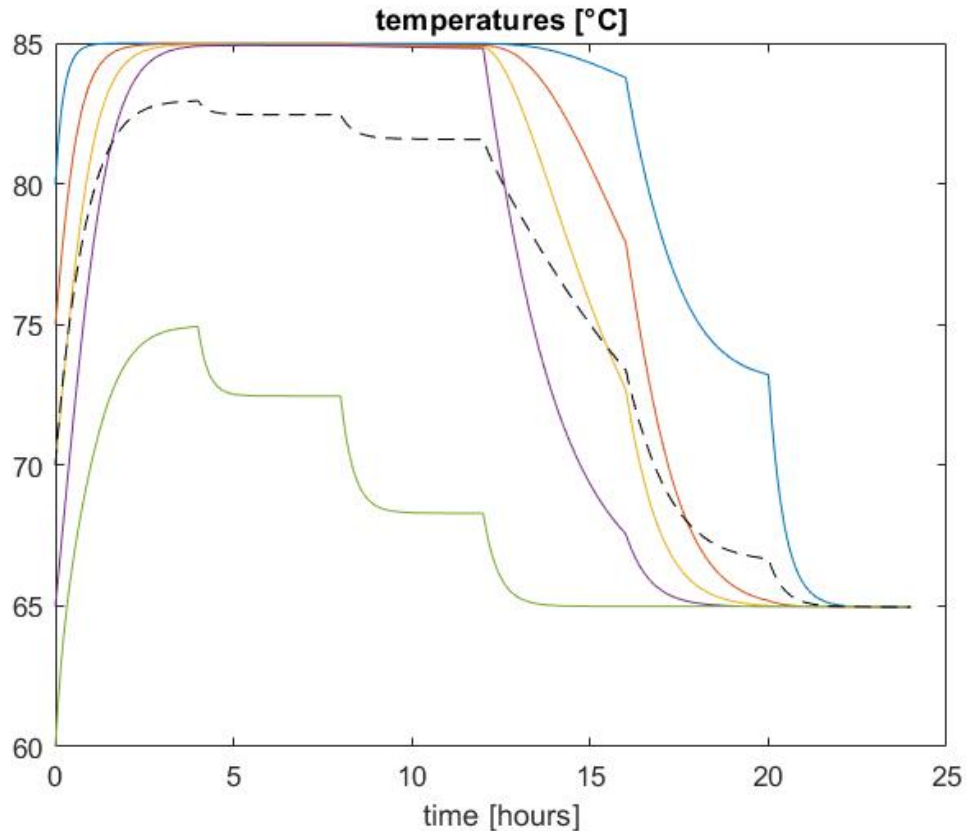


Figure 4.2: The evolution of five tank sector temperatures over 24 hours, with heat input that decreases in steps

By setting $U = 0.2 \text{ Wm}^{-2}\text{K}^{-1}$, the heat transmission through the walls is found to be more important than the one inside the tank, but still a minor phenomenon; indeed each layer temperature does not change significantly after reaching an equilibrium point, which means that neither losses nor conduction effects prevail.

The evolution of temperature is marked by stabilisation around an equilibrium value, that tends to happen in a short time frame, in the order of a few hours. In a tank with n horizontal layers, these equilibrium values are more or less one single T for the upper $n - 1$ layers, reached in different but relatively close instants in time, while the bottom layer temperature increases but stabilises at a much lower level. This result of the simulation confirms what has been found experimentally and with more detailed models in stratified tanks: when they are charged, a small pocket of colder water tends to remain in their most inferior region.

Stable temperatures are reached when the energy input from the generator equals the rate at which energy is discharged to the network. This also happens with different flow rates, because as time passes temperatures change. During charging, the stored water - more specifically the bottom region - becomes warmer, and so does the generator return, thereby decreasing the energy transferred to the tank. At the same time, the network side "sees"

warmer water exiting the tank while the entering fluid is fixed at the return temperature, and therefore more energy is withdrawn, until eventually the energy content of the tank becomes constant. During discharge, the tank temperatures fall, which means that more energy tends to be added from the generator and less energy tends to be extracted, until stabilisation.

What is more, by looking at the temperature curves like the ones in figure 4.4, we realise that the energy content of the tank, represented by the dashed line which indicates average temperature, starts decreasing as soon as the flow rate on the generator side is reduced by 20%, while still being much larger than the value on the network side. This is due to the fact that the same amount \dot{m}_g of water is taken from the bottom sector, where it is replenished by colder water from the network return and by a smaller amount of hot water from the sectors above. As the simulation progresses the share of water coming from above becomes less and less important.

Eventually, as the mass flow rate on the generator side drops below the network circulation flow rate, the temperatures quickly fall to the network return value. The uppermost control volume remains closer to a constant temperature as the rest of the tank cools down relatively quickly; this reminds us that while discharging stratified tanks, a volume of hot water is conserved at the top. The same volume then tends to settle at a higher temperature than the network return as long as there is some amount of water entering from the generator, and then finally falls to the lowest temperature level.

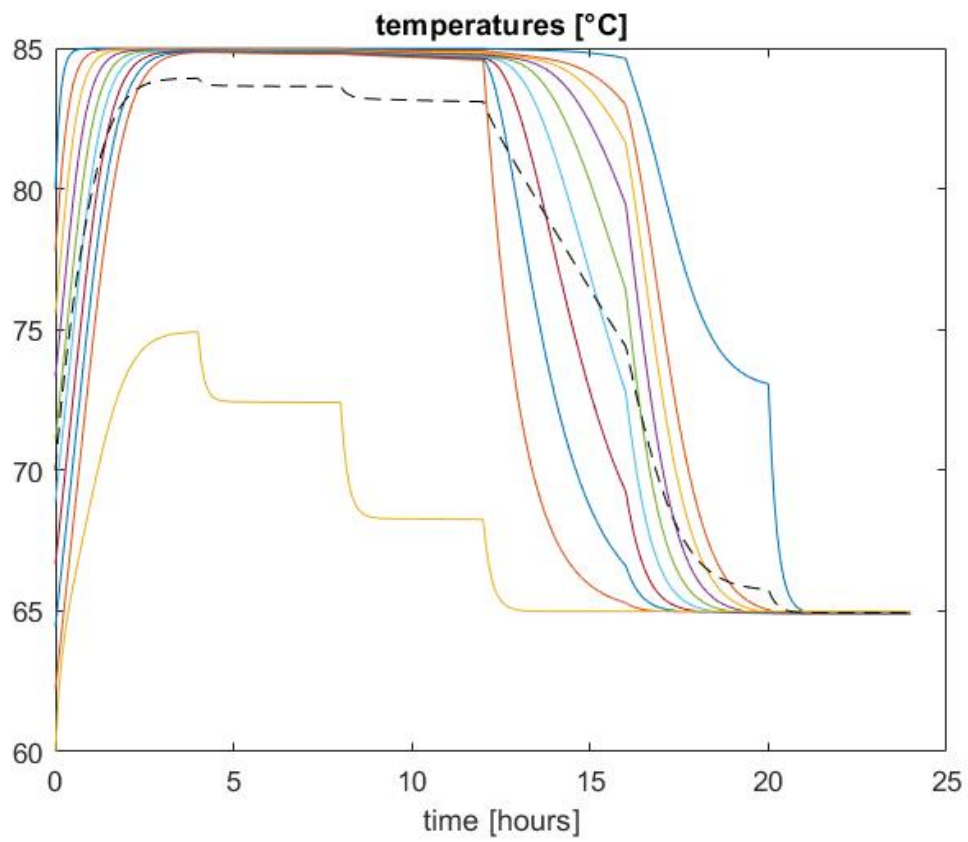


Figure 4.3: The evolution of the temperatures of ten tank sectors of equal volume over 24 hours

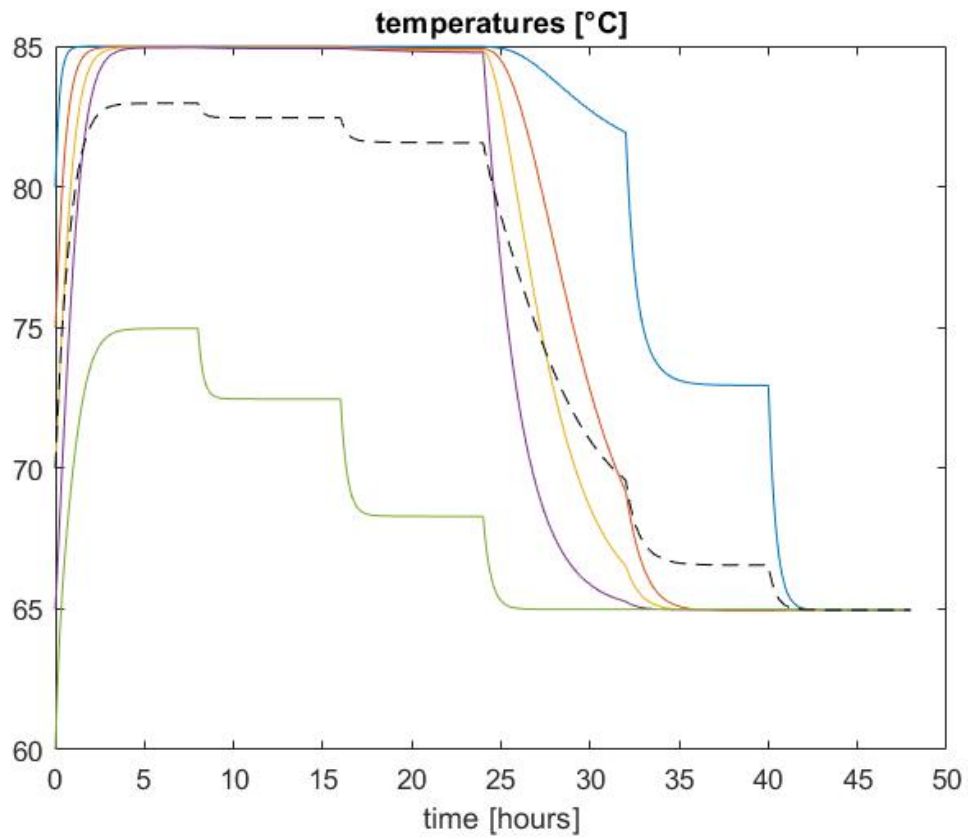


Figure 4.4: The evolution of tank sector temperatures over 48 hours, with heat input that decreases in steps, where every step lasts 8 hours

5. Model Validation

The goal of validation when modelling a system is the evaluation of the model performance, which is defined as its accuracy when it comes to mimicking the dynamical functioning of the physical system. With this objective in mind, we are going to try to compare the predictions of our MATLAB model to the information provided by a reference tank model.

5.1 The Reference Model: TRNSYS Type 534

The computer programme TRNSYS (TRaNsient SYstems Simulation program) was initially developed in 1975 at the University of Wisconsin-Madison to predict the performance of solar thermal systems and has since been expanded to conduct simulations of many different energy systems, with a focus on buildings and renewable energy integration.

TRNSYS has a vast library of sub-system models which can be connected to assemble complex systems; for our purposes, we shall use a model essentially based on one block, that represents our storage tank. Component models are known in TRNSYS as "types", and the closest of these to our MATLAB model is Type 534, described as "Vertical Cylindrical Storage Tank With Immersed Heat Exchanger", which is described quite extensively in [62].

The subroutine known as Type 534 represent a constant-volume, completely fluid-filled tank in the shape of a vertical cylinder. The fluid inside the cylinder interacts by way of heat transfer with an immersed heat exchanger and the surrounding environment, and by way of mass flow with up to two streams passing through the reservoir. The tank is divided into a certain number of isothermal, constant-volume regions called *nodes*. The nodes interact with each other via heat conduction and fluid movement (a bit like the tank sectors in our MATLAB model).

It is possible for the user to choose among four different types of heat exchangers (horizontal and vertical tube bank, serpentine tube, coiled tube) or no heat exchanger at all (which is our case). There is also the possibility of choosing a particular fluid for either the storage or the heat exchangers, specifically a mixture of water and ethylene or propylene glycol.

The tank model takes into consideration the main energy flows through the control volume boundary, as well as other phenomena that can happen in a stratified tank:

1. thermal losses to the environment, through the top surface, represented at the node 1 by the equation

$$Q_{loss,top,1} = A_{top,1}U_{top}(T_{tank,1} - T_{env,top}) \quad (5.1)$$

2. thermal losses to the environment, through the side surface:

$$Q_{loss,bottom,j} = A_{bottom,j} U_{bottom} (T_{tank,j} - T_{env,bottom}) \quad (5.2)$$

3. thermal losses to the environment, through the bottom surface:

$$Q_{loss,edge,n} = A_{edge,n} U_{edge} (T_{tank,n} - T_{env,edge}) \quad (5.3)$$

the input parameter, for this effect and the two preceding ones, is the environment temperature.

4. Thermal losses to the environment, due to flue gas passing through the tank;

$$Q_{loss,flue,j} = A_{flue,j} U (T_{tank,j} - T_{flue}) (1 - \gamma_{aux}) \quad (5.4)$$

the user provides the flue gas temperature and heat loss coefficients as inputs to the model. The parameter γ is the coefficient that indicates whether auxiliary heat is being added the tank node, in which case the gas flue losses are set to zero.

5. Heat exchange with fluid in the heat exchanger; this component is modelled with a control volume of its own, and is solved with purpose-built differential equations. The parameters of the differential equations are found with thermal fluid dynamics for forced convection, that evaluate the flow condition with the Reynolds number and calculate heat transfer coefficients with the help of the Nusselt number.

6. Conduction between adjacent tank nodes;

$$Q_{cond,j} = k_j A_j \frac{T_j - T_{j+1}}{L_{cond,j}} + k_{j-1} A_{j-1} \frac{T_j - T_{j-1}}{L_{cond,j-1}} \quad (5.5)$$

the user can set the magnitude of fluid conductivity, including at zero in order to 'turn off' this phenomenon.

7. Mass flows; there can be up to two flows entering and exiting the tank, each one through a pair of ports. The flow exiting one port must be equal to the flow entering its paired port; in any case, TRNSYS provides subroutines that simulate mixing valves, used to model a tank with an odd number of ports.

The user has to specify in which nodes the inlet and outlet ports of each stream are located, as well as the temperatures at inlet and mass flow rates.

As a default, the software calculates the temperature of each node by completely mixing the mass that has entered it during the last timestep. Anyway, it is possible for the user to decide how much of a flow mixes with every successive node (the share $f_{in,j}$, in order to represent the phenomenon of water streams "jetting past" a tank region.

There are several modes of operation when setting this kind of parameters; for example, it is possible to only assign an outlet port to a stream together with its inlet temperature, and the software will find the inlet node based on where the temperature is closest to the inlet value. The heat flow due to a mass stream entering a tank node is found with the relation:

$$Q_{flow,i,j} = \dot{m}_{in} f_{in,j} c_p T_{in} + \dot{m}_{in,j-1} c_p T_{j-1} + \dot{m}_{in,j+1} c_p T_{j+1} - \dot{m}_{push} c_p T_j \quad (5.6)$$

8. mixing between nodes, performed by the tank model to eliminate thermal instabilities; in fact, it can happen that the temperature of a node in a stratified tank is lower than the temperature of the node underneath. The solver averages out the temperatures of the two adjacent nodes, but it is also possible for the user to choose a mixing flow rate. This is a major complexity that sets TRNSYS apart from other models.
9. Mixing between nodes due to load flow through the storage tank;
10. auxiliary heat inputs in the tank nodes; this option allows to consider external temperature controls of tank nodes, by means of electrical or combustion heaters, or controls that remove heat from the specified nodes.
11. Miscellaneous heat gains or losses, that account for various minor¹, or unaccounted for, energy flows.

The subroutine relies on the solution of differential equations, that relate to the physical parameters and control surface balance of every tank node - as well as of every heat exchanger node, that however goes beyond our field of interest at least for the time being.

The differential equation for tank node j is of the type:

$$\frac{dT_{tank,j}}{dt} = \frac{Q_{aux,j} - Q_{HX,j} - Q_{loss,top,j} - Q_{loss,bottom,j} - Q_{loss,edges,j} - Q_{cond,j} - Q_{flow,i,j} - Q_{mix,j}}{C_{tank,j}} \quad (5.7)$$

where $C_{tank,j}$ is the tank node thermal capacity. It is then arranged, along with many others, in the form:

$$\frac{dT}{dt} = aT + b \quad (5.8)$$

where a and b are found from the set of physical parameters for each node. The quantity b contains the temperatures of other tank nodes, which are assumed to be constant during the timestep, at an average value. If there is a "temperature inversion" (a situation in which the node below is warmer than the one above) during the timestep, mixing can start; the software then calculates the instant at which the temperatures become unstable and archives the values at that instant, then a new solution is calculated with averaged values between the two "inverted" nodes.

The model outputs provided in the end are timestep average values.

5.2 Validation Procedure

In the TRNSYS Simulation Studio environment, the Type 534 tank model was connected with the subroutine 'Type 9a' for input values, and 'Type 25c' for printing the output values in a `.txt` file.

In the Type 534 menu, and specifically in the `Parameter` section, where the tank model *hydraulic specifications* are decided, the `Logical Unit for Data File` was left as the

¹an example given in the manual is pilot lights

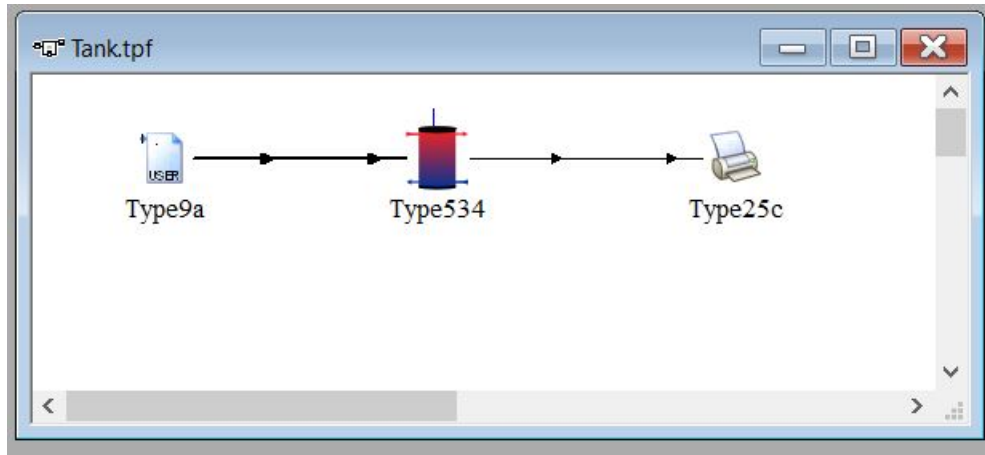


Figure 5.1: The TRNSYS deck built to read the inputs, predict temperature values and print out the outputs.

default value of 31. The Number of Tank Nodes was then set at 5 as a first approximation, and the Number of Ports at 2, since every "port" represents in reality a pair of them. The number of immersed heat exchangers was set at 0, as well as the number of miscellaneous heat flows.

The Input menu is used for the system forcing terms such as charging and discharging power, as well as energy losses to the environment. The main inputs are the flow rates and temperatures at each inlet port, and the ambient temperatures used to calculate heat losses at each node, with distinction of the side surface, relative to every node, and the bottom (or top) surface for the nodes at the ends of the tank. There are therefore in our case two Inlet temperatures and two Inlet flow rates to set, that will come from input files linked to the type 9a in order for us to have the possibility to change their values over time, especially with respect to the flow rates. There are n values of Edge Loss Temperature to set, where n is the number of tank nodes, one Top and one Bottom Loss Temperature; we shall leave all these values at the default 20°C , and remember to do the same with the parameter T_{amb} in the MATLAB model.

The Input section also contains a parameter called Gas Flue Temperature which represent the reference temperature for flue gas losses, an Inversion Mixing Flowrate and the Auxiliary Heat Input for each sector, that we are going to leave at the default values of respectively 20°C , -100 kg/hr and zero.

In the Type 534, there is another menu called Derivative where the initial conditions are set: it is equivalent to the initial vector T_0 in the MATLAB script.

Finally, the Output menu lists the model output parameters; among them it is possible to choose which ones to print in the output .txt file. A possible choice is the five node temperatures, along with the outlet temperatures and mass flow rates.

The four time-variant forcing parameters come from four columns in a text file linked in the input subroutine, in the section External Files.

The names of the headings of the four columns appear in the menu of the link between Type 9a and Type 534, and besides them we find the names of all the Type 534 input parameters.

Paired Inlet/Outlet Ports

Number of Ports: 2 Port #: 1

Inlet Flow Mode: Locations of Inlets and Outlets Provided

Entry Node: 1

Exit Node: 5

Temperature at Inlet*: 20 C

Flow Rate at Inlet*: 0 kg/hr

Figure 5.2: The menu to set the inlet and outlet levels of mass flows in TRNSYS

To ensure that the tank inputs are fed from the text file columns, each column heading name must be connected to the corresponding tank time-variant input parameter.

The Type 9a menu also contains a `Parameter` section, that regulates some aspects of the model operation. The command line `Header Lines to Skip` is set at 1 to prevent the software from reading the first line of the input file, in which there are the column headers. The number of tank input parameters is then set at 4, in the variable `No. of values to read`, and the timestep is fixed, measured in hours, as the parameter `Time interval of data`.

The software then offers the option to transform in four different ways each one of the input signals (the data columns in the file, marked by a progressive number, from 1 to 4 in this case). It is possible to interpolate the input values when there is a step change in the data, with the command `Interpolate or not?` - we choose not to and set the parameter at -1.

There is the possibility to choose a multiplication and addition factor to modify the input parameters on each side of the tank. We shall set the factors at 1 and 0 respectively to avoid modifications, except on the mass flow rates² that shall be multiplied 3600-fold in order to convert the unit of measurement of our input files ($kg\ s^{-1}$) into the one used by the software ($kg\ hr^{-1}$).

Finally, by setting the parameter `Average or instantaneous value` at 0, we declare that the inputs are average values during the timestep and not instantaneous values of the quantity, at one or the other end of the timestep itself.

The first parameter in the menu is the `Mode of operation`, which essentially determines how the software reads the input file: by choosing mode 2, we declare that the first line of the input columns contains the conditions at the initial time instant (and therefore the input file will have an odd number of lines, after the headers).

The Type 534 menu also contains a window with the tank geometric parameters. It allows to decide the tank volume, height and number of nodes, its wall, top and bottom loss coefficients, as well as the reference temperature for losses. It is also possible to pick a fluid among water (our case) or a mixture of water and ethylene or propylene glycol (the soft-

²*i.e.*: parameters 2 and 4, from the corresponding columns

ware was originally conceived for use in solar thermal systems).

For each tank node, it is also possible to assign the value of heat transfer coefficient that regulates losses to the environment through the cylindrical surface around it, by using the menu `Edge Loss`. Finally and perhaps most importantly, we can choose the number of mass flows, or equivalently of pair of ports, and for each pair of ports the entry and exit node.

The simulation duration and timestep can be set, in hours, from the `Settings` section of the TRNSYS Simulation Studio. The input text files will need as many columns as there are input variables and as many lines as there are time instants, including the initial one: the number of lines of the table shall be equal to the simulation duration divided by the timestep and increased by one.

The TRNSYS input and outputs are printed on `.txt` files. The inputs are copied from a `.xlsx` (Microsoft Excel) spreadsheet, which is also used as a source for the MATLAB script, with the help of the command `xlsread`.

Inside the MATLAB script, there are also provisions for reading the TRNSYS output in the `.txt` file, in the form of a MATLAB table, by using the command `readtable`. In parallel, the historical series of node temperatures are arranged in a similar table, comprehensive of column headers, by using the command `array2table`.

The two tables are finally copied into two spreadsheets with the command `writetable`. This way, we can bring together the outputs of TRNSYS and MATLAB and it becomes possible to make direct comparisons.

In the MATLAB script, a sub-routine was then introduced to enable the simulation to evaluate temperatures with a shorter timestep than the one separating the input values, if this necessity arises³. The time interval for calculations is decoupled from the one given in the inputs, as well as from the one given in the outputs. The latter are, in fact, fed to another sub-routine which again reduces the number of timesteps⁴. A larger number of evaluations protects the model from errors that could arise if iterative calculations are done over a series of timesteps (in the model "physical" time) instead of inside a nested loop (in a "fictitious" time interval used for recursive calculation, which would over-complicate the software).

5.3 Results and Observations

The simulation is conducted in both the MATLAB and TRNSYS environments with the fixed parameters listed in table 5.1.

- in the first simulation, the behaviour of the tank with steady-state operation of the network and the generator is studied.

The generator provides a constant flow of 143.2 kg s^{-1} of water at 85° C , while the network steadily supplies 71.6 kg s^{-1} of water at 65° C . The four columns with the

³it is called "inputmodif"

⁴see: sampling

Table 5.1: Simulation parameters for validation

tank volume	500 m ³
tank height	17 m
number of tank sectors	5
simulation timestep	900 s
wall heat transfer coefficient	0.2 Wm ⁻² K ⁻¹ (0.72 kJ m ⁻² hr ⁻¹)

constant values of mass flow and temperature are printed in a spreadsheet called `standard`, and represent a simulation with a duration of 36 hours (145 lines and the headers).

- in a second simulation, after 18 hours of operation the generator mass flow rate is reduced by 60%, to 57.3 kg s⁻¹, below the rate at which water is supplied by the return pipe, and maintained at a constant reduced value for 18 more hours. This scenario is called `mass`.
- in a third simulation regime, called `temp`, the change happens with regard to the generator side supply temperature. The parameter $T_{g,in}$ falls suddenly halfway through the 36-hour simulation, to the intermediate temperature of 72 °C.

We find slight differences between the values predicted by the two models in both transient and steady-state conditions (for a graphical representation, it is possible to see section B.2).

In the `standard` simulation regime, it is particularly evident that the MATLAB model tends to predict higher values of the temperature in the sector immediately above the bottom one, and somewhat lower values of the temperature in the other sectors. To be more precise, the temperature difference

$$\Delta T = T_{MATLAB} - T_{TRNSYS}$$

displays a tendency to quickly increase before the lower end of the tank. It is fair to say that our model, relatively to the TRNSYS one, predicts the tank to be a bit "more stratified", outside the end sectors where there is a strong effect of mass flows at the control surface. In other words, the temperatures are predicted by MATLAB to be closer together in the first $n - 1$ sectors. This is confirmed by simulations carried out with a larger number of sectors, which also show a rapid increase of ΔT in the two to three regions before the tank bottom.

It is possible to assume that the differences in the predicted temperature of the inner sectors are related to the fact that our model does not take into account the movements of mass happening because of diffusion and natural convection. The water in our tank is essentially still except for the effect of the forced circulation from generator and network.

In the `mass` scenario, temperatures tend to fall at a significantly slower pace in the MATLAB predictions, and to settle at somewhat lower values, especially in the sector that located immediately below the top one. The top sector is the only one where the values predicted

by MATLAB are higher. Since the difference in mass flow rates is much smaller under the `mass` input conditions, and mass flow is the only communication medium inside the MATLAB tank, it appears logical that transitions are slower. This is especially true for the top sector, which "sees" two water inflows: one of hot water from the generator, that tends to conserve temperatures, and one of cooler water from the tank lower regions. The former is the larger one, by a factor of four, and this explains the slow temperature change compared to when all the water entering the tank comes from the "hot" generator side and causes a quick temperature increase.

In the `temp` scenario, there is strong matching of temperature evolution as calculated in the two models, during both transient and steady-state conditions.

Natural convection

It has been observed that natural convection causes movement of water in stratified tanks. This is due to the cooling of water located next to the tank walls, which tends to fall and cause, because of the conservation of mass, a slow rising movement of the water in the central region [12].

The speed of this flow has been found to be inversely proportional to the gradient of temperature, according to the equation:

$$w_B = 0.0021 \cdot (\text{grad } T)^{-0.838} \quad (5.9)$$

in a finite difference environment, gradient is calculated for each boundary between two adjacent sectors with the simple formula:

$$\text{grad } T(j) = \frac{T(j+1) - T(j)}{z(j+1) - z(j)} = \frac{T(j+1) - T(j)}{\Delta z} \quad (5.10)$$

The buoyancy-induced mass flow rate is then evaluated from the speed by taking into account the thickness t_B of the external layer in which the phenomenon happens, which is reported to be around 1 cm, or 8 mm on average [12]. Since this length is much smaller than the diameter of the cylinder, we believe it is legitimate to find the section of the boundary layer by simply multiplying the tank perimeter by t_B . The mass flow will finally be equal to this section multiplied by the velocity and the fluid density.

$$\dot{m}_B(j) = S_B \cdot w_B(j) \cdot \rho(j) = 2\pi r \cdot t_B \cdot w_B(j) \cdot \rho(j) \quad (5.11)$$

The quantity $\dot{m}_B(j)$, or \dot{m}_B^j , as is predictable from the formulae used for its quantification, refers to the mass flow *exiting* the j -th sector and *entering* the $(j+1)$ -th sector; there will be $n - 1$ values of \dot{m}_B at every timestep.

Balance equations

The balance equation for sector 1, where the conduction terms have been eliminated for the sake of simplicity, becomes:

$$\frac{T^1}{C} = \frac{T_0^1}{C} + \dot{m}_g c_p T_{g,in} - \dot{m}_d c_p T^1 - \dot{m}_{net} c_p T^1 - \dot{m}_B^1 c_p T^1 + \dot{m}_B^1 c_p T^2 - U(A+S)(T^1 - T_{amb}) \quad (5.12)$$

which rearranged means:

$$\left[\frac{1}{C} + \dot{m}_d c_p + \dot{m}_{net} c_p + \dot{m}_B^1 c_p + U(A + S) \right] T^1 - \dot{m}_B^1 c_p T^2 = \frac{T_0^1}{C} + U(A + S) T_{amb} + \dot{m}_g c_p T_{g,in} \quad (5.13)$$

in the intermediate sectors, the energy balance shall be:

$$\frac{T^j - T_0^j}{C} = \dot{m}_{net} c_p (T^{j-1} - T^j) - UA(T^j - T_{amb}) + \dot{m}_B^{j-1} c_p (T^{j-1} - T^j) - \dot{m}_B^j c_p (T^j - T^{j+1}) \quad (5.14)$$

in linear system form, it becomes:

$$(-\dot{m}_{net} c_p - \dot{m}_B^{j-1} c_p) T^{j-1} + \left(\frac{1}{C} + \dot{m}_{net} c_p + UA + \dot{m}_B^{j-1} c_p + \dot{m}_B^j c_p \right) T^j + (-\dot{m}_B^j) T^{j+1} = \frac{T_0^j}{C} + UA T_{amb} \quad (5.15)$$

regarding the bottom end, we can write:

$$\frac{T^n}{C} = \frac{T_0^n}{C} + \dot{m}_d c_p T_{d,in} - \dot{m}_g c_p T^n + \dot{m}_{net} c_p T^{n-1} + \dot{m}_B^{n-1} c_p T^{n-1} - \dot{m}_B^n c_p T^n - U(A + S)(T^n - T_{amb}) \quad (5.16)$$

which results in:

$$(-\dot{m}_{net} c_p - \dot{m}_B^{n-1} c_p) T^{n-1} + \left(\frac{1}{C} + \dot{m}_g c_p + \dot{m}_B^{n-1} c_p + U(A + S) \right) T^n = \frac{T_0^n}{C} + \dot{m}_d c_p T_{d,in} + U(A + S) T_{amb} \quad (5.17)$$

Under the hypothesis that the natural convection flow is uniquely dependent on losses to the environment, there is no need to change the position of the terms with \dot{m}_B in the matrix used when \dot{m}_{net} takes negative values.

In simulations where the mass flows on the two sides of the tank are significantly different, the MATLAB outputs match the TRNSYS ones a bit more closely.

From the simulations under the regime `mass`, on the other hand, it becomes clear that as soon as \dot{m}_{net} becomes negative, a model where the buoyancy-induced mass flow is taken into account produces severe instabilities in the temperature profiles in time, especially in the intermediate sectors.

Meanwhile, the simpler model, where there is no "natural" flow between sectors, predicts some thermal inversions and is vulnerable to the case in which $\dot{m}_{net} = 0$, as in this peculiar situation sectors are "isolated" from one another. Nevertheless, is reasonably robust and can be retained as an acceptable compromise solution for a tank model integrated into a larger network simulation with moderate requirements of computing power.

Table 5.3: Evolution of temperature as predicted by the two models: in the MATLAB model, mass flow by natural convection has been introduced

t [h]	T ₁			T ₂			T ₃			T ₄			T ₅		
	M	T	ε[%]	M	T	ε[%]	M	T	ε[%]	M	T	ε[%]	M	T	ε[%]
0	80	80	0	75	75	0	70	70	0	65	65	0	60	60	0
0.25	83.28	81.28	2.45	78.12	76.81	1.70	72.98	72.08	1.24	67.93	67.43	0.74	64.10	63.74	0.56
0.50	84.35	82.55	2.17	80.51	79.04	1.86	75.80	74.94	1.14	70.84	70.83	0.01	66.44	67.50	-1.58
0.75	84.68	83.24	1.74	81.97	80.56	1.75	78.08	77.19	1.16	73.53	73.50	0.04	68.13	69.70	-2.25
1.00	84.78	83.68	1.32	82.74	81.60	1.40	79.71	78.83	1.11	75.79	75.44	0.46	69.49	71.26	-2.49
1.25	84.80	83.98	0.99	83.08	82.33	0.91	80.70	79.99	0.89	77.51	76.84	0.88	70.56	72.39	-2.53
1.50	84.81	84.19	0.74	83.17	82.84	0.41	81.21	80.81	0.50	78.67	77.83	1.07	71.35	73.20	-2.53
1.75	84.80	84.33	0.56	83.17	83.19	-0.03	81.42	81.38	0.04	79.33	78.54	1.02	71.87	73.77	-2.57
2.00	84.80	84.43	0.43	83.15	83.44	-0.35	81.47	81.79	-0.39	79.65	79.03	0.79	72.18	74.18	-2.69
2.25	84.80	84.51	0.34	83.13	83.62	-0.59	81.47	82.08	-0.74	79.77	79.39	0.49	72.34	74.46	-2.86
2.50	84.79	84.56	0.28	83.12	83.74	-0.75	81.46	82.28	-1.00	79.81	79.63	0.22	72.40	74.67	-3.03
2.75	84.79	84.59	0.24	83.11	83.83	-0.86	81.46	82.43	-1.18	79.81	79.81	0.00	72.43	74.81	-3.18
3.00	84.79	84.62	0.21	83.11	83.89	-0.93	81.45	82.53	-1.30	79.81	79.93	-0.16	72.44	74.91	-3.30
3.25	84.79	84.64	0.19	83.11	83.94	-0.99	81.45	82.60	-1.39	79.81	80.02	-0.27	72.44	74.98	-3.39
3.50	84.79	84.65	0.17	83.11	83.97	-1.02	81.45	82.65	-1.45	79.81	80.08	-0.35	72.44	75.03	-3.45
3.75	84.79	84.66	0.16	83.11	83.99	-1.05	81.45	82.69	-1.49	79.81	80.13	-0.40	72.44	75.07	-3.50
4.00	84.79	84.66	0.15	83.11	84.01	-1.06	81.45	82.71	-1.52	79.81	80.16	-0.44	72.44	75.09	-3.53
4.25	84.79	84.67	0.15	83.11	84.02	-1.08	81.45	82.73	-1.54	79.81	80.18	-0.47	72.44	75.11	-3.55
4.50	84.79	84.67	0.14	83.11	84.02	-1.09	81.45	82.74	-1.56	79.81	80.19	-0.48	72.44	75.12	-3.57
4.75	84.79	84.67	0.14	83.11	84.03	-1.09	81.45	82.75	-1.57	79.81	80.20	-0.50	72.44	75.13	-3.58
5.00	84.79	84.68	0.14	83.11	84.03	-1.10	81.45	82.76	-1.58	79.81	80.21	-0.51	72.44	75.14	-3.59
5.25	84.79	84.68	0.14	83.11	84.04	-1.10	81.45	82.76	-1.58	79.81	80.22	-0.51	72.44	75.14	-3.59
5.50	84.79	84.68	0.14	83.11	84.04	-1.10	81.45	82.76	-1.59	79.81	80.22	-0.52	72.44	75.14	-3.60
5.75	84.79	84.68	0.14	83.11	84.04	-1.10	81.45	82.77	-1.59	79.81	80.22	-0.52	72.44	75.15	-3.60
6.00	84.79	84.68	0.14	83.11	84.04	-1.11	81.45	82.77	-1.59	79.81	80.23	-0.52	72.44	75.15	-3.60

6. The Verona Case Study

The work described in the present thesis has been conducted with the goal of, eventually, studying flexibility solutions in the real-life context of a DH network in the city of Verona. More specifically, the tank model is to be integrated into a detailed model of the whole system. Our aim is to provide the first elements for comparing the opportunities and shortcomings of using the network or a storage tank to uncouple demand from supply.

6.1 Network Description

The Verona DH network provides space heating and DHW to 247 consumers near the central part of the city. The main heat carrier pipes have a combined length of about 40 km, and deliver about 70'000 MWh of heat per year to customer buildings with a combined volume of around 3.2 million cubic metres.

Three main heat supply plants are considered, each one employing a variety of generators:

- The *Centrale Centro Città* (CCC) has an installed thermal power of roughly 37 MW, provided by the waste heat of five natural gas internal combustion engines (11 MW), by five heat pumps (2 MW) and by three gas boilers, which are accountable for most of the heating capacity (25.5 MW).
- The *Centrale Sede* (CSD) relies on three natural gas HOBs, with a nameplate power of 1200 kW for the first two and 600 kW for the third one. It is mostly used as support for the other two plants during both winter and summer demand peaks. The three boilers heat the water in a primary circuit, which then transfers heat to the network with the help of a single plate heat exchanger (rated of course at 3 MW). The

Table 6.1: Types of generators with installed power in the Verona district heating network, from [72]

Supply station	Heat generation	Units	Total installed power
CCC	Gas-fired internal combustion engines	5	11 MWth (11.25 MWe)
	Heat pumps	5	2.0 MWth
	Gas boilers	3	25.5 MWth
CRV	Waste heat from foundry	1	4.4 MWth
CSD	Gas boilers	3	3.4 MWth

water circulates in the heat exchanger cold side due to a 55 kW pump that withdraws and supplies water from the main transport lines.

- The *Centrale di Recupero Termico* (CRV) recovers heat from a steel plant owned by the Pittini company, at a nominal capacity of about 4.4 MW, which enables it to provide about 15% of the network energy demand.

Around the year, the network relies on the waste heat provided in the CRV station, which in the summer accounts for the vast majority of the energy needs.

The CCC plant, on the other hand, is mostly used when the water circulation in the network exceeds $150 \text{ m}^2 \text{ s}^{-1}$, *i. e.* during the winter. Nonetheless there is the opportunity to operate the station in the summer, with a pressure differential between supply and return of only 1.5 bar, whereas the value for the winter is 6 bar. The three gas boilers are regulated in order to maintain a supply temperature of 80 °C.

The CSD plant is instead used as a support of both the CCC and CRV facilities, to match peaks in demand that can occur in both summer and winter.

In summary, four different energy sources are employed, and it is fair to assume that there is an *order of merit* at any given moment that defines which sources are to be favoured, with priority given to the least expensive ones (from a marginal cost standpoint). Generally speaking, we can expect the lowest marginal cost source to be the foundry waste heat, and the gas boilers to be the most expensive type of power plant, to be used as a "last resort".

The transport and distribution pipelines have been laid since 1986, and are made of many different materials. As of 2017, the operator identified 1080 joined branches, forming 11 "meshes".

The heat is delivered to consumers in 247 substations in which heat exchangers transfer energy in parallel to both the space heating and DHW circuits. In some buildings, DHW is provided by an autonomous system. The evaluation of consumption is carried out manually three times a year [53].

6.2 The Network Model

To analyse the use of DH networks to improve flexibility and more generally to simulate their dynamic behaviour, researchers at the University of Padua have developed an implicit model called NeMo.

NeMo is a model based on *graph theory*: the network is represented as a set of nodes connected by branches. The connections between nodes are represented in an *adjacency matrix*. Adjacency matrices are square matrices where the n nodes are represented in their mutual relations: each element $m_{i,j}$ depends on the connection between the nodes numbered with i and j , and is equal to 0 if there is no connection, 1 if there is a connection from i to j , and -1 if the connection is oriented and goes from j to i .

There are a certain number of fundamental assumptions in the NeMo model:

- the movement of water is fully dependent on forced convection: as a result there is no relation between temperature and velocity, and the thermal and hydraulic models can be uncoupled.
- The mass flow is completely incompressible;
- water runs in the conduits as a full slug flow: its velocity is constant in the radial direction.
- Heat conduction inside the wall pipe in the axial direction is neglected;
- heat conduction happens through the wall pipe in the radial direction. The forced convection resistance of the carrier fluid is considered, as well as the conduction resistance of the pipe wall and of the ground;
- the heat capacity of the ground is neglected.

6.2.1 The hydraulic problem

The hydraulic problem is solved through the continuity equation and the momentum equation, that completely describe the pressure and velocity fields of the incompressible fluid. From the conservation of mass, we can write for the node i :

$$G_{i,in} - G_{i,out} = G_{i,ext} \quad (6.1)$$

where $G_{i,ext}$ is the mass flow exiting (or entering) the network from node i . The pressure drop on branch j comes from:

$$\Delta p_j = \frac{1}{2} \rho \left(f_j \frac{L_j}{D_j} + \sigma_j \right) v_j^2 - \Delta p_{pump,j} \quad (6.2)$$

if we know that the mass flow rate is naturally related to the velocity according to $G_j = \rho S_j v_j$, and if we set the term:

$$r_j = \frac{1}{2 \rho S_j^2} \left(f_j \frac{L_j}{D_j} + \sigma_j \right) \quad (6.3)$$

that contains the characteristic parameters of the branch j , we can put the pressure drop directly in relation with the mass flow rate.

In matrix notation, with A equal to the adjacency matrix, it becomes possible to write together the continuity equations (6.1) for all the nodes:

$$A\dot{G} + \dot{G}_{ext} = 0 \quad (6.4)$$

while the branch pressure drops are rendered as:

$$A^T P = r\dot{G}^2 - h \quad (6.5)$$

where the vector h contains the pump hydraulic heads.

The two equations form a non-linear system that can be solved with a semi-implicit method built into the model and based on the SIMPLE method by Patankar and Spalding [48].

6.2.2 The thermal problem

The thermal problem is solved by doing a thermal balance on the nodes of the network. Let us consider the node i , which is connected to branches $j-1$ and j , with a control volume that is equivalent to half the volume of the connected branches; L and Ω are the branch length and perimeter, G is the mass flow rate and T_∞ is the ground undisturbed temperature. The energy flow balance comprises mass flow and conduction heat flow:

$$\rho V_i c_p \frac{\partial T_i}{\partial \tau} = G_{j-1} c_p T_{j-1} - G_j c_p T_j - \frac{1}{2} (L_j \Omega_j U_j + L_{j-1} \Omega_{j-1} U_{j-1}) (T_i - T_\infty) \quad (6.6)$$

the derivative is then discretised as a finite difference between two subsequent instants in time, called $\tau - \Delta\tau$ and τ , and the temperature of the mass flows in the branches entering the node is set as equal to the temperature of the nodes whence they come. The temperature in the branches exiting the node, meanwhile, can be set as equal to the temperature of the node itself.

$$\rho V_i c_p \frac{T_i^{(\tau)} - T_i^{(\tau-\Delta\tau)}}{\Delta\tau} = G_{j-1} c_p T_{j-1}^{(\tau)} - G_j c_p T_i^{(\tau)} - \frac{1}{2} (L_j \Omega_j U_j + L_{j-1} \Omega_{j-1} U_{j-1}) (T_i^{(\tau)} - T_g) \quad (6.7)$$

If we write this equation for every node, separating the terms with node temperature from the ones with the ground temperature, we obtain a system that can be represented in matrix form as:

$$M\dot{T} = s - KT \quad (6.8)$$

the system can be solved with an ODE numerical solution software, or linearised as

$$\frac{M}{\Delta t} (T - T_0) = s - KT \quad (6.9)$$

$$\left(K + \frac{M}{\Delta t} \right) T = s + \frac{M}{\Delta t} T_0 \quad (6.10)$$

and solved with Gauss elimination; the temperature in every time instant T is found starting from the previous time instant T_0 [72].

6.2.3 Network analysis and results

In the case of Verona, research has been conducted on the possibilities of using the circulating water as a storage instrument. With the help of the NeMo model researchers have predicted the return temperatures given a fixed load profile and different hydraulic control strategies, and then a series of performance parameters.

In the simulations, the primary input is the global network heat demand profile during two representative weeks of the year. The first is called the "Winter Week" and starts in February, the second is called the "Middle Season Week" and is taken from late April. The demand data, provided by the network operator AGSM, are split between a total of 65 users with coefficients loaded through the input spreadsheets, making two simplifications: the number of consumers is reduced, and the demand curve shape is considered identical for everyone,

Table 6.2: Topology of the real network and of the one used in NeMo simulations, as per [72] and [53]

Parameter	Real Network	Model Network
Number of substations	247	65
Number of heat supply points	3	1
Number of branches	1080	159
Total length [km]	22.6	16.3
Length of transmission pipes	15.0	12.0
Length of service pipes	7.6	4.3
Loops	11	11

with only amplitude changing, partly due to the fact that the installed meters only give the consumption integral. The network water volume is instead equal in the simulation and in reality.

The goal of the simulations is to evaluate the effects of different water flow regimes on some performance parameters. During a certain span of time the water flow, in order to store heat in the pipelines, must be different from the "standard" one which is always directly proportional to heat consumption.

This divergence is represented with five parameters:

- α depends on the mass flow rate increase occurring when the modified mass flow diverges from the standard one for the first or the last time;
- β is related to the instant in which the peak of the modified mass flow is reached;
- γ fixes the value of the maximum modified flow rate;
- ε establishes the duration of the mass profile divergence *after* the predicted peak of the standard load evolution;
- τ complements ε by setting the duration of the mass profile divergence *before* the predicted peak of the standard load evolution. It is of particular interest in the context of this research, because it expresses the duration of the network *pre-charge*.

Three different *pre-charge* flow regimes are applied to the system, each characterised by a specific set of the parameters α β and γ . Every flow regime, in turn, can take on four different values of τ , from 1.5 to 4.5 hours.

These different mass flow profiles are meant to shift heat loads in time; the results are evaluated by the computer model in the form of six parameters, of which the first three are particularly important and are considered Key Performance Indicators (KPI).

- the relative reduction in the peak load seen by the production plant:

$$\Delta q_{max} = \frac{q_{max,ref} - q_{max,mod}}{q_{max,ref}} \quad (6.11)$$

- the temporal shift of the peak, which is negative when the peak is brought forward and positive when it is delayed:

$$\Delta t_{q,max} = t_{max,mod} - t_{max,ref} \quad (6.12)$$

- the *available network capacity* is the amount of energy that it becomes possible to provide in a different period in time:

$$C_{net} = \int_{t_0}^{t_1} (q_{mod} - q_{ref}) dt \quad (6.13)$$

where t_0 is the instant in time where the flow regulation starts and t_1 is time when the modified flow matches exactly the reference one. C_{net} is roughly proportional to one of the two areas between the curves in chart 6.1, and is positive when the network is pre-charged.

It is also important to consider other effects of the flow regulation that might affect the ability of the network to meet its obligations to the customers and to limit its operational costs. For these effects there are other parameters:

- the integrated discomfort indicator, which for simplicity is considered proportional to the drop in return temperatures compared to the standard regime:

$$PD_{rel} = \begin{cases} \int_0^{168} (T_{r,ref} - T_{r,mod}) dt & \text{if } T_{r,ref} > T_{r,mod} \\ 0 & \text{if } T_{r,ref} < T_{r,mod} \end{cases} \quad (6.14)$$

- the relative variation of the energy supplied by the plant:

$$\Delta Q_t = \frac{Q_{t,mod} - Q_{t,ref}}{Q_{t,ref}} \quad (6.15)$$

it is important to remark that the deeper goal of flexibility is not necessarily the reduction of the energy supplied; it is more likely, for example, to be the reduction of *primary* energy consumption.

- Finally, the model calculates the variation in electrical energy consumed for pumping:

$$\Delta W_{el} = \frac{W_{el,mod} - W_{el,ref}}{W_{el,ref}} \quad (6.16)$$

The working principle of network storage is to increase the mass flow rate so that, for a fixed amount of heat withdrawn by the consumers, the temperature drops at the substations will fall and the return temperatures will increase, also increasing the average network temperature and reducing the specific energy addition at the generating plant.

It is important to remark that, normally, the mass flow rate in the network is the sum of the flow rates demanded by the substations. This prevents the operator from actually managing the evolution of water flows. It has been proposed to install bypass lines between

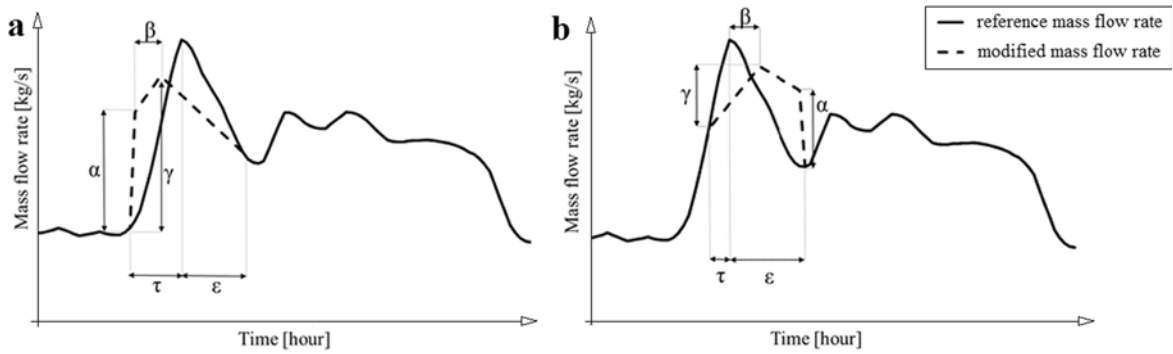


Figure 6.1: Visual representation of the five mass flow regulation parameters in the pre-charge and post-charge regime [72]

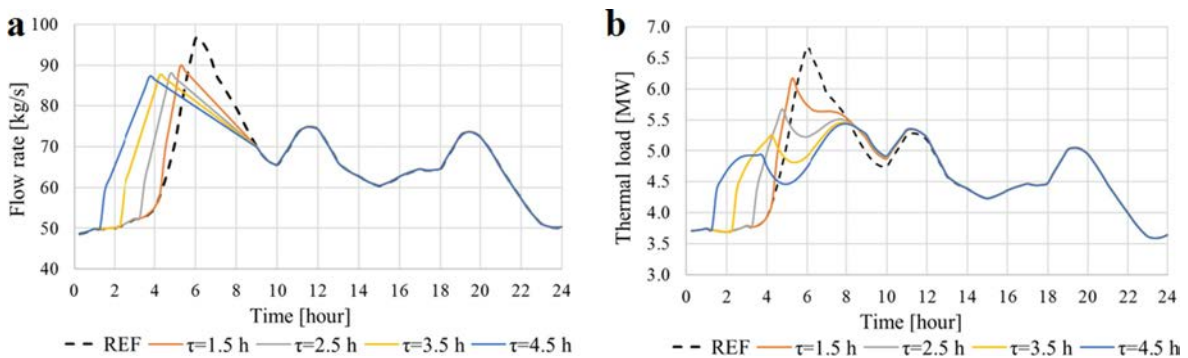


Figure 6.2: Changing the mass flow rate creates two peaks in the heat demand [72]

the supply and return of a number of substations, in order to increase the mass flow in the network without degrading the pressure levels or the level of service to the customers.

Simulations have been conducted with different shapes of the flow regime profile, indicated by the symbols C1, C2 and C3 when the peak was brought forward in time. Each profile has been simulated with four different values of τ , from 1.5 to 4.5 hours, and therefore a different duration of the pre-charging interval.

It was observed, during the simulated scenarios, that two successive temperature peaks propagate through the network, and that the heat flow supplied also undergoes two cycles of rise and fall.

- At first, the increasing mass flow rates cause the power transferred to the network to increase;
- then, the rise of the return temperatures (due to the fact that energy is not consumed and is instead being stored in the network) prevails, and the smaller temperature increases at the generators cause a decline in the supplied power.
- Finally, there is the consumption peak which discharges the network and allows the generators to produce more power thanks to the lower return temperature.

The difference in magnitude between the two peaks indicates how much *peak shaving* is

Table 6.3: The performance parameters with the mass flow regulated as in the C1 regime, with four different starting points related to the reference peak [72]

Week	$q_{max,ref}$ [MW]		τ [h]	Δq_{max} [%]		Δt_{max} [h]		C_{net} [MWh]		PD_{rel} [°C h]	
	TUE	SUN		TUE	SUN	TUE	SUN	TUE	SUN	TUE	SUN
FEB	25.71	20.64	1.5	7.5	11.8	0.5	1	1.36	2.06	10	12
			2.5	8.5	12.4	0.75	1	3.25	4.56	14	14
			3.5	8.7	12.8	0.75	1.25	6.06	5.63	16	15
			4.5	8.7	12.8	0.75	1.25	7.46	6.98	17	15
APR	6.67	6.69	1.5	7.6	2	-0.75	-0.5	0.08	0.08	4	3
			2.5	14.9	6.9	-1.25	-1	1.48	0.45	5	6
			3.5	18.2	13.3	1.75	-1.5	2.24	1.39	5	7
			4.5	18.4	17	2	1.25	2.8	2.31	5	7

achieved.

The performance indicators Δq_{max} , Δt_{max} and C_{net} increase progressively as the flow regulation starts earlier and earlier (greater τ), as can be seen in table 6.3; this is true with different regulation profiles.

The peak load reduction is particularly pronounced in the mid-season simulation, probably due to the fact that peaks are particularly important since less energy is used for the more constant space heating load. On the other hand, significantly more energy is stored in the network during winter days; it is also important to notice that, in the winter, customer satisfaction is more sensitive to alternative control strategies (PD_{rel} is 2 to 4 times larger) and therefore a certain degree of caution is warranted.

In the April week, the network stores less heat but, by increasing the duration of the pre-charge interval, the largest relative increases of performance parameters are observed: this is due to the lower speed of the heat carrier fluid, that allows slower propagation and longer retention of heat.

The amount of energy supplied tends to increase by a small amount, around 0.09% to 0.33% in the February week and 0.19% on average in the days of the April simulation. More unpredictable is the change in the required pumping power.

On a final note, the performance indicators are strongly affected by the day of the week: this is a property of the individual DH system that mostly depends on its consumer base.

6.3 Model Integration and Application

It has been estimated that Danish DH networks, which provide on average 115 GWh of heat per day, can set aside around 5 GWh of energy (roughly one hour of average consumption) by increasing their average temperature by 10 K. In Helsinki, where the network provides about 20 GWh of energy per day, an increase of 15 K allows to conserve 1.2 GWh. Hot water tanks, where implemented, might be able to accumulate one order of magnitude

more energy: their capacity has been estimated at 50 GWh in Denmark and 42 GWh in Sweden (over 40% and 25% of the daily demand respectively) [26]. It would be interesting to know, in the case of Verona, how a reservoir compares to the network from the point of view of the flexibility provided.

6.3.1 Computer model structure

The MATLAB programme integrating the tank and NeMo models is built around a main script, which takes as input databases:

- a MATLAB script containing the tank simulation parameters¹, among which the volume, the number of sectors, the height, the environment temperature;
- a MATLAB script where many network simulation parameters are stored²;
- five multi-spreadsheet files, containing:
 - the demand load profile, expressed as total mass flow rate³, and then the coefficients to distribute the mass flow among the customers and the heat load profiles at every substation;
 - the status of every substation, signalled with a "logical" quantity: 1 for producer, 2 for consumer;
 - the incidence matrix, where for every branch of the network the origin (upstream) and destination (downstream) nodes are declared, geometric parameters about the pipelines and support data for calculations;
 - the ground temperature at every timestep, which is the same in the whole network;
 - some topological, geometric and operational parameters of the network, like the number of nodes, the number of branches, the depth of pipelines, the minimum pressure differential to maintain in the node which is furthest from the supply station.

The data are then saved into a file and loaded in the workspace, before the start of the actual dynamic simulation.

The vector of tank node temperatures is first determined with `linspace`, and then a function⁴ is employed to evaluate the inner wall temperature used to calculate the natural convection heat transfer coefficient.

The main `for` loop then begins, with the reading of the tank input temperature from the generator side (which is a model input) and from the network side (which is the return

¹called `Storage_preProcessingModule`

²called `NeMo_preProcessingModule`

³in a sheet called `ccc` because, in the tankless network model, the network circulation is the one at the boundaries of the single CCC power plant

⁴called `initialFun`

temperature predicted by NeMo at node 148). Other model inputs are the mass flow rates on the two sides of the tank, which, together with the generator outlet temperature, come from an independent spreadsheet⁵ read by one of the support scripts. The fluid specific heat capacity is then calculated for the two flows entering the tank, and a new function⁶ evaluates the other fluid properties and finally determines the vector of global heat transfer coefficient for the current timestep (the values of the convection coefficient and of the heat transfer are recorded).

Then, the function `fserbatoio`, in one of its versions, evaluates the distribution of temperatures in the n tank layers, by taking as inputs values:

- the generator water supply temperature;
- the mass flow rate out of the generator, which is the main input to be changed from one simulation to another;
- the mass flow rate in the network, which is the same in the various simulations but different for each "season";
- the tank geometric parameters;
- the network return temperature, provided at every timestep by another section of the model.

Each one of the mass flow and temperature variables comes in the form of a *vector* which shows its evolution over the simulation timesteps.

The tank simulation function equally evaluates the wall inner temperature.

At this point the network supply temperature is set equal to the amount found in the tank top sector. The newly found tank vector is set equal to T_0 in order to act as input for the next iteration, and, at last, the script evaluates the power effectively released by the generator into the tank at the present instant.

The parameters obtained by the function are afterwards "archived" into vectors, along with the a marker of the time elapsed since the beginning of the simulation.

Later on, the function `pNeMoFun` is introduced. A series of inputs are extracted from linked files in order to be fed to it: the mass flow rates in all the nodes, the heat loads from the substations, the supply temperature (*i. e.*, the uppermost tank temperature), the temperature of the ground at all the nodes. By implementing a procedure built around a second function, `pNeMoFun` evaluates:

- mass flow rates in the 159 branches;
- fluid velocities in the 159 branches;

⁵"dati_nsim"

⁶see: `UTotFun`

- supply pressures at the nodes;
- return pressures;
- supply temperatures at the nodes;
- return temperatures.

The power effectively delivered to the consumers is now calculated: it considers the mass flow rate in the network and the difference between the tank top temperature (supply) and the newly found return at node 148.

The outputs, which paint the near-instantaneous picture of the network, are then archived and the loop inputs are updated. The tank will take new temperatures for its levels and the network inflow - the latter equal to the return temperature calculated by NeMo for node 148 (formerly the power station).

In the final part of the code, the output vectors are sampled over the course of time in order to match, if necessary, the temporal precision of the simulation to the frequency of input variations, and plotted.

The most important plot is the one of the energy flows on the two sides of the reservoir: from the history of these, it is possible to evaluate the Key Performance Indicators discussed in section 6.2.3, especially the peak shaving (equation 6.11). Moreover, our script evaluates the relative increase in delivered energy caused by the presence of a reservoir, according to equation 6.15. These amounts are evaluated for every day of the week by a function⁷ taking as one of its inputs the number of "cycles", that is to say, of days, in the period considered. In all cases, the "reference" power curve is the one demanded by the network, which would be the exact power curve supplied by the generators if there were no storage capability. The "modified" power evolution is instead the actual generator operation programme, based on the input mass flow on generator hot side.

6.3.2 Performance indicators

When NeMo simulations were carried out to quantify the ability of the network to act as a heat reserve, different regimes of the production-side mass flow are tested in the face of a fixed profile of the same value on the consumer side, within fixed limits to the temperature rise.

Now, the network is fed with energy and mass flows that are exactly equal to those demanded by the consumers, and the uncoupling happens at the tank. The tank, for its part, is injected with many different profiles of the generator mass flow and we wish to evaluate a series of parameters in order to compare with each other and those found in April:

- Δq_t : the relative difference between the energy supplied to the tank by the generator in every scenario and the energy supplied by the tank, which acts as the new "power plant" seen by the network, to the customers. These two energy flows depend on the

⁷see: `fpshaving`

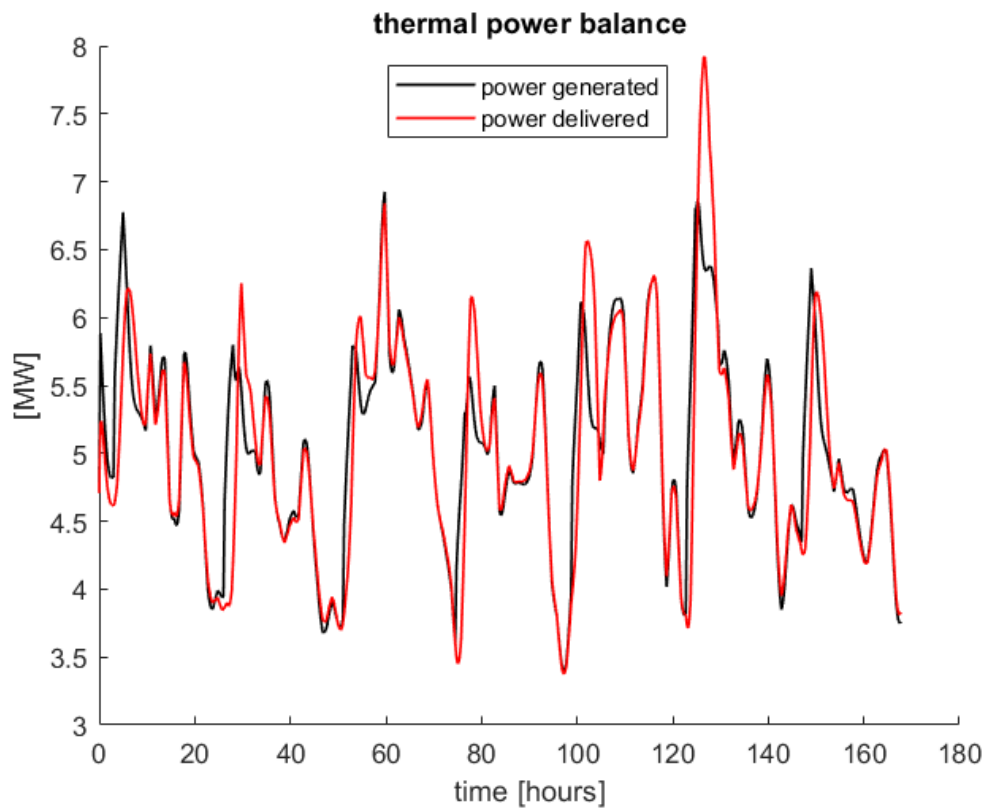


Figure 6.3: The energy flows in a simulation week from the April scenario, where the generators are operated in the regime C1, with mass flow abruptly increasing 3.5 hours before the demand ("reference") peak.

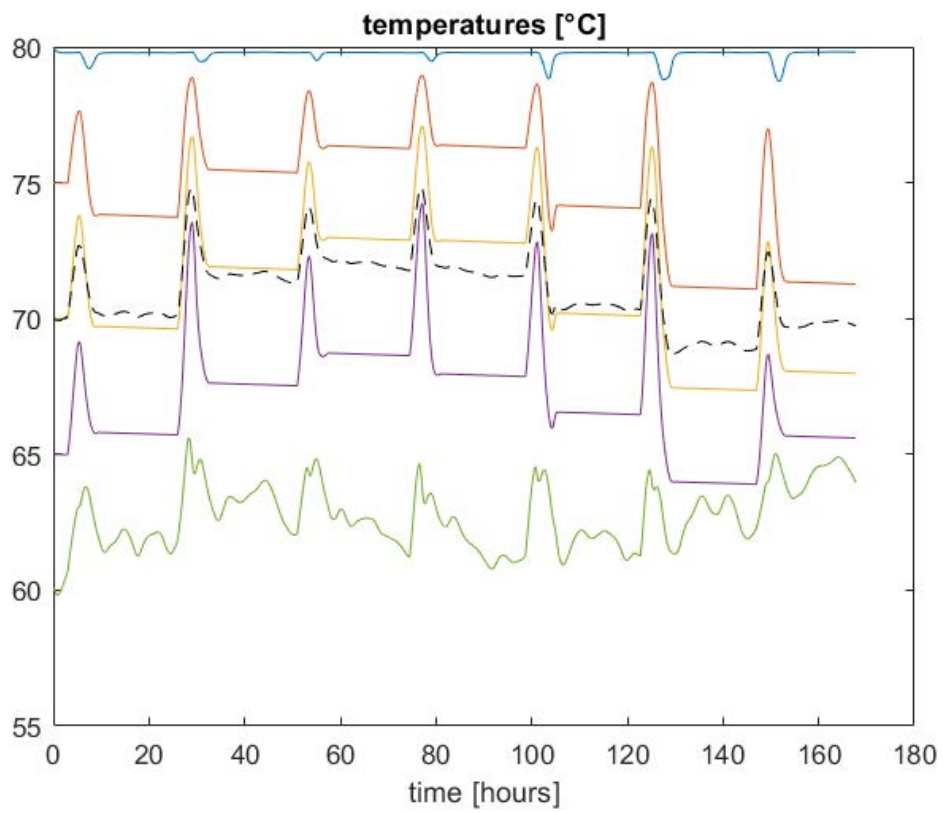


Figure 6.4: The evolution of tank temperatures during the week whose power profiles are shown in figure 6.3. The inner sectors are relatively insulated from the quick variations of the lowest one

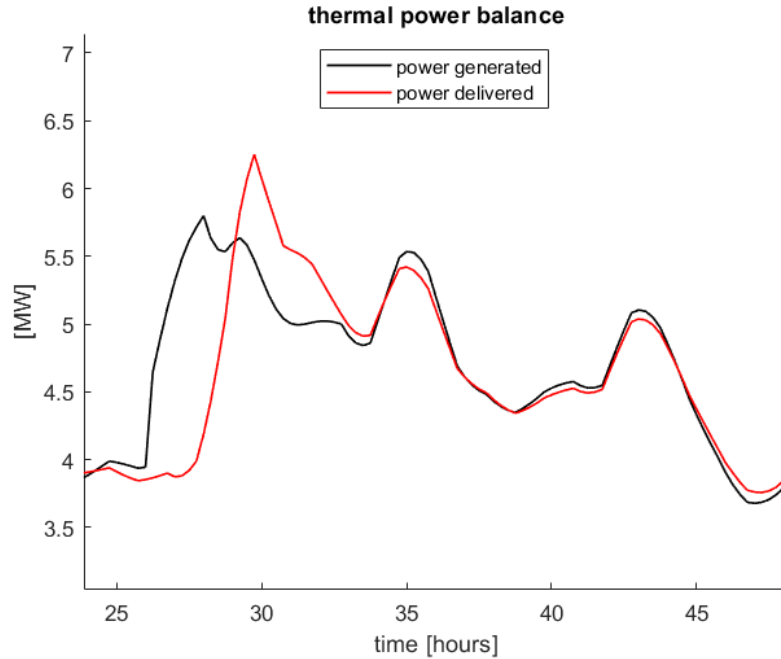


Figure 6.5: Detail ("Tuesday") of the week shown in figure 6.3.

temperatures and on the mass flow rates of the "modified" and "reference" scenarios respectively, as per equation 6.15.

- the relative decrease in the maximum value of power produced by the generator ΔQ_{max} (eq. 6.11). This particular parameter is strongly influenced by the mass flow rates, which have been set in order to evaluate the network performance as a reservoir.
- the energy shifted from one moment in time to another, evaluated by the parameter C_{net} (eq. 6.13), that is evaluated for every day of the week with a Microsoft Excel spreadsheet prepared at the University of Padua, in which the weekly evolution of Q_{gen} and Q_{dist} are loaded.

When using the network as an instrument of flexibility, simulations allowed to record variations of the temperature levels on the return lines of the consumer substations, due to the unconventional management of the heat carrier flow rates. These temperature variations allowed to evaluate the discomfort parameter PD_{rel} . In the simulations where the reservoir is introduced, the network mass flow is kept in tune with the customer demands, and therefore measuring the customer dissatisfaction would be quite misleading. For the same reasons, the time span between the peak of generated and delivered power is of little interest.

In the first series of simulations, the parameters described above were evaluated within the framework of the heat demand of a standard week of April and the generator flow management scenario C1, that had given the most promising results with network storage. The three versions of the scenario were then compared to the case in which the mass flow rate on the generator side was kept constant, at a value of 66.8 kg s^{-1} obtained by dividing the

Table 6.4: The parameters obtained from the simulations of the April week, with the various versions of the C1 scenario, compared to a reference week in which the same mass flow always circulates in the generator.

parameter	τ [h]	MON	TUE	WED	THU	FRI	SAT	SUN
ΔQ_t [%]	1.5	0.24	0.30	0.28	0.04	0.25	-0.18	0.45
	2.5	0.14	0.82	0.27	0.00	0.05	-0.37	0.61
	3.5	0.42	1.12	0.49	0.17	-0.27	-0.33	0.84
	4.5	0.82	1.06	0.66	0.20	-0.57	-0.22	1.12
	constant \dot{m}_g	2.58	0.11	-2.99	4.50	-2.85	0.31	0.55
ΔQ_{max} [%]	1.5	-2.28	-1.14	-1.20	-2.49	-2.82	0.76	-4.86
	2.5	-1.85	4.53	-1.21	2.57	-0.89	3.03	-6.22
	3.5	0.87	11.43	-1.17	7.77	3.95	13.89	-2.66
	4.5	2.95	12.57	-1.16	8.21	4.61	18.02	5.55
	constant \dot{m}_g	1.70	17.74	6.04	10.25	11.94	12.50	9.61
C_{net} [MWh]	1.5	0.73	0.84	0.51	0.24	0.41	0.77	0.26
	2.5	1.14	2.05	1.09	0.98	1.00	1.28	0.69
	3.5	1.86	2.92	1.79	1.87	1.80	2.51	1.92
	4.5	2.66	3.24	2.27	2.21	2.23	3.43	3.16
	constant \dot{m}_g	3.38	1.55	1.69	4.60	1.13	3.43	2.39

approximate amount of heat delivered in the week (823 MWh) by the duration and the enthalpy change of the fluid over an approximate average temperature change of 17.5° C. Generally speaking, more energy enters the tank than is delivered to the customers over the course of the week, by an extent typically smaller than 1%. It is interesting to notice that this quantity tends to increase (which might also mean, to decrease in absolute terms when it is negative) the sooner the generator flow regulation starts.

Another important remark is that the ratio of tank input to output energy is strongly dependent on the demand and production profiles of the particular days: in all regimes, on Saturdays the tank tends to discharge more energy than it absorbs from the generator.

The values of the "peak shaving" are rather inconsistent, with the generator often having to provide more power than the maximum energy flow absorbed by the network on the same day. This is quite predictable for the reasons explained above, however it might be worth mentioning that the highest amount of peak shaving is achieved on the simulated Saturday, with $\tau = 4.5$ h, and the "constant \dot{m}_g " simulation always gives a decrease in the power that the generator has to provide.

The parameter C_{net} , on the other hand, exhibits a marked tendency to increase as the flow rate "decoupling" is initiated earlier and earlier. From $\tau = 1.5$ h to $\tau = 4.5$ h it can increase by a factor of anywhere between 3 and 10, and it presents the highest values in the regime with constant generator flow. Besides, it does not appear to be influenced by the discrepancy between the heat consumption of workdays and the demand of weekend days. From a

Table 6.5: Different regimes with mass flow divergence at the instant corresponding to $\tau = 2.5$ h, in the April week.

parameter	regime	MON	TUE	WED	THU	FRI	SAT	SUN
ΔQ_t [%]	C1	0.14	0.82	0.27	0.00	0.05	-0.37	0.61
	C2	0.41	1.04	0.58	0.16	-0.28	-0.35	0.64
	C3	0.24	0.80	0.33	0.00	0.05	-0.37	0.78
ΔQ_{max} [%]	C1	-1.85	4.53	-1.21	2.57	-0.89	3.03	-6.22
	C2	-9.34	-3.83	-1.12	0.30	-4.58	0.02	-13.21
	C3	-4.16	2.71	-1.26	4.91	-1.26	5.47	-7.24
C_{net} [MWh]	C1	1.14	2.05	1.09	0.98	1.00	1.28	0.69
	C2	1.62	2.56	1.59	1.48	1.43	1.94	1.23
	C3	1.56	2.52	1.55	1.59	1.63	1.98	1.41

comparison with the data resulting from the network storage simulation, it appears that a 500 cubic metre tank allows to shift a similar, often slightly larger, amount of heat in time. These data are collected in table 6.4; from 6.5 it appears that the regimes C3 and C2 may allow a greater temporal shift of energy.

Other simulations were performed by taking as input the reference February week, in the various forms of the C1 strategy and with a constant generator mass flow scenario for completeness. This time, the constant mass flow was 159.4 kg s^{-1} , which comes from the total energy produced (about 2468 MWh) and an approximate average temperature difference between the generator supply and the tank bottom (22°C).

The relative difference between the heat originally produced and the heat delivered to the network tends to be smaller in winter, which is probably related to the much larger energy flows involved, of which we give a general overview in table 6.7.

What is more, there are some days of the week (Monday and Thursday) in which, for any time shift of the flow rate divergence, the energy injected in the tank is a smaller amount than the one ultimately distributed.

The peak shaving, instead, is consistently positive: the maximum amount of energy produced by the generator is, every day, smaller than the maximum consumption by an amount anywhere between 9 and 23%.

Similarly to what happens in the April simulation, the shifted energy C_{net} increases as long as the value of τ is incremented. It can reach, on Friday and Saturdays, values as high as 9 to 10 MWh. It is interesting that in the scenarios where \dot{m}_g is constant there is a sharp drop of the amount of energy that is "moved in time" (table 6.6).

Generally speaking, the values of C_{net} with a 500 cubic metre tank are also somewhat higher than those found with the circulating water providing heat storage.

From the integration of the power profiles, it becomes evident that the model tends to pre-

Table 6.6: Values selected from the simulations of the winter week, with different versions of the regime C1 compared to the constant generator mass flow

parameter	τ [h]	MON	TUE	WED	THU	FRI	SAT	SUN
ΔQ_t [%]	1.5	-1.00	0.20	0.62	-0.10	0.07	0.66	0.34
	2.5	-1.10	0.25	0.60	-0.10	0.05	0.70	0.41
	3.5	-1.09	0.28	0.63	-0.06	0.07	0.74	0.46
	4.5	-1.08	0.31	0.66	-0.01	0.09	0.78	0.48
	constant \dot{m}_g	0.23	0.27	0.74	-0.29	0.24	-0.28	1.29
ΔQ_{max} [%]	1.5	8.74	12.29	15.97	13.96	14.54	13.44	11.22
	2.5	14.39	19.06	21.67	15.32	20.97	19.68	16.38
	3.5	16.06	19.97	23.10	15.41	23.39	20.86	18.36
	4.5	15.79	19.27	23.29	15.01	23.43	20.35	19.62
	constant \dot{m}_g	7.17	10.62	10.58	9.91	9.03	12.43	17.68
C_{net} [%]	1.5	2.87	4.67	5.47	5.79	5.30	5.23	3.70
	2.5	3.93	7.75	8.21	7.66	8.15	8.43	6.94
	3.5	4.41	8.78	9.05	8.57	9.05	9.52	8.08
	4.5	4.93	9.40	9.57	9.05	9.69	10.10	8.45
	constant \dot{m}_g	3.73	3.05	2.53	0.91	1.29	0.97	2.86

dict a higher amount of energy inserted into the tank than is extracted. This difference is always smaller than 1%, tends to increase with τ and in the winter is generally not as important as in the mid-season.

The thermal losses have also been evaluated, and found to be rather small in relative terms. They amount to less than 0.1% of thermal energy discharged in all scenario, and this is especially true in the winter (as is predictable since the weekly cumulative energy flow is much larger). The change in tank energy content, at the end of the week, can be either positive or negative, and together with the losses it does not arrive to explain the discrepancy of the cumulative energy exchanges on the two sides of the tank. The evaluation of *energy* (as opposed to *power*) is likely to require further study, since these "errors" might be due to the low precision of the method of integration used for the power flows.

Table 6.8: Results in the April week with the same regulation strategy ($C1, \tau = 3.5$) and two different values of the tank volume

parameter	$V [m^3]$	MON	TUE	WED	THU	FRI	SAT	SUN
ΔQ_t [%]	500	0.42	1.12	0.49	0.17	-0.27	-0.33	0.84
	1000	0.68	1.77	0.54	0.43	-0.28	-0.27	0.74
ΔQ_{max} [%]	500	0.87	11.43	-1.17	7.77	3.95	13.89	-2.66
	1000	-2.08	5.40	-1.44	7.80	4.32	12.60	-3.18
C_{net}	500	1.86	2.92	1.79	1.87	1.80	2.51	1.92
	1000	2.26	3.64	2.15	2.33	2.14	2.84	2.39

Table 6.9: Results in the February week with the same regulation strategy ($C1, \tau = 3.5$) and two different values of the tank volume

parameter	$V [m^3]$	MON	TUE	WED	THU	FRI	SAT	SUN
ΔQ_t [%]	500	-1.09	0.28	0.63	-0.06	0.07	0.74	0.46
	1000	-1.69	0.44	0.76	-0.22	0.06	1.11	0.69
ΔQ_{max} [%]	500	16.06	19.97	23.10	15.41	23.39	20.86	18.36
	1000	19.98	21.28	26.21	22.30	27.24	23.21	21.10
C_{net}	500	4.41	8.78	9.05	8.57	9.05	9.52	8.08
	1000	6.83	13.72	13.82	13.25	14.36	14.43	11.85

Table 6.7: Different regimes with *weekly* data of energy produced and distributed, and the difference between these two values, in both absolute and percentage. Also shown are the tank energy content increase and the total losses, in absolute and percentage. All absolute quantities are expressed in MWh.

scenario	E_{gen}	E_{dist}	ΔE_w	ΔE_w [%]	ΔE_{tank}	$E_{loss,w}$	$E_{loss,rel}$ [%]
Apr, $\tau = 1.5$	825.0	823.4	1.589	0.193	-1.172	0.640	0.077
Apr, $\tau = 2.5$	824.7	823.0	1.701	0.207	-0.999	0.646	0.079
Apr, $\tau = 3.5$	825.3	822.6	2.697	0.328	-0.157	0.661	0.080
Apr, $\tau = 4.5$	826.4	823.0	3.440	0.418	0.386	0.672	0.082
Apr, const.	822.2	820.1	2.082	0.254	-0.370	0.647	0.079
Feb, $\tau = 1.5$	2469.8	2467.6	2.150	0.087	-3.600	0.581	0.024
Feb, $\tau = 2.5$	2469.7	2467.5	2.175	0.088	-3.576	0.518	0.024
Feb, $\tau = 3.5$	2469.9	2467.0	2.905	0.118	-3.598	0.587	0.024
Feb, $\tau = 4.5$	2470.4	2466.8	3.605	0.146	-3.679	0.591	0.024
Feb, const.	2473.2	2466.0	7.284	0.295	3.483	0.061	0.025

Other simulations were performed after doubling the value of the tank *volume*. It can be observed that there are no consistent variations of the energy consumption; the peak power reduction, instead, while largely unchanged in the April scenarios, shows a tendency to increase in February.

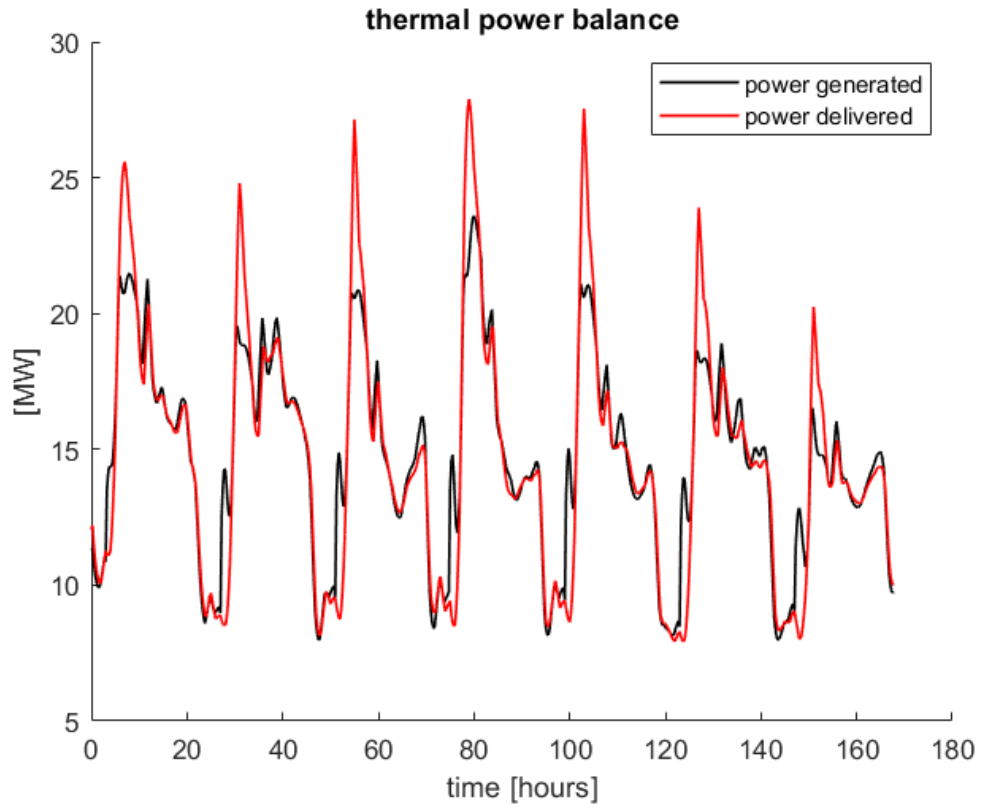


Figure 6.6: The power profiles in the February week with C1 management regime and $\tau = 3.5h$

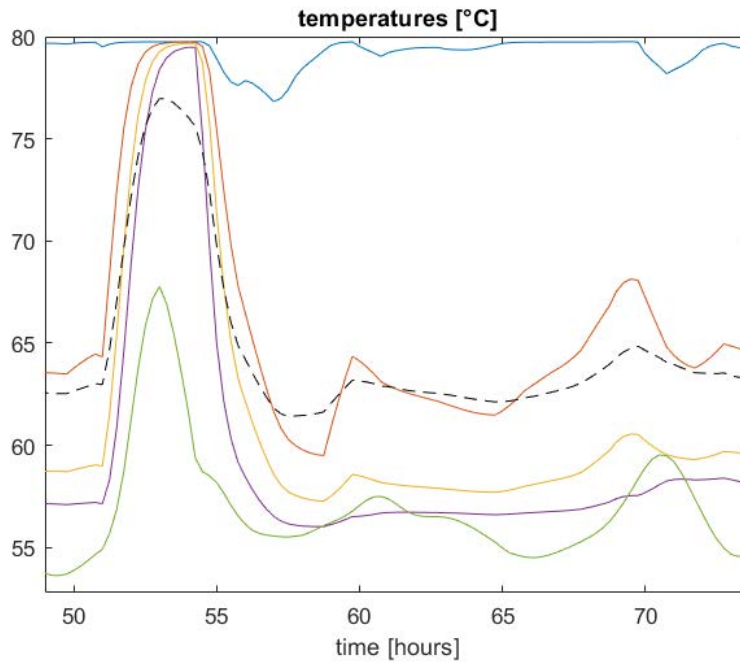


Figure 6.7: The temperature levels inside the tank during a short interval of time ("Wednesday") of the week shown in figure 6.6

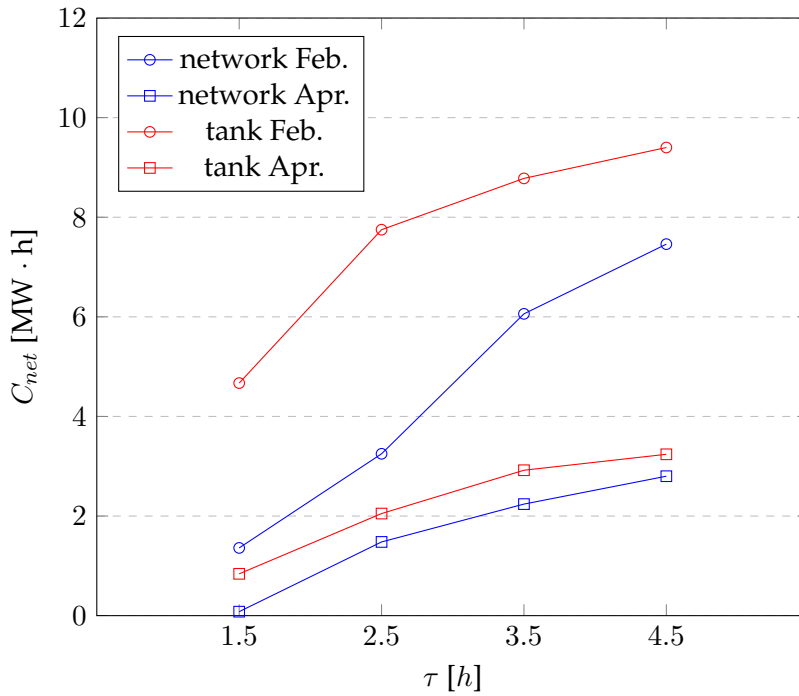


Figure 6.8: Evolution of the shifted energy for the "Tuesday" cycle with different pre-charge durations and flexibility tools

The most notable aspect of simulations with an increased tank volume is quite certainly the larger values of the energy displaced in time C_{net} . The rise is certainly not linear but definitely consistent, especially in February (tables 6.8, 6.9).

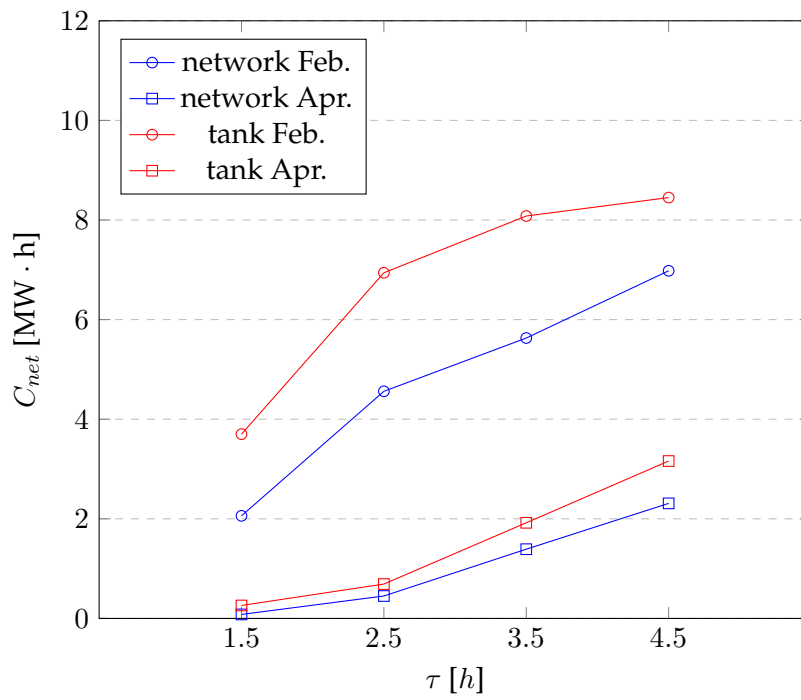


Figure 6.9: Evolution of the shifted energy for the "Sunday" cycle with different pre-charge durations and flexibility tools

7. Conclusions

The problem of whether to decouple demand from supply in district heating, and of the extent to which this should be done, lies at the intersection of economic, technological and social considerations. The choice of what instrument of flexibility to use is complex, and beyond the scope of this work.

At the core of our research, there has been the production of a simple model of a stratified reservoir, to be included in a much broader numerical representation of the whole district network of Verona. The reservoir model is based on mass and energy balance equations written for each of its sectors, where the vast majority of the energy exchanges are accounted for by the forced mass flows directly produced by the heat generator and network operation.

From a mathematical standpoint, fluid mechanics is perhaps the most complex branch of classical physics. One would expect a model almost exclusively considering conduction and forced mass flows to fall short of the goal of representing a large volume of stored stratified water. Indeed, it is possible to observe some short-lived "intersections" of the temperature profiles in the lower part of the tank, related to a certain degree of thermal inversion. Apart from these phenomena, however, the temperatures predicted by the model for return to the generator and supply to the network take reasonable values, consistent with the charging and discharging cycles that happen when the generated power overtakes consumption and then the reverse happens. It could be argued that simple models are suitable to quick-changing systems like load-following district heating networks.

By looking at the daily cycles of the average tank temperature, we find out a variation of a few degrees Celsius in the April simulations, and of around 15 degrees in the February week. This is consistent with the values of C_{net} increasing by roughly a factor of 3 between the two seasons.

A decrease of 15 °C during discharge renders an energy density, for practical purposes, of little over 60 MJ, or less than 20 kWh, per cubic metre. There are now two important considerations to make about this value.

The first is that it is compatible with the energy shift observed on winter days, which at around 10 MWh is never far away from the product of the energy density and the tank volume used in simulations.

On the other hand, 20 kWh m⁻³ is significantly smaller¹ than the numbers reported in the literature for TTES: we realise that it is important to consider the specific operational con-

¹by a factor of four compared to the numbers in [9]

ditions when evaluating a thermal storage technology.

Besides, it is interesting to notice that, by increasing the pre-charge time through the parameter τ , the increase obtained in the shifted energy is faster in April than in February. This is similar to what happens when using the network, in which case it is explained by the slower circulation of water in the pipelines during mid-season [72]. The reasons why the same phenomenon seems to happen with the tank need to be the subject of further analysis; it could be that with smaller average consumption of heat, more capacity is left to fill the reserve at every cycle.

By looking at the relative values of the additional energy consumed by the reservoir, or more correctly at the amounts by which the injected heat exceeds the heat released to the network, we find them to be consistently smaller than 1%, an acceptable value compared to the primary energy savings that are generally achieved with better generator scheduling. However, more detailed network studies are required to find out how and how much the scheduling can be improved in the specific case of Verona.

Finally, a glance at the absolute values of the shifted energy C_{net} reveals that a 500 cubic metre reservoir may be able to set aside more heat than the pre-charged network, which in the simulations has a volume of about 700 cubic metres (as per [72]).

The use of the mass of the heat distribution water as an instrument of flexibility has been found to cause discomfort to the users, while the main drawbacks of stratified reservoirs are the losses through the walls, that risk to degrade the quality of the heat, and especially the installation cost. Furthermore, in the network used in the simulations there are simple integrator meters and the control of heat withdrawal is essentially left to the customers: by investing in demand response and having the users plan, to a certain extent, their consumption, better results could be obtained from network storage. Since controls and meters need to be replaced during the lifetime of a DHN, it might be a sound strategy to introduce more advanced specimens of these machines before investing in TTES.

However, involving the consumers in the system flexibility might be seen as a way of shifting on them the costs and possible inconveniences, while the use of reservoirs is a much more "internal" decision on the part of the operator.

Ultimately, the choice is not strictly technical. In order to make informed decisions, more research can and should be conducted. For example, it would be useful to simulate the network in different conditions, like the presence of a storage system, the use of the network fluid, the introduction of demand response, or even a combination of these three options (or others). Such numerical representations should incorporate the different generators with the purpose of studying their possible scheduling regimes. Thus, it will become possible to know which choices, in both design and operation, are optimal with regard to various design objectives such as primary energy conservation, carbon emissions reduction, or integration of larger shares of waste and renewable heat.

A. MATLAB Code

The following scripts have been uploaded with the help of the `mcode.sty` package developed by Florian Knorn.

A.1 Tank Model

A.1.1 Tank Linear System Function

This function comes from the file where internal conduction was "switched off" and as a result occurrences of the parameter G were replaced with zeroes.

```
1 function[T]=fserbatoio_v1(T_g_in, mg, T_d_in, md, U_tot, A, S, C, c_p, c_p_g, c_p_d, ...
2     T_amb, n, T0)
3     mnet=mg-md;
4     %% Definition of matrix M - parameters that multiply T
5     if mnet>=0
6         M(1,:)=[1/C(1)+md*c_p(1)+mnet*c_p(1)+0+U_tot(1)*(A+S)    -0    zeros(1,n-2)];
7         M(2,:)=[-mnet*c_p(2)-0    mnet*c_p(2)+2*0+U_tot(2)*A+1/C(2)    -0 ...
8             zeros(1,n-3)];
9         h2=0;
10        for j=3:1:n-1
11            h2=h2+1;
12            filler=j-2;
13            M(j,:)=[zeros(1, filler)    -mnet*c_p(j-1)-0    ...
14                mnet*c_p(j)+2*0+U_tot(j)*A+1/C(j)    -0    zeros(1,n-3-filler)];
15        end
16        M(n,:)=[zeros(1,n-2)    -mnet*c_p(n)-0    1/C(n)+mg*c_p(n)+0+U_tot(n)*(A+S)];
17    else
18        M(1,:)=[1/C(1)+md*c_p(1)+0+U_tot(1)*(A+S)    mnet*c_p(1)-0    zeros(1,n-2)];
19        M(2,:)=[-0    -mnet*c_p(2)+2*0+U_tot(2)*A+1/C(2)    mnet*c_p(2)-0....
20            zeros(1,n-3)];
21        h2=0;
22        for j=3:1:n-1
23            h2=h2+1;
24            filler=j-2;
25            M(j,:)=[zeros(1, filler)    -0    -mnet*c_p(j)+2*0+U_tot(j)*A+1/C(j) ...
26                mnet*c_p(j)-0    zeros(1,n-3-filler)];
27        end
28        M(n,:)=[zeros(1,n-2)    -0    1/C(n)+mg*c_p(n)-mnet*c_p(n)+0+U_tot(n)*(A+S)];
29    end
30    %% Definition of known values vector
```

```

31     b(1,1)=T0(1)/C(1)+U_tot(1)*(A+S)*T_amb+mg*c_p_d*T_g_in;
32     for j2=2:1:n-1
33         b(j2,1)=T0(j2)/C(j2)+U_tot(j2)*A*T_amb;
34     end
35     b(n,1)=T0(n)/C(n)+U_tot(n)*(A+S)*T_amb+md*c_p_g*T_d_in;
36     T=M\b;
37 end

```

A.2 Code for TRNSYS Validation

A.2.1 Main Script

The script includes REFPROP evaluations of fluid properties, a calculation of the coefficient of natural convection at every step and its integration into the general energy balance.

```

1  clc
2  clear all
3  close all
4  % global V U A S tm C G c_p T_amb
5  %% Definition of parameters
6  Vtot=500; % tank volume
7  U=0.2; % global heat transfer coefficient [W m-2 K-1]
8  H=17; % tank height
9  S=Vtot/H; % horizontal surface
10 r=sqrt(S/pi); % tank radius
11 f=H/(2*r); % aspect ratio
12 tm=300; % duration of timestep (linear system)
13 tau=900; % timestep of inputs (boundary conditions)
14 n=5; % number of tank sectors
15 deltax=H/n; % height of a tank sector
16 A=2*pi*r*deltax; % lateral surface of a sector
17 V=Vtot/n; % sector volume
18 T_amb=20; % ambient temperature
19 deltaT=20; % approximate temp difference to estimate energy flow
20 g=9.81; % gravitational acceleration
21
22 T0=linspace(80, 60, n); % initial tank temperatures (simplified representation)
23 T0_initial=T0; % for completeness of plots
24
25 BCinputs_00=xlsread('dati_in_sim','mass1'); % input reading
26 BCinputs_0=BCinputs_00(2:length(BCinputs_00),:); % elimination of t=0
27 BCinputs=inputmodif(BCinputs_0, tm, tau); % "expansion" of input...
28 % ...vectors: make a more detailed simulation
29 % than the inputs, with timestep tm instead of
30 % tau (NB: tau/tm must be INTEGER)
31 simulationTime=length(BCinputs); % number of *model* timesteps
32
33 T_hist = zeros(simulationTime, n); % preallocation of temp matrix
34 h_in=100; % first approx value of nat conv coeff

```

```

35 T0_av=mean(T0); % Tank uniform T in first approx
36
37 U_tot=1/(1/h_in+1/U)*ones(1,n); % global wall HTC
38 T_s0=T_amb+U_tot/U*(T0_av-T_amb); % Wall inner T in first approx
39 T_s_initial=T_s0;
40
41 %% Dynamic evaluation of tank temperature
42 for t=1:1:simulationTime
43     T_g_in=BCinputs(t,1);
44     T_d_in=BCinputs(t,3);
45     mg=BCinputs(t,2);
46     md=BCinputs(t,4);
47
48     c_p_g=refpropm('C','T',T_g_in+273.15,'P',101.325,'water');
49     c_p_d=refpropm('C','T',T_d_in+273.15,'P',101.325,'water');
50
51     T_av=mean(T0);
52
53     for i=1:1:n
54         T_s(i)=T_s0(i); % Wall inner T in this timestep
55         Tf(i)=(T_s(i)+T0(i))/2;
56         rho(i)=refpropm('D','T',T0(i)+273.15,'P',101.325,'water');
57         c_p(i)=refpropm('C','T',T0(i)+273.15,'P',101.325,'water');
58
59         lambda(i)=refpropm('L','T',T0(i)+273.15,'P',101.325,'water');
60
61         beta(i)=refpropm('B','T',Tf(i)+273.15,'P',101.325,'water');
62         nu(i)=refpropm('$','T',Tf(i)+273.15,'P',101.325,'water');
63         alpha(i)=refpropm('%','T',Tf(i)+273.15,'P',101.325,'water');
64         C(i)=tm./(rho(i).*V.*c_p(i)); % for synthesis in formulae
65         G(i)=lambda(i).*S./deltaz;
66
67         Ra(i)=g*beta(i)*abs(T0(i)-T_s(i))*(2*r)^3/(nu(i)*alpha(i)*(1/10^8));
68         C_Nu=0.125; % parameters for Nusselt, from MATES, 1987
69         m=0.3333; % (Ra is very large)
70         Nu(i)=C_Nu*Ra(i)^m;
71         h_in(i)=lambda(i)*Nu(i)/(2*r);
72         U_tot(i)=1/(1/h_in(i)+1/U);
73     end
74     h_in_hist0(t,:)=h_in;
75     Ra_hist0(t,:)=Ra;
76
77     T=fserbatoio_v1(T_g_in, mg, T_d_in, md, U_tot, A, S, C, c_p, c_p_g, c_p_d,...
78         T_amb, n, T0);
79
80     for i=1:1:n % Calculation of the new value
81                 % of the wall inner temperature
82         T_s0(i)=T_amb+U_tot(i)/U*(T(i)-T_amb);
83     end
84
85     mnet=mg-md; % mass flow rate inside the tank
86     T_d_supply=T(1);
87     T_g_return=T(n);
88     T0='T'; % definition of the new value of T0

```

```

89
90     Q_g_eff=mg*c_p_g*(T_g_in-T(n))/10^6;    % power actually delivered to tank [MW]
91     Q_d_eff=md*c_p(1)*(T(1)-T_d_in)/10^6;    % power actually delivered to net [MW]
92
93     T_hist_0(t,:)=T';                        % compilation of matrices with
94                                           % recorded values of temp...
95     T_s_hist_0(t,:)=T_s0;
96     mg_hist_0(t,:)=mg;                       %...mass flow rates...
97     md_hist_0(t,:)=md;
98     mnet_hist_0(t,:)=mnet;
99     Q_g_eff_hist_0(t,:)=Q_g_eff;             %...and delivered heating power
100    Q_d_eff_hist_0(t,:)=Q_d_eff;
101    hora_0(t)=t*tm/3600;                       % time in hours, used in charts
102    Q_g_hist_0(t)=mg*c_p_g*deltaT/10^6;       % approx enthalpy from gen w.r.t.0 C
103    Q_d_hist_0(t)=md*c_p_d*deltaT/10^6;       % approx enthalpy from net w.r.t.0 C
104 end
105 %% Extraction of vector values to match the number of simulation timesteps
106 h_in_hist=sampling(h_in_hist0, tm, tau);
107 Ra_hist=sampling(Ra_hist0, tm, tau);
108 T_hist=sampling(T_hist_0, tm, tau);
109 T_s_hist=sampling(T_s_hist_0, tm, tau);
110 mg_hist=sampling(mg_hist_0, tm, tau);
111 md_hist=sampling(md_hist_0, tm, tau);
112 mnet_hist=sampling(mnet_hist_0, tm, tau);
113 Q_g_eff_hist=sampling(Q_g_eff_hist_0, tm, tau);
114 Q_d_eff_hist=sampling(Q_d_eff_hist_0, tm, tau);
115 hora=sampling(hora_0', tm, tau);             % time in seconds, used in charts
116 Q_g_hist=sampling(Q_g_hist_0', tm, tau);     % absolute enthalpy from gen supply
117 Q_d_hist=sampling(Q_d_hist_0', tm, tau);     % absolute enthalpy from net return
118 %% Matrices and vectors are overwritten to include instant zero (for plots)
119 T_hist=[T0_initial; T_hist];
120 T_s_hist=[T_s_initial; T_s_hist];
121 mg_hist=[BCinputs(1,2); mg_hist];
122 md_hist=[BCinputs(1,4); md_hist];
123 Q_g=[BCinputs(1,2)*c_p(1)*deltaT/10^6; Q_g_hist];
124 Q_d=[BCinputs(1,4)*c_p(n)*deltaT/10^6; Q_d_hist];
125 Q_g_eff_hist=[BCinputs(1,2)*c_p(1)*deltaT/10^6; Q_g_eff_hist];
126 Q_d_eff_hist=[BCinputs(1,4)*c_p(n)*deltaT/10^6; Q_d_eff_hist];
127 mnet_hist=mg_hist-md_hist;
128 hora=[0; hora];
129 Hist=[hora T_hist mg_hist md_hist mnet_hist Q_g_eff_hist Q_d_eff_hist];
130
131 %% Print output values in a digital spreadsheet (valid for n=5 sectors)
132 filename='outputs_2.xlsx';
133 % writematrix(T_hist,filename,'Sheet',2,'Range','A2:J97');
134 TM = array2table(T_hist,'VariableNames',{'T1','T2','T3','T4','T5'});
135
136 writetable(TM,filename,'Sheet','MATLABresults','WriteVariableNames',true);
137 TT = readtable('output_tank.txt','Format','auto');    % Read .txt file with
138                                           % TRNSYS values and print them on spreadsheet
139 writetable(TT,filename,'Sheet','TRNSYSresults','WriteVariableNames',true);
140
141 T_av=mean(T_hist');                            % average tank temperature
142 %% PLOTS

```

```

143 figure(1);
144 plot(hora, T_hist(:, 1));
145 hold on
146 plot(hora, T_hist(:, 2));
147 plot(hora, T_hist(:, 3));
148 plot(hora, T_hist(:, 4));
149 plot(hora, T_hist(:, n));
150 plot(hora, T_av, 'k--');
151 hold off
152 title('temperatures [ C ]');
153 xlabel('time [hours]');
154 figure(2);
155 yyaxis left;
156 plot(hora, mg_hist, 'k--');
157 hold on
158 plot(hora, md_hist, 'r--');
159 ylabel('[kg/s]');
160 yyaxis right;
161 plot(hora, Q_g, 'k-');
162 plot(hora, Q_d, 'r-');
163 plot(hora, Q_g_eff_hist, 'k-.');
164 plot(hora, Q_d_eff_hist, 'r-.');
165 hold off
166 ylabel('[MW]');
167 title('flow rates and thermal power balance');
168 xlabel('time [hours]');
169 legend('generator mass flow', 'network mass flow', 'gen power (1st approx)',...
170       'net power (1st approx)', 'power consumed', 'power delivered');

```

A.2.2 Support Functions

The goal of these functions is to produce an input signal with closer values than the original one, and then to "summarise" the model output so that it has the same number of timesteps as the input.

```

1 function BCinputs=inputmodif(BCinputs_0, tm, tau)
2 BCinputs=[];
3     for i=1:1:length(BCinputs_0(:,1))
4         riga=BCinputs_0(i,:);
5         righe=repmat(riga,tau/tm,1);
6         BCinputs=[BCinputs; righe];
7     end
8 end

1 function output=sampling(output_0, tm, tau)
2 freq=tau/tm;
3 indici=freq:freq:length(output_0);
4 output=output_0(indici,:);
5 end

```

A.3 Full Simulation

This script requires many more functions to work; we have only included the "original" scripts.

```
1
2 clc; clear all; close all;
3
4 %% Parameters pre-processing Storage Tank
5 % calculates all parameters
6 Storage_preProcessingModule;
7 % saves storage parameters into .mat file
8 save('storagePars')
9 storageParams = load('storagePars');
10
11 %% Load input files NeMo
12 filename_load = 'input_sim-standard\nemo_item1_loads_FEB_ED_AGSM_CCC_standard.xlsx';
13 filename_subs = 'input_sim-standard\substationStatus.xlsx';
14 filename_net = 'input_sim-standard\nemo_item3_net_AGSM_CCC_standard.xlsx';
15 filename_ground = 'input_sim-standard\nemo_item4_ground_FEB_AGSM_CCC.xlsx';
16 filename_prms = 'input_sim-standard\nemo_params_AGSM_CCC.xlsx';
17
18 %% Start simulation
19 start_time = datetime('now');
20 start_time_str = {datestr(start_time)};
21
22 %% Parameters pre-processing NeMo
23 % calculates all parameters
24 NeMo_preProcessingModule;
25 % saves network parameters into .mat file
26 save('netPars')
27 netParams = load('netPars');
28
29 %% Simulation start
30 tStart = tic;
31 T0=linspace(T_0(148), 60, n); % initial tank temperatures
32 T0_initial=T0; % for completeness of plots
33 [T_s0] = Ts0_initialFun(storageParams, T0);
34 T_s_initial=T_s0;
35
36 for t=1:1:SimulationTime
37
38 % STORAGE TANK -----
39 % Update boundary conditions Storage Tank -----
40 T_g_in=BCinputs(t,1);
41 T_d_in=Tr_0(148);
42 mg=BCinputs(t,2);
43 md=BCinputs(t,3);
44 c_p_g=refpropm('C','T',T_g_in+273.15,'P',101.325,'water');
45 c_p_d=refpropm('C','T',T_d_in+273.15,'P',101.325,'water');
46
47 % Run U_tot function
```

```

48 [U_tot, C, c_p, h_in, Ra, rho] = UtotFun(storageParams, T0, T_s0);
49 h_in_hist0(t,:)=h_in;
50 Ra_hist0(t,:)=Ra;
51
52 % Run Storage Tank function
53 [T_st, T_s0] = fserbatoio_v1(storageParams, T0, T_g_in, mg, T_d_in, md,...
54     U_tot, C, c_p, c_p_g, c_p_d);
55
56 A = storageParams.A; %% calculation of LOSSES at timestep
57 S = storageParams.S;
58 Area_loss=A*ones(1,n);
59 Area_loss(1)=Area_loss(1)+S;
60 Area_loss(n)=Area_loss(n)+S;
61 Q_loss_sec_coeff=U_tot.*Area_loss;
62 Q_loss_sec=Q_loss_sec_coeff.*(T_st-T_amb)';
63 Q_loss=sum(Q_loss_sec)/10^6;
64
65 T_d_supply=T_st(1);
66
67 mnet=mg-md; % mass flow rate inside the tank
68 T0=T_st'; % definition of the new value of T0
69
70 Q_g_eff=mg*c_p_g*(T_g_in-T_st(n))/10^6; % power actually delivered to tank [MW]
71
72 % Save values Storage Tank-----
73 T_st_hist_0(t,:)=T_st'; % compilation of matrices with temp...
74 T_s_hist_0(t,:)=T_s0;
75 mg_hist_0(t,:)=mg; %...mass flow rates...
76 md_hist_0(t,:)=md;
77 mnet_hist_0(t,:)=mnet;
78 Q_g_eff_hist_0(t,:)=Q_g_eff; %...and delivered heating power
79 hora_0(t)=t*tm/3600; % time in hours, used in charts
80 Q_g_hist_0(t)=mg*c_p_g*deltaT/10^6; % enthalpy entering from gen w.r.t.0
81 Q_loss_hist_0(t,:)=Q_loss;
82
83 % Update boundary conditions NeMo -----
84 G_ext = G_extm(t,:); % update users mass flow rates
85 heatLoad = q_loads(t,:); % update users heat demand
86 temp_inlet = T_d_supply; % update supply temperatures
87 T_ground = groundTemp(t);
88
89 % Run NeMo function -----
90 [G,v,P,Pr,T,Tr] = pNeMoFun(netParams, T_0, Tr_0, G_0, G_1, P_0, ...
91     G_ext, temp_inlet, heatLoad, T_ground);
92
93 Q_d_eff = md*c_p(1)*(T_st(1)-Tr(148))/10^6; % power actually delivered
94 %to network [MW]
95
96 % Save values NeMo-----
97 G_hist(t,:) = G;
98 v_hist(t,:) = v;
99 P_hist(t,:) = P;
100 Pr_hist(t,:) = Pr;
101 T_hist(t,:) = T;

```

```

102     Tr_hist(t,:) = Tr;
103     Q_d_eff_hist_0(t,:) = Q_d_eff;
104     Q_d_hist_0(t)=md*c_p_d*deltaT/10^6;           % enthalpy entering from net w.r.t.0
105
106     % Update initial state -----
107     T_0 = T;
108     Tr_0 = Tr;
109
110     % Update guess vectors for G and P -----
111     G_0 = G;
112     G_1 = 0.8*G_0 + 0.2*G_0.*rand(nb,1);
113
114     % Print simulation time -----
115     time = t*tstep/3600           % hr
116
117 end
118
119 tElapsed = toc(tStart);
120 % stop_time = datetime('now');
121 % stop_time_str = {datestr(stop_time)};
122
123
124 %% Post-processing Storage Tank
125 h_in_hist=sampling(h_in_hist0, tm, Tau);
126 Ra_hist=sampling(Ra_hist0, tm, Tau);
127
128 T_st_hist=sampling(T_st_hist_0, tm, Tau);
129 T_s_hist=sampling(T_s_hist_0, tm, Tau);
130 mg_hist=sampling(mg_hist_0, tm, Tau);           %...mass flow rates...
131 md_hist=sampling(md_hist_0, tm, Tau);
132 mnet_hist=sampling(mnet_hist_0, tm, Tau);
133 Q_g_eff_hist=sampling(Q_g_eff_hist_0, tm, Tau); %...and delivered heating power
134 Q_d_eff_hist=sampling(Q_d_eff_hist_0, tm, Tau); % time in seconds, used in charts
135 hora=sampling(hora_0', tm, Tau);
136 Q_g_hist=sampling(Q_g_hist_0', tm, Tau);       % absolute enthalpy, gen supply
137 Q_d_hist=sampling(Q_d_hist_0', tm, Tau);       % absolute enthalpy, net return
138 Q_loss_hist=sampling(Q_loss_hist_0, tm, Tau);
139 %% Matrices and vectors are overwritten to include instant zero
140 T_st_hist=[T0_initial; T_st_hist];             % commands to include t=0
141 T_s_hist=[T_s_initial; T_s_hist];
142 mg_hist=[BCinputs(1,2); mg_hist];             %...mass flow rates...
143 md_hist=[BCinputs(1,3); md_hist];
144 Q_g=[BCinputs(1,2)*c_p(1)*deltaT/10^6; Q_g_hist];
145 Q_d=[BCinputs(1,3)*c_p(n)*deltaT/10^6; Q_d_hist];
146 Q_g_eff_hist=[BCinputs(1,2)*c_p(1)*deltaT/10^6; Q_g_eff_hist];
147 Q_d_eff_hist=[BCinputs(1,3)*c_p(n)*deltaT/10^6; Q_d_eff_hist];
148
149     Q_loss_sec_coeff=U_tot.*Area_loss;
150     Q_loss_sec0=Q_loss_sec_coeff.*(T0_initial-T_amb);
151     Q_loss0=sum(Q_loss_sec0)/10^6;
152 Q_loss_hist=[Q_loss0; Q_loss_hist_0];
153 mnet_hist=mg_hist-md_hist;
154
155 hora=[0; hora];

```



```

156 Hist=[hora T_st_hist mg_hist md_hist mnet_hist Q_g_eff_hist Q_d_eff_hist];
157
158 T_av=mean(T_st_hist'); % average tank temperature
159 %% Copy energy flows into spreadsheet
160 filename='power_results_apr.xlsx';
161 Qeff_hist=[Q_g_eff_hist Q_d_eff_hist];
162 QEFF=array2table(Qeff_hist, 'VariableNames', {'Q_gen [MW]', 'Q_net [MW]'});
163 writetable(QEFF,filename,'Sheet','power','WriteVariableNames',true);
164 %% Evaluate performance parameters
165 Eth_ref_week=sum(Q_d_eff_hist*(Tau/3600)); %[MWh] energy on the two sides in a week
166 Eth_mod_week=sum(Q_g_eff_hist*(Tau/3600));
167 deltaQt_week_abs=Eth_mod_week-Eth_ref_week;
168 deltaQt_week=(Eth_mod_week-Eth_ref_week)/Eth_ref_week;
169 deltaQt_week_pc=deltaQt_week*100;
170
171 Eth_loss=sum(Q_loss_hist*(Tau/3600)); % energy lost in the week [MWh]
172 Eth_loss_pc=(Eth_loss/Eth_ref_week)*100;
173 %% Power peak shaving and energy production variation, day by day
174 NC=7; % Number of cycles
175 % Results_para=fpshaving(NC,Q_d_eff_hist,Q_g_eff_hist, Tau);
176 % deltaQmax_pc=deltaQmax_dd_hist*100;
177 [Qmax_ref_dd_hist, Qmax_mod_dd_hist, absDeltaQmax_hist, deltaQmax_dd_hist, Eth_ref_hist,...
178 Eth_mod_hist, deltaQt_hist,deltaQt_pc_hist]=fpshaving(NC,Q_d_eff_hist,Q_g_eff_hist,Tau
179 deltaQmax_pc=deltaQmax_dd_hist*100;
180 para_perf=[deltaQt_pc_hist; deltaQmax_pc];
181 PARA=array2table(para_perf, 'VariableNames', {'MON', 'TUE', 'WED', 'THU', 'FRI', 'SAT',...
182 'SUN'}, 'RowNames', {'deltaQt [%]', 'deltaQmax [%]'});
183 writetable(PARA,filename,'Sheet','performances','WriteVariableNames',true,...
184 'WriteRowNames', true);
185 %% Calculation of approximate tank energy content increase
186 Vtot=storageParams.Vtot;
187 Tinterm=(T_av(1)+T_av(length(T_av)))/2;
188 rho_interm=refpropm('D','T',Tinterm+273.15,'P',101.325,'water');
189 c_p_interm=refpropm('C','T',Tinterm+273.15,'P',101.325,'water');
190 deltaEnergyTank=c_p_interm*rho_interm*Vtot*(T_av(length(T_av))-T_av(1))/(3.6*10^9);
191 %% Plots Storage Tank
192 figure(1);
193 plot(hora, T_st_hist(:, 1));
194 hold on
195 plot(hora, T_st_hist(:, 2));
196 plot(hora, T_st_hist(:, 3));
197 plot(hora, T_st_hist(:, 4));
198 plot(hora, T_st_hist(:, n));
199 plot(hora, T_av, 'k--');
200 hold off
201 title('temperatures [ C ]');
202 xlabel('time [hours]');
203 figure(2);
204 yyaxis left;
205 plot(hora, mg_hist, 'k--');
206 hold on
207 plot(hora, md_hist, 'r--');
208 ylabel(' [kg/s] ');
209 yyaxis right;

```

```

210 plot(hora, Q_g_eff_hist, 'k-.');
211 plot(hora, Q_d_eff_hist, 'r-.');
212 hold off
213 ylabel(' [MW] ');
214 title('flow rates and thermal power balance');
215 xlabel('time [hours]');
216 legend('generator mass flow', 'network mass flow', 'generator power', 'demanded power',...
217        'power consumed', 'power delivered');
218 figure(3);
219 plot(T_hist(:,148), 'Linewidth',1.5)
220 hold on
221 plot(Tr_hist(:,148), 'Linewidth',1.5)
222 hold on
223 legend('T', 'Tr')
224 grid on
225 figure(4);
226 hold on
227 plot(hora, Q_g_eff_hist, 'k', 'Linewidth', 1.0);
228 plot(hora, Q_d_eff_hist, 'r', 'Linewidth', 1.0);
229 hold off
230 ylabel(' [MW] ');
231 title('thermal power balance');
232 xlabel('time [hours]');
233 legend('power generated', 'power delivered');

```

Function for performance parameter evaluation:

```

1 function [Qmax_ref_dd_hist, Qmax_mod_dd_hist, absDeltaQmax_hist, deltaQmax_dd_hist,...
2         Eth_ref_hist, Eth_mod_hist, deltaQt_hist,deltaQt_pc_hist]=...
3         fppshaving(NC,Q_d_eff_hist,Q_g_eff_hist,Tau)
4         cyclength=length(Q_d_eff_hist)/NC;
5         for dd=0:1:(NC-1)
6             Q_d_eff_hist_dd=Q_d_eff_hist(dd*cyclength+1:(dd+1)*cyclength);
7             Q_g_eff_hist_dd=Q_g_eff_hist(dd*cyclength+1:(dd+1)*cyclength);
8             Qmax_ref_dd=max(Q_d_eff_hist_dd);
9             Qmax_mod_dd=max(Q_g_eff_hist_dd);
10            absDeltaQmax=Qmax_mod_dd-Qmax_ref_dd;
11
12            deltaQmax_dd=(Qmax_ref_dd-Qmax_mod_dd)/Qmax_ref_dd;
13            Eth_ref=sum(Q_d_eff_hist_dd*(Tau/3600)); %[MWh] energy
14            Eth_mod=sum(Q_g_eff_hist_dd*(Tau/3600));
15            deltaQt=(Eth_mod-Eth_ref)/Eth_ref;
16            deltaQt_pc=deltaQt*100;
17
18            Qmax_ref_dd_hist(dd+1)=Qmax_ref_dd;
19            Qmax_mod_dd_hist(dd+1)=Qmax_mod_dd;
20            absDeltaQmax_hist(dd+1)=absDeltaQmax;
21            deltaQmax_dd_hist(dd+1)=deltaQmax_dd;
22            Eth_ref_hist(dd+1)=sum(Q_d_eff_hist_dd*(Tau/3600)); %[MWh] energy
23            Eth_mod_hist(dd+1)=sum(Q_g_eff_hist_dd*(Tau/3600));
24            deltaQt_hist(dd+1)=(Eth_mod-Eth_ref)/Eth_ref;
25            deltaQt_pc_hist(dd+1)=deltaQt_pc;
26        end
27 end

```

B. Tables and Charts

B.1 General Notes

Table B.1: Selected DH heat storage structures, from [9] and [31]

Country	City	Technology	Volume [m ³]	Height [m]	Width [m]	A/V ratio
D	Hamburg	buried tank TES	4500	10.7	25.7	0.37
D	Friedrichshafen	buried tank TES	1200	19.4	32.4	0.23
D	Crailsheim	buried tank TES	480	14.5	6.3	0.75
AT	Linz	freestanding TTES	34500	65	29	0.18
D	Jena	freestanding TTES	13000	43	21	0.27
D	Ulm	freestanding TTES	2500	27	11.5	0.47
I	Turin	freestanding TTES	833 (9×)	24.0	6.7	0.68
NL	Diemen	freestanding TTES	23715	56	26	0.23
D	Chemnitz	pit TES, gravel-water	8000	7	39	0.42
D	Egenhausen	pit TES, sand/soil- water	300	4	8.7	1.2
S	Anneberg	BTES, ground	60000	-	-	-

Table B.2: Materials used as latent thermal storage media. Selection from [1], based on phase change conditions reasonably close to DH temperatures.

Type	Material	Phase change temperature [°C]	Density [kg m ⁻³]	Thermal conductivity [W m ⁻¹ K ⁻¹]	Latent Heat [kJ kg ⁻¹]	Volumetric storage capacity [MJ m ⁻³]
paraffins	n-hexadecane	20	733 (l)	0.21	236	182.4
	n-eicozane	36.6	788 (l)	\	247	194.6
	n-pentacozane	53.5	801 (l)	\	238	190.6
fatty acids	palmitic acid	64	989 (l)	0.162 (68.4 °C)	185.4	183.4
	stearic acid	69	940 (l)	\	209	196.5
alcohols	D-sorbitol	97	1490	\	110	163.9
	xylitol	93	1520	\	280	425.6
salt hydrates	Ba(OH) ₂ ·8H ₂ O	78	2070 (s) 1937 (l, 84 °C)	1.225 (s) 0.653 (l)	265.7	550
	MgCl ₂ · 6H ₂ O	117	1569 (s) 1450 (l, 120°C)	0.694 (s) 0.570 (l, 120 °C)	168.6	264.5
salts	AlCl ₃	192	\	\	280	\
	KNO ₃	335	2109 (s)	0.5	266	561
	LiF	850	2640 (s) 1810 (l)	\		2756.2
metals	zinc	419	7140	116	113	806.8
	aluminium	660	2707	204	397	1074.7
alloys	Zn-Mg (53.7-46.3)	340	4600 (s)	\	185	851

Table B.3: Solid materials used as sensible thermal storage media, selected from [1] and with information on concrete provided by [60].

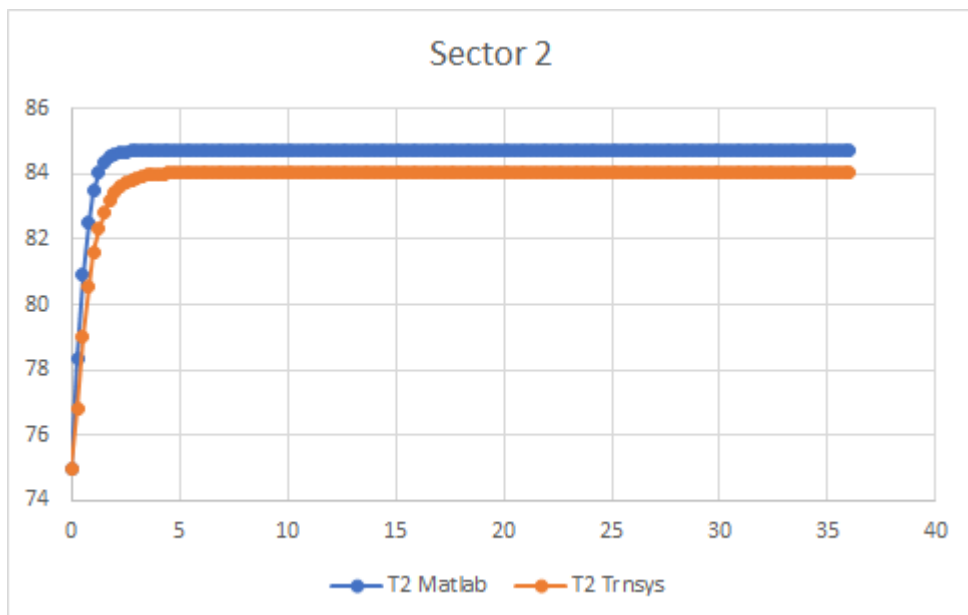
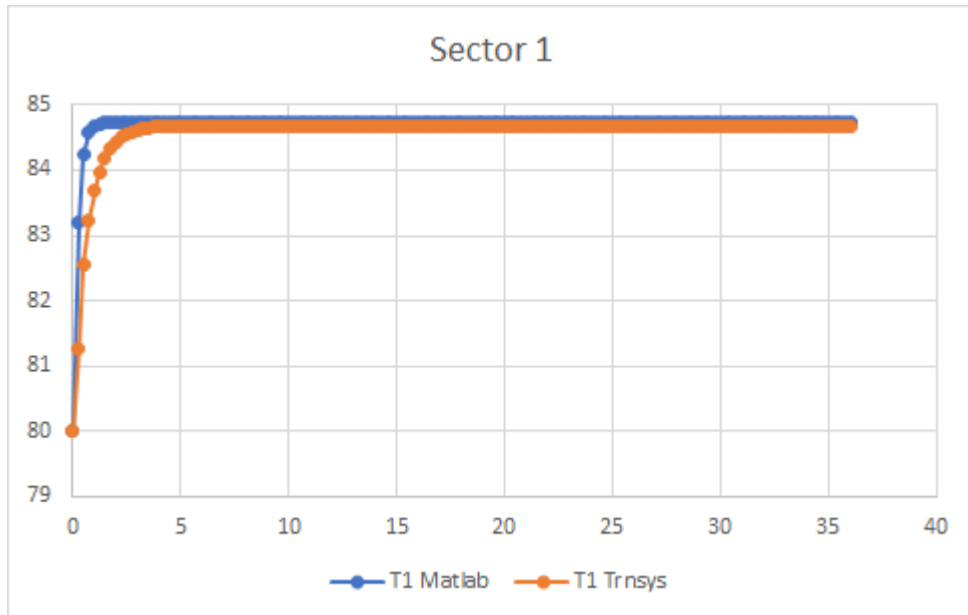
Material	Density [kg m ⁻³]	Thermal cond. [W m ⁻¹ K ⁻¹]	Spec. heat capacity [kJ kg ⁻¹]
concrete (normal, gravel aggregate)	2248	1.98	0.741
concrete (structural lightweight, Stalite aggregate)	1811	1.21	0.932
concrete (structural lightweight, Argex aggregate)	1541	0.94	1
cement paste	1990	0.52	0.703
cement paste, with 0.8% Methylcellulose	1840	0.38	0.742
granite	2530-2620	2.8	0.6-1.2
basalt	2610-2670	3.2	1.47

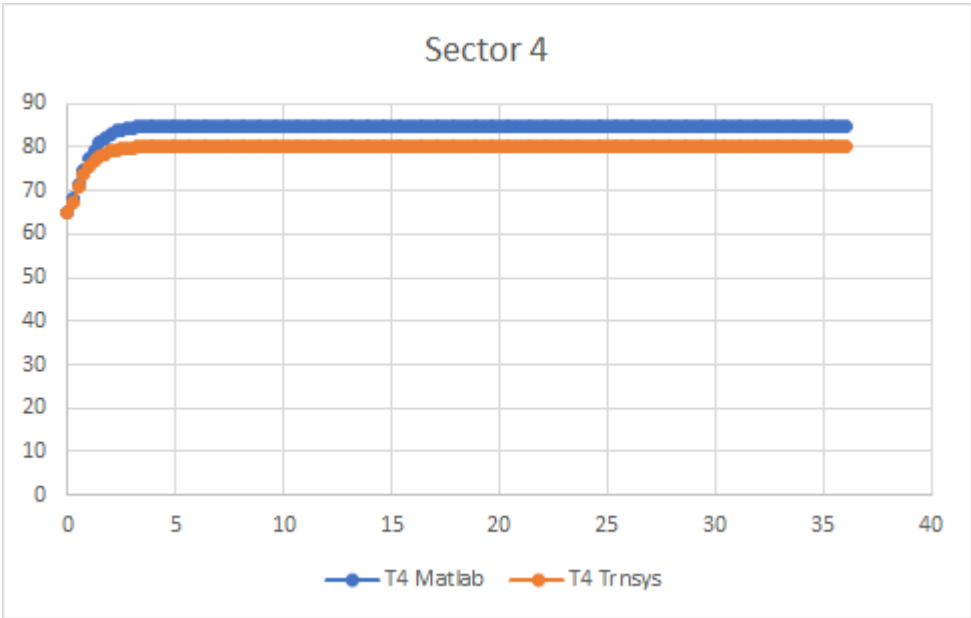
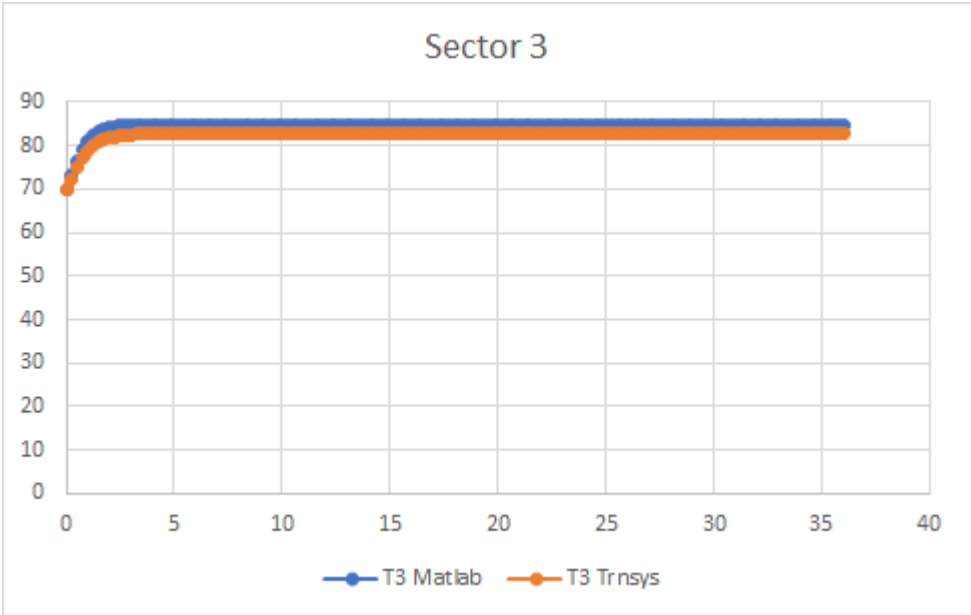
Table B.4: Liquid materials used as sensible thermal storage media, from [1]

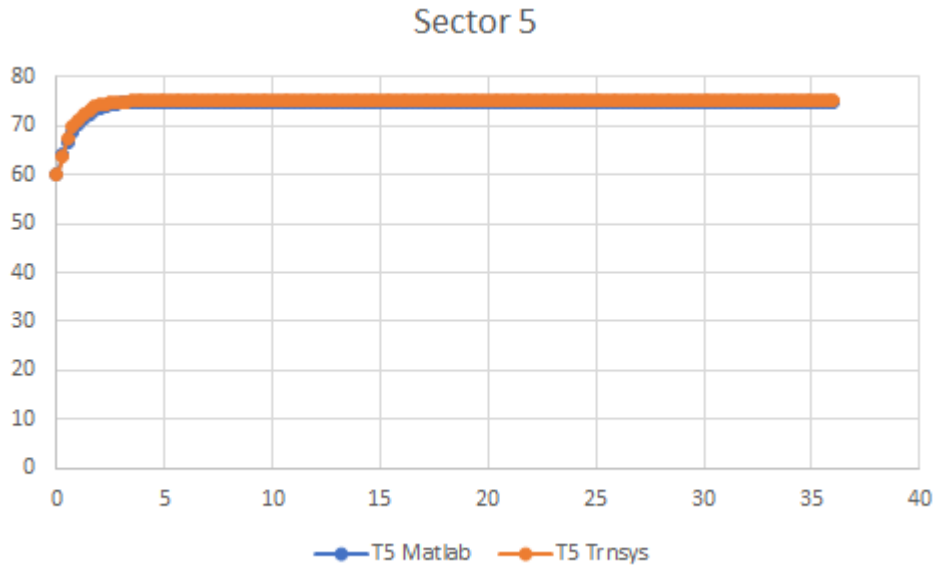
Type	Material	Melting Point [°C]	Atm. Boiling Point [°C]	Density (liq., 40 °C) [kg m ⁻³]	Density (liq., 210 °C) [kg m ⁻³]	Thermal cond. at 40°C [W m ⁻¹ K ⁻¹]	Thermal cond. at 210°C [W m ⁻¹ K ⁻¹]	Spec. heat capacity at 210 °C [kJ kg ⁻¹ K ⁻¹]
inorganic	water	0	100	992	853	0.63	0.65	4.55
diphenyl oil	Therminol® VP-1	12	257	1068	904	\	0.11	2.075
polysiloxane	Syltherm XLT®	-111	200	834	660	\	0.06	2.171
paraffinic oil	Xceltherm 600®	\	301	841	736	\	0.12	2.643
vegetable	triglycerids	\	\	926	802	\	0.11	2.509

B.2 Validation Results

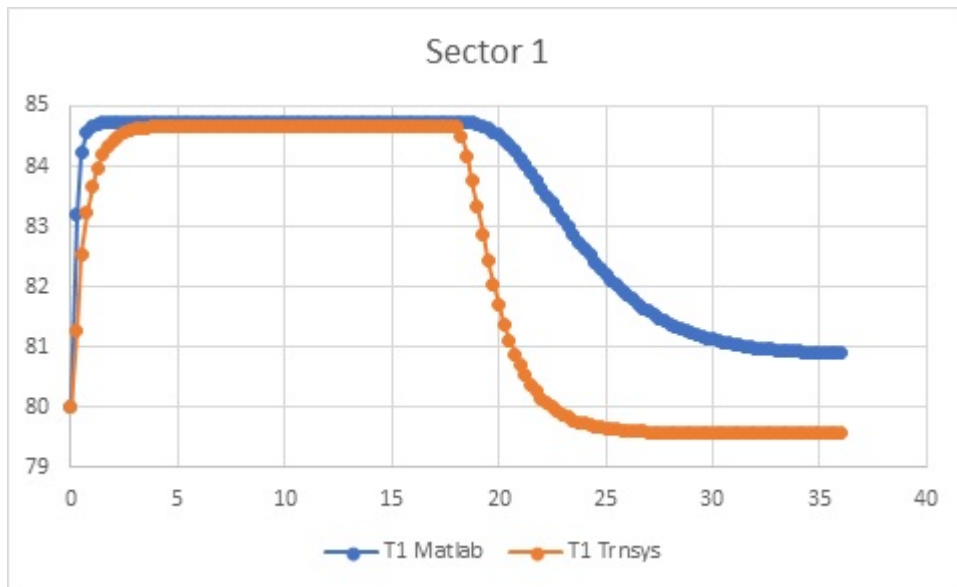
Comparison of results given for every tank sector by the TRNSYS model and by our own script, in steady-state operation with different mass flows on the two sides of the tank.

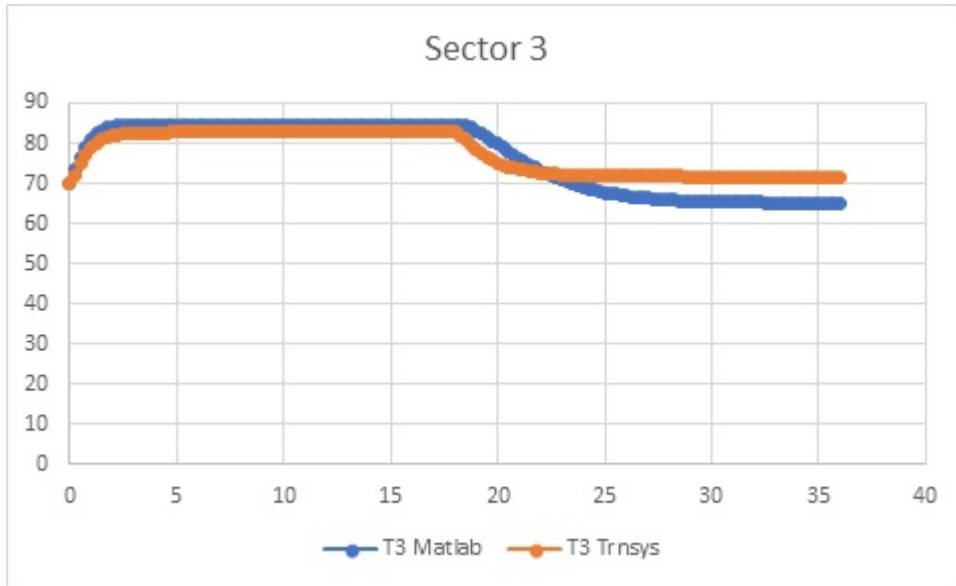




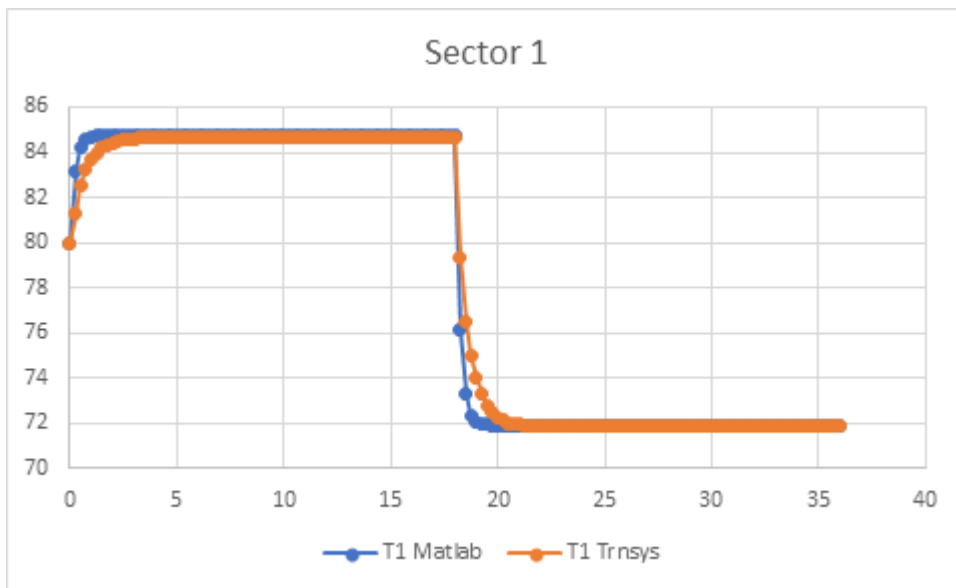


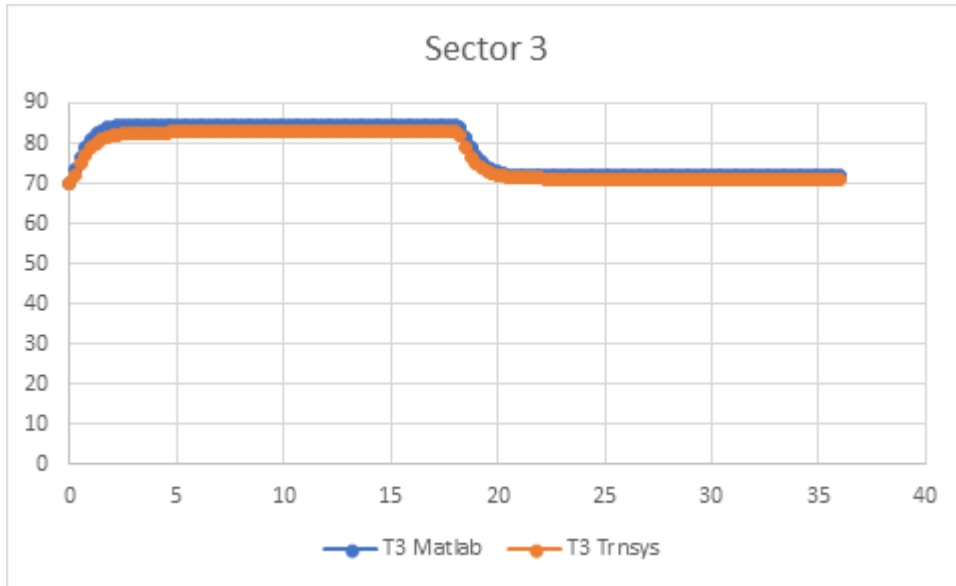
Now let us introduce the validation results in a situation where the mass flow rates were changed and brought close together: as it is evident, the MATLAB model shows a slower response.





The two simulations behave in a reasonably similar way when the change happens at the temperature level.





B.3 Selected Simulations

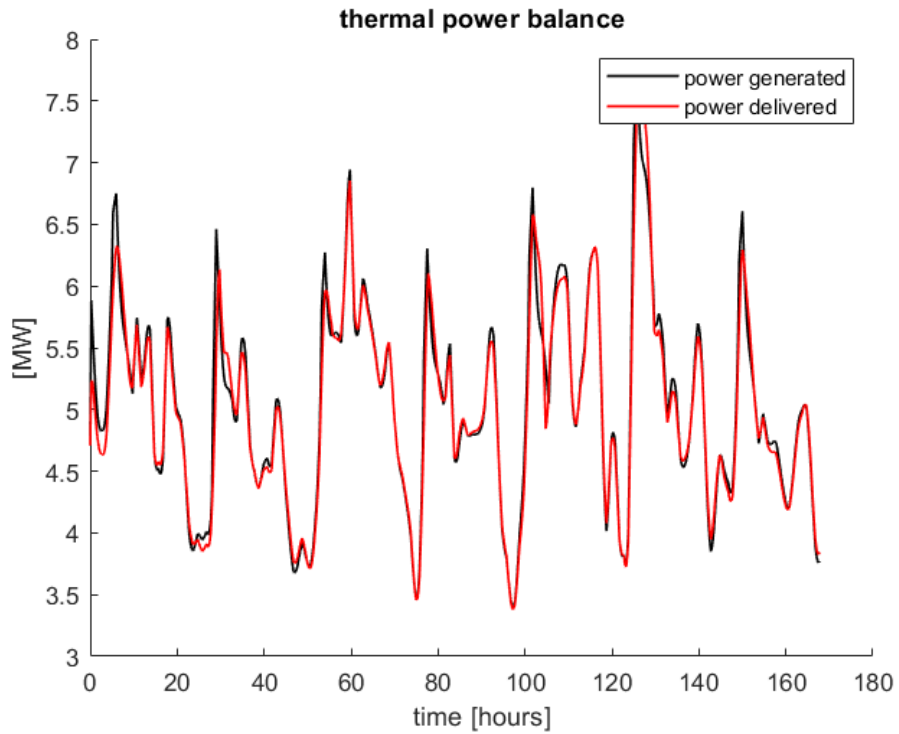


Figure B.1: The power profiles in the April week simulated with $\tau = 1.5h$

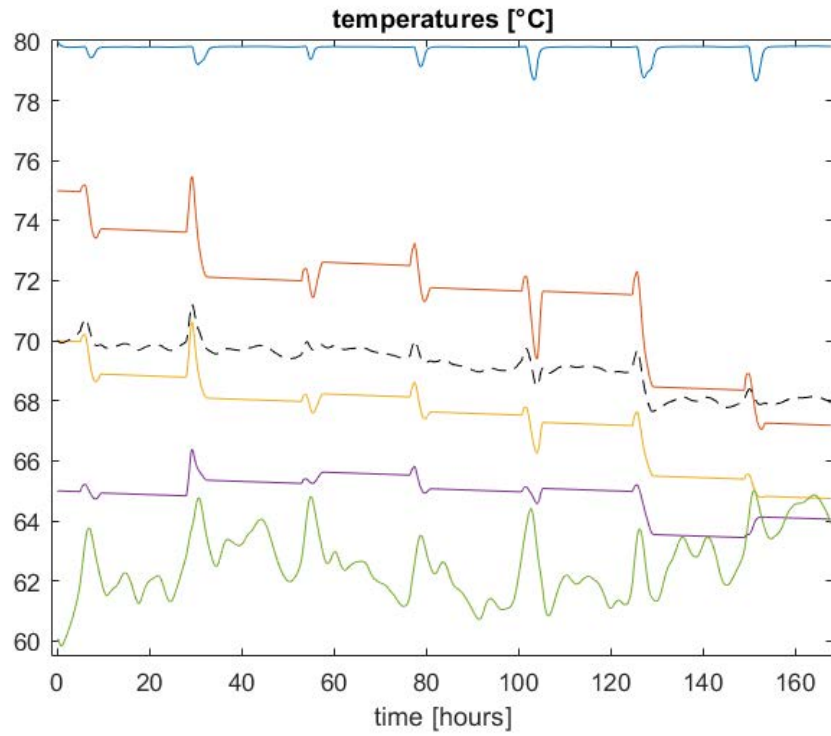


Figure B.2: The tank temperatures in the April week with $\tau = 1.5h$

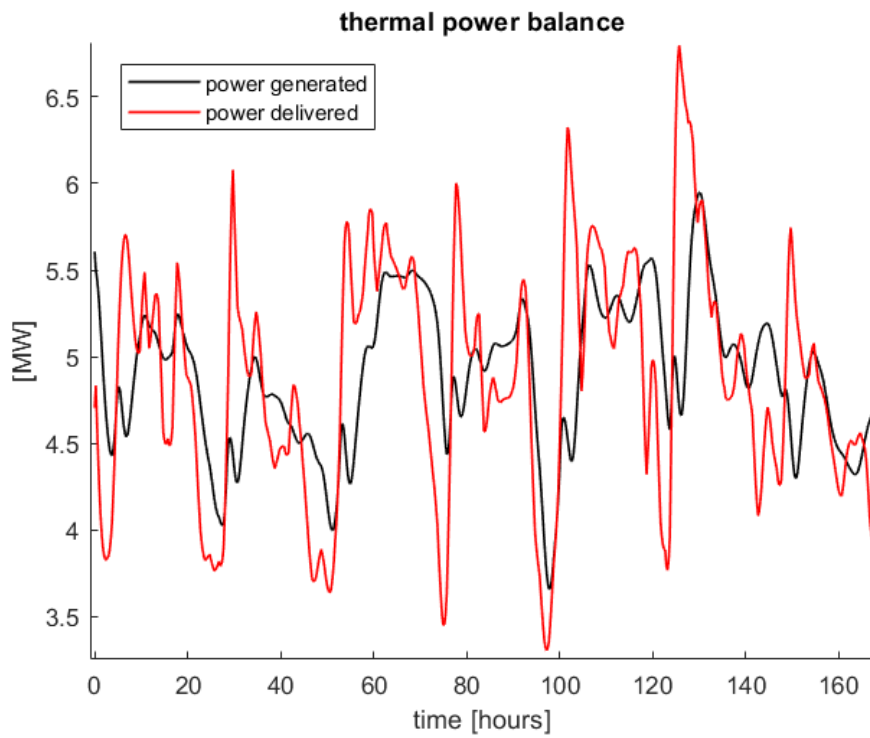


Figure B.3: The power profiles in the April week with constant \dot{m}_g

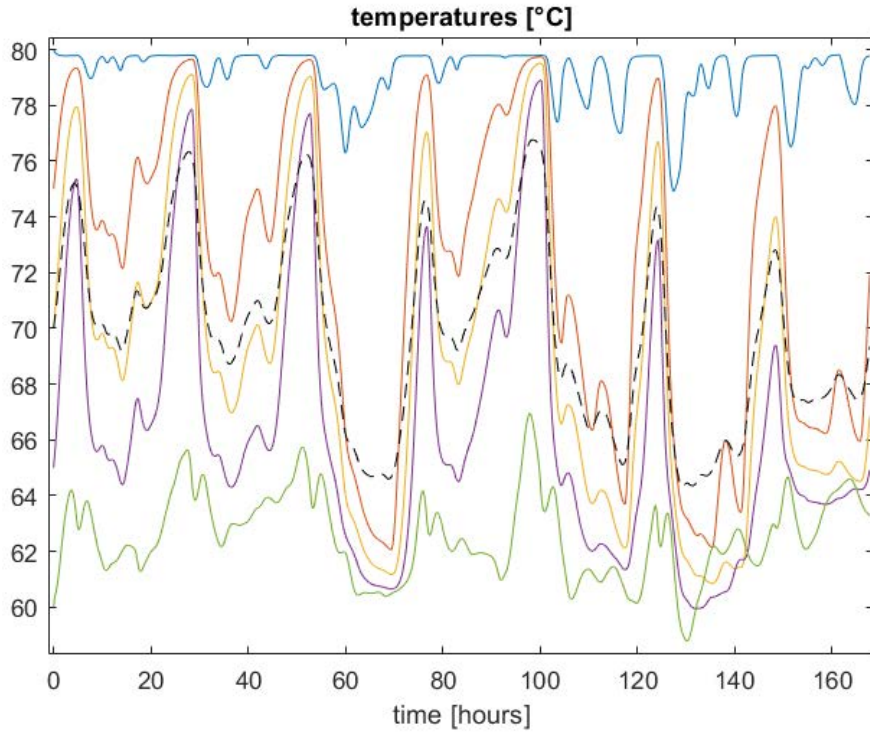


Figure B.4: Tank level temperatures in the April week with constant \dot{m}_g

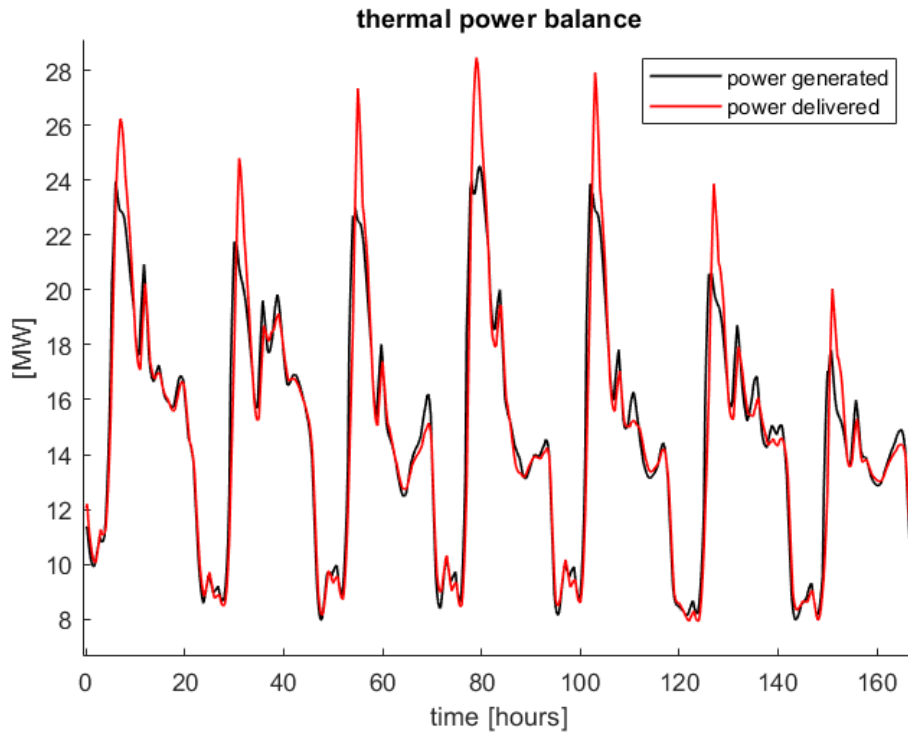


Figure B.5: The power profiles in the February week simulated with $\tau = 1.5h$

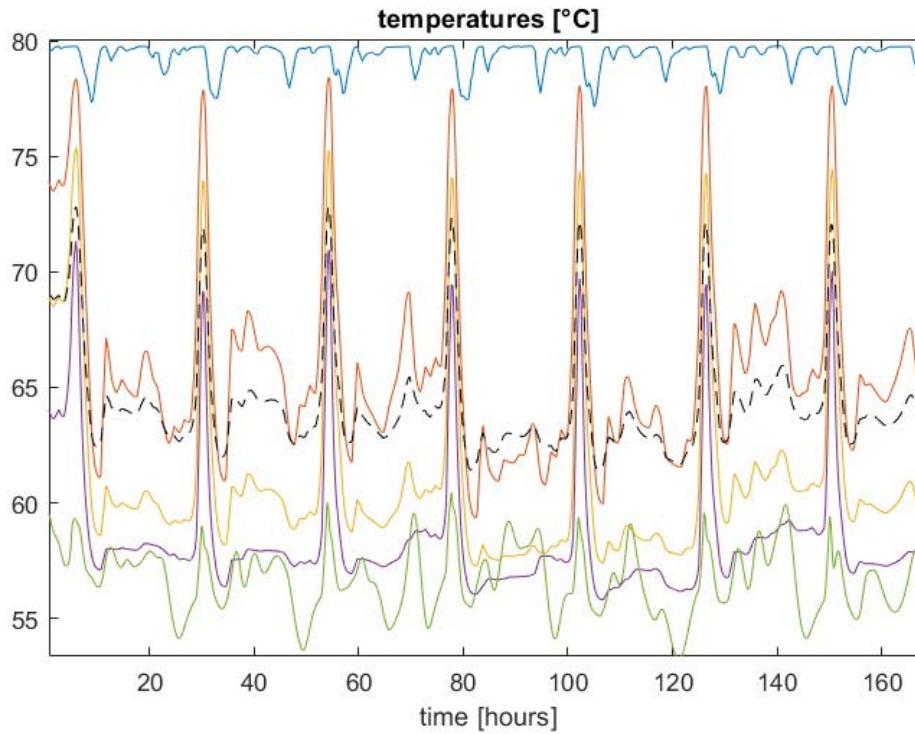


Figure B.6: The tank temperatures in the February week with $\tau = 1.5h$

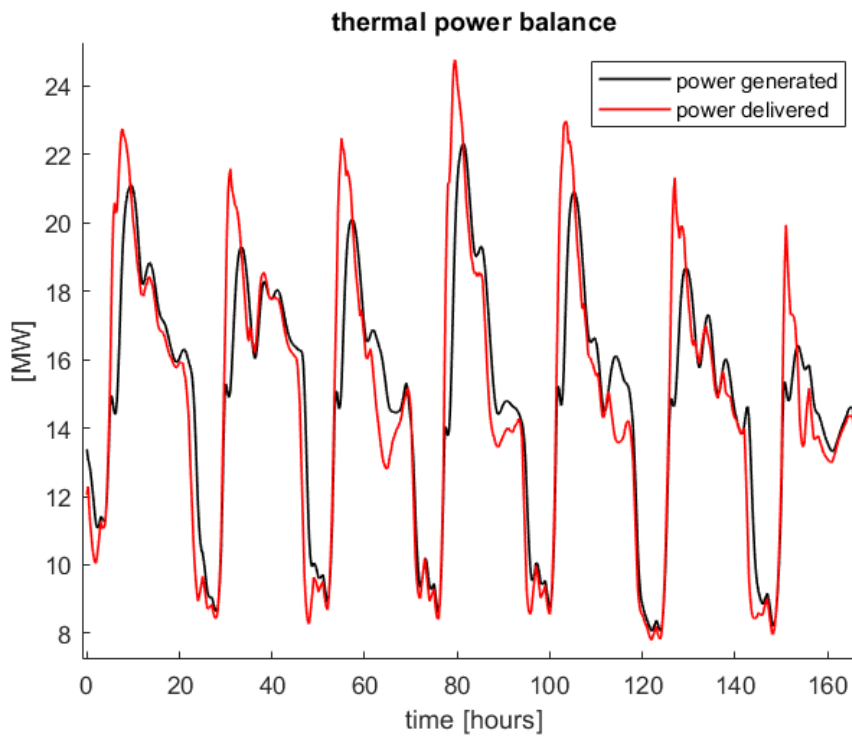


Figure B.7: Power profiles in the February week in which mass circulation on the generator side was always constant

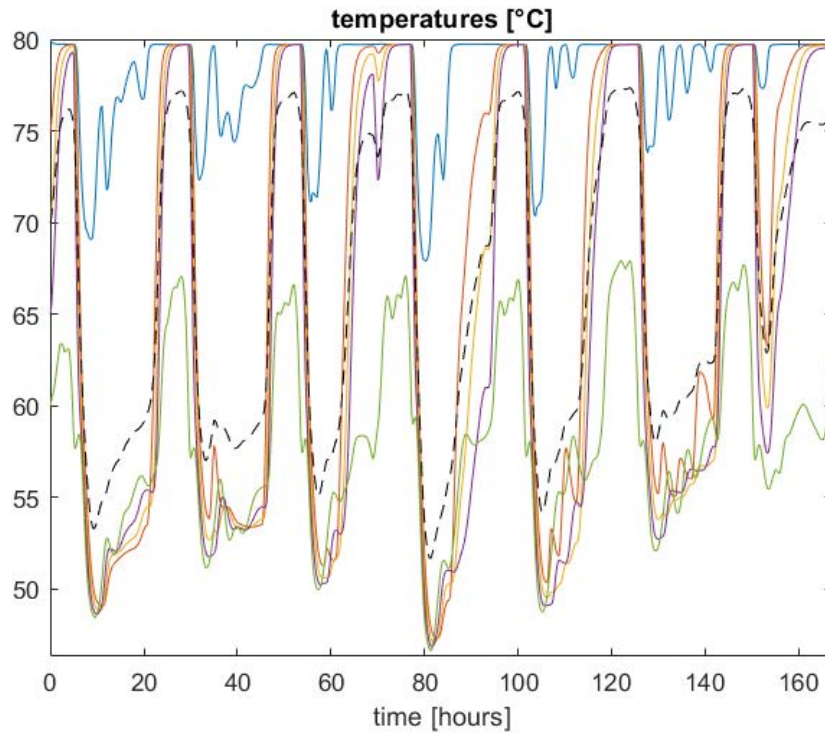


Figure B.8: Tank level temperatures in the February week in which mass circulation on the generator side was always constant

Bibliography

- [1] Guruprasad Alva, Yaxue Lin, and Guiyin Fang. “An overview of thermal energy storage systems”. In: *Energy* 144 (2018), pp. 341–378. ISSN: 0360-5442. DOI: <https://doi.org/10.1016/j.energy.2017.12.037>. URL: <https://www.sciencedirect.com/science/article/pii/S036054421732056X>.
- [2] *ASHRAE Handbook*. Atlanta, Georgia: ASHRAE, 2020.
- [3] Helge Averfalk, Paul Ingvarsson, Urban Persson, Mei Gong, and Sven Werner. “Large heat pumps in Swedish district heating systems”. In: *Renewable and Sustainable Energy Reviews* 79 (2017), pp. 1275–1284. ISSN: 1364-0321. DOI: <https://doi.org/10.1016/j.rser.2017.05.135>. URL: <https://www.sciencedirect.com/science/article/pii/S1364032117307839>.
- [4] Sergio Bazzoli, ed. *Approcci alla costruzione ed installazione di sistemi di accumulo per sistemi di teleriscaldamento*. AIRU (Italian Urban [District] Heating Association). Milano, 2016.
- [5] Cesare Bonacina, Alberto Cavallini, and Lino Mattarolo. *Trasmissione del calore*. Padova: CLEUP, 1985.
- [6] Helge Brattebø and Marte Reenaas. “Comparing CO₂ and NO_x emissions from a district heating system with mass-burn waste incineration versus likely alternative solutions – City of Trondheim, 1986-2009”. In: *Resources, Conservation and Recycling* 60 (2012), pp. 147–158. ISSN: 0921-3449. DOI: <https://doi.org/10.1016/j.resconrec.2011.11.001>. URL: <https://www.sciencedirect.com/science/article/pii/S0921344911002345>.
- [7] Simone Buffa, Marco Cozzini, Matteo D’Antoni, Marco Baratieri, and Roberto Fedrizzi. “5th generation district heating and cooling systems: A review of existing cases in Europe”. In: *Renewable and Sustainable Energy Reviews* 104 (2019), pp. 504–522. ISSN: 1364-0321. DOI: <https://doi.org/10.1016/j.rser.2018.12.059>. URL: <http://www.sciencedirect.com/science/article/pii/S1364032118308608>.
- [8] Paola Caputo, Giulio Ferla, and Simone Ferrari. “Evaluation of environmental and energy effects of biomass district heating by a wide survey based on operational conditions in Italy”. In: *Energy* 174 (2019), pp. 1210–1218. ISSN: 0360-5442. DOI: <https://doi.org/10.1016/j.energy.2019.03.073>. URL: <https://www.sciencedirect.com/science/article/pii/S0360544219304773>.

- [9] Abdulrahman Dahash, Fabian Ochs, Michele Bianchi Janetti, and Wolfgang Streicher. “Advances in seasonal thermal energy storage for solar district heating applications: A critical review on large-scale hot-water tank and pit thermal energy storage systems”. In: *Applied Energy* 239 (2019), pp. 296–315. ISSN: 0306-2619. DOI: <https://doi.org/10.1016/j.apenergy.2019.01.189>. URL: <https://www.sciencedirect.com/science/article/pii/S0306261919301837>.
- [10] A. Dalla Rosa, R. Boulter, K. Church, and S. Svendsen. “District heating (DH) network design and operation toward a system-wide methodology for optimizing renewable energy solutions (SMORES) in Canada: A case study”. In: *Energy* 45.1 (2012). The 24th International Conference on Efficiency, Cost, Optimization, Simulation and Environmental Impact of Energy, ECOS 2011, pp. 960–974. ISSN: 0360-5442. DOI: <https://doi.org/10.1016/j.energy.2012.06.062>. URL: <https://www.sciencedirect.com/science/article/pii/S0360544212005142>.
- [11] Danica Djurić Ilić. “Classification of Measures for Dealing with District Heating Load Variations – A Systematic Review”. In: *Energies* 14.1 (2021). ISSN: 1996-1073. DOI: 10.3390/en14010003. URL: <https://www.mdpi.com/1996-1073/14/1/3>.
- [12] Jianhua Fan and Simon Furbo. “Buoyancy driven flow in a hot water tank due to standby heat loss”. In: *Solar Energy* 86.11 (2012), pp. 3438–3449. ISSN: 0038-092X. DOI: <https://doi.org/10.1016/j.solener.2012.07.024>. URL: <https://www.sciencedirect.com/science/article/pii/S0038092X12002873>.
- [13] Hao Fang, Jianjun Xia, and Yi Jiang. “Key issues and solutions in a district heating system using low-grade industrial waste heat”. In: *Energy* 86 (2015), pp. 589–602. ISSN: 0360-5442. DOI: <https://doi.org/10.1016/j.energy.2015.04.052>. URL: <https://www.sciencedirect.com/science/article/pii/S0360544215005071>.
- [14] Sam Foster, Jenny Love, Ian Walker, and Martin Crane. *Heat Pumps in District Heating - Final Report*. Tech. rep. United Kingdom Department of Energy and Climate Change, 2016. URL: https://www.gshp.org.uk/pdf/DECC_Heat_Pumps_in_District_Heating.pdf.
- [15] Svend Frederiksen and Sven Werner. *District Heating and Cooling*. Lund: Studentlitteratur, 2013.
- [16] Henrik Gadd and Sven Werner. “Thermal energy storage systems for district heating and cooling”. In: *Advances in Thermal Energy Storage Systems - Methods and Applications* (2015), pp. 467–478. DOI: <https://doi.org/10.1533/9781782420965.4.467>. URL: <https://www.sciencedirect.com/science/article/pii/B9781782420880500183>.
- [17] Roman Geyer, Diego Hangartner, Markus Lindahl, and Svend Vinther Pedersen. *Heat Pumps in District Heating and Cooling Systems – Final Report*. Tech. rep. International Energy Agency, Technology Collaboration Programme on Heat Pump Technology, 2020. URL: <https://heatpumpingtechnologies.org/publications/heat-pumps-in-district-heating-and-cooling-systems-final-report/>.

- [18] Eric Granryd, Ingvar Ekroth, and Per Lundqvist. *Refrigerating Engineering*. Stockholm: Royal Institute of Technology - KTH Press, 2011.
- [19] Elisa Guelpa. "Impact of thermal masses on the peak load in district heating systems". In: *Energy* 214 (2021). DOI: <https://doi.org/10.1016/j.energy.2020.118849>.
- [20] Elisa Guelpa, Giulia Barbero, Adriano Sciacovelli, and Vittorio Verda. "Peak-shaving in district heating systems through optimal management of the thermal request of buildings". In: *Energy* 137 (2017), pp. 706–714. ISSN: 0360-5442. DOI: <https://doi.org/10.1016/j.energy.2017.06.107>. URL: <https://www.sciencedirect.com/science/article/pii/S0360544217311040>.
- [21] Elisa Guelpa and Vittorio Verda. "Thermal energy storage in district heating and cooling systems: A review". In: *Applied Energy* 252 (2019), p. 113474. ISSN: 0306-2619. DOI: <https://doi.org/10.1016/j.apenergy.2019.113474>. URL: <https://www.sciencedirect.com/science/article/pii/S0306261919311481>.
- [22] Einar Gunnlaugsson, ed. *GEOTHERMAL DISTRICT HEATING IN REYKJAVÍK, ICELAND*. Zakopane, Poland, 2004.
- [23] Stefanie Haehnlein, Peter Bayer, and Philipp Blum. "International legal status of the use of shallow geothermal energy". In: *Renewable and Sustainable Energy Reviews* 14.9 (2010), pp. 2611–2625. ISSN: 1364-0321. DOI: <https://doi.org/10.1016/j.rser.2010.07.069>. URL: <https://www.sciencedirect.com/science/article/pii/S1364032110002492>.
- [24] Elín Hallgrímsdóttir, Claus Ballzus, and Ingólfur Hrólfsson. "The Geothermal Power Plant at Hellisheiði, Iceland". In: *GRC Transactions* 36 (2012), pp. 1067–1072.
- [25] Y.M. Han, R.Z. Wang, and Y.J. Dai. "Thermal stratification within the water tank". In: *Renewable and Sustainable Energy Reviews* 13.5 (2009), pp. 1014–1026. ISSN: 1364-0321. DOI: <https://doi.org/10.1016/j.rser.2008.03.001>. URL: <https://www.sciencedirect.com/science/article/pii/S1364032108000385>.
- [26] Jay Hennessy, Hailong Li, Fredrik Wallin, and Eva Thorin. "Flexibility in thermal grids: a review of short-term storage in district heating distribution networks". In: *Energy Procedia* 158 (2019). Innovative Solutions for Energy Transitions, pp. 2430–2434. ISSN: 1876-6102. DOI: <https://doi.org/10.1016/j.egypro.2019.01.302>. URL: <https://www.sciencedirect.com/science/article/pii/S1876610219303224>.
- [27] Frank P. Incropera and David P. DeWitt. *Fundamentals of Heat and Mass Transfer. Sixth Edition*. Hoboken, New Jersey: John Wiley and Sons Inc., 2007.
- [28] Brescia CHP operator website (in Italian). URL: <https://www.a2a.eu/it/gruppo/i-nostri-impianti/termoutilizzatori/brescia>.
- [29] S. P. Kavanaugh and K. Rafferty. *Ground-source Heat Pumps, Design of Geothermal Systems for Commercial and Institutional Buildings*. Atlanta, Georgia: ASHRAE, 1997.

- [30] Johan Kensby, Anders Trüschel, and Jan-Olof Dalenbäck. “Potential of residential buildings as thermal energy storage in district heating systems – Results from a pilot test”. In: *Applied Energy* 137 (2015), pp. 773–781. ISSN: 0306-2619. DOI: <https://doi.org/10.1016/j.apenergy.2014.07.026>. URL: <https://www.sciencedirect.com/science/article/pii/S0306261914007077>.
- [31] Domenico Lattanzio, ed. *Strategie efficienti per l’esercizio della rete mediante accumuli in pressione*. AIRU (Italian Urban [District] Heating Association). Milano, 2016.
- [32] R. Lazzarin and M. Noro. “District heating and gas engine heat pump: economic analysis based on a case study”. In: *Applied Thermal Engineering* 26.2-3 (2006), pp. 193–199.
- [33] J. Le Dréau and P. Heiselberg. “Energy flexibility of residential buildings using short term heat storage in the thermal mass”. In: *Energy* 111 (2016), pp. 991–1002. ISSN: 0360-5442. DOI: <https://doi.org/10.1016/j.energy.2016.05.076>. URL: <https://www.sciencedirect.com/science/article/pii/S0360544216306934>.
- [34] E.W. Lemmon, I.H. Bell, M.L. Huber, and M.O. McLinden. *NIST Standard Reference Database 23: Reference Fluid Thermodynamic and Transport Properties (REF-PROP)*. Tech. rep.
- [35] Martin Leurent, Frédéric Jasserand, Giorgio Locatelli, Jenny Palm, Miika Rämä, and Andrea Trianni. “Driving forces and obstacles to nuclear cogeneration in Europe: Lessons learnt from Finland”. In: *Energy Policy* 107 (2017), pp. 138–150. ISSN: 0301-4215. DOI: <https://doi.org/10.1016/j.enpol.2017.04.025>. URL: <https://www.sciencedirect.com/science/article/pii/S0301421517302501>.
- [36] Maciej Lipka and Adam Rajewski. “Regress in nuclear district heating. The need for rethinking cogeneration”. In: *Progress in Nuclear Energy* 130 (2020), p. 103518. ISSN: 0149-1970. DOI: <https://doi.org/10.1016/j.pnucene.2020.103518>. URL: <https://www.sciencedirect.com/science/article/pii/S0149197020302663>.
- [37] Giovanni Lozza. *Turbine a gas e cicli combinati*. Bologna: Società editrice Esculapio, 2016.
- [38] Henrik Lund, Sven Werner, Robin Wiltshire, Svend Svendsen, Jan Eric Thorsen, Frede Hvelplund, and Brian Vad Mathiesen. “4th Generation District Heating (4GDH) Integrating smart thermal grids into future sustainable energy systems”. In: *Energy* 68 (2014), pp. 1–11.
- [39] Yrjö Majanne and Luis Vázquez Seisdedos. “Sliding Back Pressure Control in Industrial CHP Plants”. In: *IFAC Proceedings Volumes* 45.21 (2012). 8th Power Plant and Power System Control Symposium, pp. 639–644. ISSN: 1474-6670. DOI: <https://doi.org/10.3182/20120902-4-FR-2032.00112>. URL: <https://www.sciencedirect.com/science/article/pii/S1474667016320444>.
- [40] Robert Edward Mates Jr. “Model for an Immersed, Collector Side Heat Exchanger”. MA thesis. Madison, Wisconsin: University of Wisconsin-Madison, 1987.
- [41] Amy Musser and William Bahnfleth. “Parametric Study of Charging Inlet Diffuser Performance in Stratified Chilled Water Storage Tanks with Radial Diffusers: Part 1-Model Development and Validation”. In: *HVAC&R Research* 7 (Jan. 2001), pp. 31–49. DOI: [10.1080/10789669.2001.10391428](https://doi.org/10.1080/10789669.2001.10391428).

- [42] G. Nardin, G. Ciotti, F. Dal Magro, A. Meneghetti, and P. Simeoni. “Waste heat recovery in the steel industry: better internal use or external integration?” In: *University of Udine, XXIII Summer School “Francesco Turco” – Industrial Systems Engineering* (2016).
- [43] Lidia Navarro, Alvaro de Gracia, Shane Colclough, Maria Browne, Sarah J. McCormack, Philip Griffiths, and Luisa F. Cabeza. “Thermal energy storage in building integrated thermal systems: A review. Part 1. active storage systems”. In: *Renewable Energy* 88 (2016), pp. 526–547. ISSN: 0960-1481. DOI: <https://doi.org/10.1016/j.renene.2015.11.040>. URL: <https://www.sciencedirect.com/science/article/pii/S0960148115304584>.
- [44] Hassan Nazir, Mariah Batool, Francisco J Bolivar Osorio, Marllory Isaza-Ruiz, Xinhai Xu, K Vignarooban, Patrick Phelan, Arunachala M Kannan, et al. “Recent developments in phase change materials for energy storage applications: a review”. In: *International Journal of Heat and Mass Transfer* 129 (2019), pp. 491–523.
- [45] F. Ochs, W. Heidemann, and H. Müller-Steinhagen. “Performance of Large-Scale Seasonal Thermal Energy Stores”. In: *Journal of Solar Energy Engineering* (2009). DOI: <https://doi.org/10.1115/1.3197842>.
- [46] Dave Olsthoorn, Fariborz Haghighat, Alain Moreau, and Gino Lacroix. “Abilities and limitations of thermal mass activation for thermal comfort, peak shifting and shaving: A review”. In: *Building and Environment* 118 (2017), pp. 113–127. ISSN: 0360-1323. DOI: <https://doi.org/10.1016/j.buildenv.2017.03.029>. URL: <https://www.sciencedirect.com/science/article/pii/S0360132317301282>.
- [47] Daniele Pasinelli, ed. *Accumuli termici. Schemi di installazione e regolazione*. AIRU (Italian Urban [District] Heating Association). Milano, 2016.
- [48] S.V. Patankar and D.B. Spalding. “A calculation procedure for heat, mass and momentum transfer in three-dimensional parabolic flows”. In: *International Journal of Heat and Mass Transfer* 15.10 (1972), pp. 1787–1806. ISSN: 0017-9310. DOI: [https://doi.org/10.1016/0017-9310\(72\)90054-3](https://doi.org/10.1016/0017-9310(72)90054-3). URL: <https://www.sciencedirect.com/science/article/pii/0017931072900543>.
- [49] T. Pauschinger. “5 - Solar thermal energy for district heating”. In: *Advanced District Heating and Cooling (DHC) Systems*. Ed. by Robin Wiltshire. Woodhead Publishing Series in Energy. Oxford: Woodhead Publishing, 2016, pp. 99–120. ISBN: 978-1-78242-374-4. DOI: <https://doi.org/10.1016/B978-1-78242-374-4.00005-7>. URL: <https://www.sciencedirect.com/science/article/pii/B9781782423744000000>
- [50] Kinga Pielichowska and Krzysztof Pielichowski. “Phase change materials for thermal energy storage”. In: *Progress in Materials Science* 65 (2014), pp. 67–123. ISSN: 0079-6425. DOI: <https://doi.org/10.1016/j.pmatsci.2014.03.005>. URL: <https://www.sciencedirect.com/science/article/pii/S0079642514000358>.
- [51] Carlo Piemonte, ed. *Esempi di realizzazione di sistemi di teleriscaldamento geotermici*. Italian Geothermal Union (Unione Geotermica Italiana). Milan, 2019. URL: <https://www.unionegeotermica.it/pdf/files/8-PIEMONTE.pdf>.

- [52] Carlo Piemonte, Andrea Masella, and Mauro Piemonte, eds. *Esperienze nell'impiego di pompe di calore acqua/acqua di media e grossa taglia*. Ordine degli Ingegneri della Provincia di Milano. Milan, 2017. URL: https://www.cittametropolitana.mi.it/export/sites/default/ambiente/doc/Community/Archivio_lifelong_learning/23_11mag2017/C.Piemonte-presentazione-v2.pdf.
- [53] Edoardo Ploner. "Analisi del comportamento idraulico e termico della rete di teleriscaldamento di Verona centro città mediante modello alle differenze finite". MA thesis. Università degli Studi di Padova, 2018.
- [54] Michal Pomianowski, Per Heiselberg, and Rasmus Lund Jensen. "Dynamic heat storage and cooling capacity of a concrete deck with PCM and thermally activated building system". In: *Energy and Buildings* 53 (2012), pp. 96–107. ISSN: 0378-7788. DOI: <https://doi.org/10.1016/j.enbuild.2012.07.007>. URL: <https://www.sciencedirect.com/science/article/pii/S0378778812003192>.
- [55] Di Qin, Zhun (Jerry) Yu, Tingting Yang, Shuishen Li, and Guoqiang Zhang. "Thermal performance evaluation of a new structure hot water tank integrated with phase change materials". In: *Energy Procedia* 158 (2019). Innovative Solutions for Energy Transitions, pp. 5034–5040. ISSN: 1876-6102. DOI: <https://doi.org/10.1016/j.egypro.2019.01.659>. URL: <https://www.sciencedirect.com/science/article/pii/S1876610219306939>.
- [56] J. Raccanello, S. Rech, and A. Lazzaretto. "Simplified dynamic modeling of single-tank thermal energy storage systems". In: *Energy* 182 (2019), pp. 1154–1172. ISSN: 0360-5442. DOI: <https://doi.org/10.1016/j.energy.2019.06.088>. URL: <https://www.sciencedirect.com/science/article/pii/S0360544219312204>.
- [57] M. Ramirez, M. Epelde, M. Gomez de Arteche, A. Panizza, A. Hammerschmid, M. Baresi, and N. Monti. "Performance evaluation of an ORC unit integrated to a waste heat recovery system in a steel mill". In: *Energy Procedia* 129 (2017). 4th International Seminar on ORC Power Systems, September 13-15th, 2017, POLITECNICO DI MILANO BOVISA CAMPUS MILANO, ITALY, pp. 535–542. ISSN: 1876-6102. DOI: <https://doi.org/10.1016/j.egypro.2017.09.183>. URL: <https://www.sciencedirect.com/science/article/pii/S1876610217340973>.
- [58] Benjamin L. Ruddell, Francisco Salamanca, and Alex Mahalov. "Reducing a semiarid city's peak electrical demand using distributed cold thermal energy storage". In: *Applied Energy* 134 (2014), pp. 35–44. ISSN: 0306-2619. DOI: <https://doi.org/10.1016/j.apenergy.2014.07.096>. URL: <https://www.sciencedirect.com/science/article/pii/S0306261914007879>.
- [59] Thomas Schmidt, Thomas Pauschinger, Per Alex Sørensen, Aart Snijders, Reda Djebbar, Raymond Boulter, and Jeff Thornton. "Design Aspects for Large-scale Pit and Aquifer Thermal Energy Storage for District Heating and Cooling". In: *Energy Procedia* 149 (2018). 16th International Symposium on District Heating and Cooling, DHC2018, 9–12 September 2018, Hamburg, Germany, pp. 585–594. ISSN: 1876-6102. DOI: <https://doi.org/10.1016/j.egypro.2018.08.223>. URL: <https://www.sciencedirect.com/science/article/pii/S1876610218305198>.

- [60] Payam Shafigh, Iman Asadi, and Norhayati Binti Mahyuddin. “Concrete as a thermal mass material for building applications - A review”. In: *Journal of Building Engineering* 19 (2018), pp. 14–25. ISSN: 2352-7102. DOI: <https://doi.org/10.1016/j.jobeb.2018.04.021>. URL: <https://www.sciencedirect.com/science/article/pii/S2352710218301992>.
- [61] Wijbrand Sommer, Johan Valstar, Ingo Leusbrock, Tim Grotenhuis, and Huub Rijnaarts. “Optimization and spatial pattern of large-scale aquifer thermal energy storage”. In: *Applied Energy* 137 (2015), pp. 322–337. ISSN: 0306-2619. DOI: <https://doi.org/10.1016/j.apenergy.2014.10.019>. URL: <https://www.sciencedirect.com/science/article/pii/S0306261914010605>.
- [62] TESS – Thermal Energy Systems Specialists. *TESSLibs 17 Component Libraries for the TRNSYS Simulation Environment - Storage Tank Library Mathematical Reference*. Madison, Wisconsin, 2012.
- [63] A. Thomson and G. Claudio. “The Technical and Economic Feasibility of Utilising Phase Change Materials for Thermal Storage in District Heating Networks”. In: *Energy Procedia* 159 (2019). Renewable Energy Integration with Mini/Microgrid, pp. 442–447. ISSN: 1876-6102. DOI: <https://doi.org/10.1016/j.egypro.2018.12.042>. URL: <http://www.sciencedirect.com/science/article/pii/S1876610218313377>.
- [64] Zhiyong Tian, Shicong Zhang, Jie Deng, Jianhua Fan, Junpeng Huang, Weiqiang Kong, Bengt Perers, and Simon Furbo. “Large-scale solar district heating plants in Danish smart thermal grid: Developments and recent trends”. In: *Energy Conversion and Management* 189 (2019), pp. 67–80. ISSN: 0196-8904. DOI: <https://doi.org/10.1016/j.enconman.2019.03.071>. URL: <https://www.sciencedirect.com/science/article/pii/S0196890419303759>.
- [65] Masaki Toyoshima and Seiji Okawa. “An effect of a horizontal buoyant jet on the temperature distribution inside a hot water storage tank”. In: *International Journal of Heat and Fluid Flow* 44 (2013), pp. 403–413. ISSN: 0142-727X. DOI: <https://doi.org/10.1016/j.ijheatfluidflow.2013.07.009>. URL: <https://www.sciencedirect.com/science/article/pii/S0142727X13001513>.
- [66] Annelies Vandermeulen, Bram van der Heijde, and Lieve Helsen. “Controlling district heating and cooling networks to unlock flexibility: A review”. In: *Energy* 151 (2018), pp. 103–115. ISSN: 0360-5442. DOI: <https://doi.org/10.1016/j.energy.2018.03.034>. URL: <https://www.sciencedirect.com/science/article/pii/S0360544218304328>.
- [67] Vittorio Verda, ed. *L’accumulo termico giornaliero e stagionale in sistemi di teleriscaldamento*. AIRU (Italian Urban [District] Heating Association). Milano, 2016.
- [68] Vittorio Verda and Francesco Colella. “Primary energy savings through thermal storage in district heating networks”. In: *Energy* 36.7 (2011), pp. 4278–4286. ISSN: 0360-5442. DOI: <https://doi.org/10.1016/j.energy.2011.04.015>. URL: <https://www.sciencedirect.com/science/article/pii/S0360544211002647>.

- [69] Jacopo Vivian, P. Monsalvete Álvarez de Uribarri, U. Eicker, and A. Zarrella. “The effect of discretization on the accuracy of two district heating network models based on finite-difference methods”. In: *Energy Procedia* 149 (2018). 16th International Symposium on District Heating and Cooling, DHC2018, 9-12 September 2018, Hamburg, Germany, pp. 625–634. ISSN: 1876-6102. DOI: <https://doi.org/10.1016/j.egypro.2018.08.227>. URL: <https://www.sciencedirect.com/science/article/pii/S187661021830523X>.
- [70] Jacopo Vivian, Giuseppe Emmi, Angelo Zarrella, Xavier Jobard, Dirk Pietruschka, and Michele De Carli. “Evaluating the cost of heat for end users in ultra low temperature district heating networks with booster heat pumps”. In: *Energy* 153 (2018), pp. 788–800. ISSN: 0360-5442. DOI: <https://doi.org/10.1016/j.energy.2018.04.081>. URL: <https://www.sciencedirect.com/science/article/pii/S0360544218306893>.
- [71] Jacopo Vivian, Davide Quaggiotto, E Ploner, F D’Isep, and Angelo Zarrella. “Load-shifting strategies in district heating networks with constant supply temperature: the case study of Verona”. In: *Journal of Physics: Conference Series* 1599 (2020), p. 012038. DOI: [10.1088/1742-6596/1599/1/012038](https://doi.org/10.1088/1742-6596/1599/1/012038). URL: <https://doi.org/10.1088/1742-6596/1599/1/012038>.
- [72] Jacopo Vivian, Davide Quaggiotto, and Angelo Zarrella. “Increasing the energy flexibility of existing district heating networks through flow rate variations”. In: *Applied Energy* 275 (2020), p. 115411. ISSN: 0306-2619. DOI: <https://doi.org/10.1016/j.apenergy.2020.115411>. URL: <https://www.sciencedirect.com/science/article/pii/S0306261920309235>.
- [73] Sven Werner. “International review of district heating and cooling”. In: *Energy* 137 (2017), pp. 617–631.
- [74] Wahiba Yaïci, Mohamed Ghorab, Evgueniy Entchev, and Skip Hayden. “Three-dimensional unsteady CFD simulations of a thermal storage tank performance for optimum design”. In: *Applied Thermal Engineering* 60.1 (2013), pp. 152–163. ISSN: 1359-4311. DOI: <https://doi.org/10.1016/j.applthermaleng.2013.07.001>. URL: <https://www.sciencedirect.com/science/article/pii/S1359431113004894>.
- [75] Martin Zogg. *History of heat pumps - Swiss contributions and international milestones*. Tech. rep. 2008. URL: <https://www.osti.gov/etdeweb/servlets/purl/21381633>.